PERFORMANCE ANALYSIS OF COMPOSITE
PROPULSION SYSTEMS

PHASE II FINAL REPORT

(25 March 1968 through 24 March 1969)

By

J. A. Wrubel

Prepared For

National Aeronautics and Space Administration

April 1969

Contract NAS7-521

Rocketdyne
A Division of North American Rockwell Corporation
6633 Canoga Avenue, Canoga Park, California 91304

PERFORMANCE ANALYSIS OF COMPOSITE
PROPULSION SYSTEMS

Phase I Final Report

(25 March 1968 through 24 March 1969)

By

J. A. Wrubel

Prepared For

National Aeronautics and Space Administration

April 1969

Contract NAS7-521

APPROVAL

The draft of this report, dated 25 April 1969, was approved for
formal printing on 20 May 1969 by letter S&E-AERO-AT, dated 16 May
1969 signed by David C. Seymour, NASA Technical Manager.

FOREWORD

ABSTRACT

The improved understanding of gas-stream turbulent mixing is contingent upon obtaining a more comprehensive description of the resultant flow field and a more precise evaluation of the turbulent transport properties. The second phase of a continuing program to accomplish these goals is described herein. The flow field being experimentally studied is the two-dimensional mixing of fuel-rich supersonic hydrogen-oxygen combustion products and a subsonic heated airstream. The mixing is accomplished in a chamber accessible to both optical- and probe-type instrumentation systems. The second phase of the program included flow facility check-out, instrumentation installation, probe instrumentation survey, and preliminary testing.

CONTENTS

ILLUSTRATIONS

TABLES

INTRODUCTION

Technological developments are required for advanced vehicle
propulsion systems. One of the required technology development
efforts, which is the subject of this study, is the improved under-
standing of high-speed gas mixing. Both fundamental and applied
knowledge of turbulent mixing are required by engine designers to
optimize the design of composite propulsion systems such as ramjets,
scramjets, and air-augmented rockets. In addition, this information
is applicable to the study of rocket engine exhaust plume after-
burning. Here it can be utilized in such diverse fields as missile
base heating and radio-frequency communication interference.

An extensive body of phenomenological theory on turbulent mixing
exists. However, the proof of the validity of these theories, which
are usually formulated in terms of an eddy transport coefficient or
eddy viscosity, is greatly impeded by the limited knowledge of
turbulent transport properties. This is particularly true in the
case of mixing involving chemical reactions, as in flames. Therefore,
the goal of this investigation is to experimentally determine in
detail the developing free shear layer in a particular turbulent
mixing process with combustion. The data thus obtained will be used
to generate a comprehensive description of the flow field and to
determine the turbulent transport properties of the mixing process.

In the past, probe-type instrumentation systems have been the primary
source of data collection. These systems have the common disadvantage
of disrupting the flow field in the vicinity of the measurement
station which in turn introduces an inherent uncertainity into these
data. This fundamental problem is overcome through utilization of
optical instrumentation devices which can gather the same data, except
velocity, without disturbing the flow field. These devices have been
successfully used at Rocketdyne for a number of years.

1

The three optical instruments (spectroradiometer, large aperture
spectrometer/spectrograph (LASS), and photographic pyrometer) utilized
on this program were designed and constructed by the Rocketdyne Physics
organization to conduct spectroscopic studies of rocket plume radiation.
Measurements are taken through appropriate internal optics from a line
of sight through the region of interest. If this region is confined,
care must be taken in the selection of the window materials to ensure
that they allow transmission of the particular specie radiation.
Quartz is usually selected because of its excellent mechanical and
optical properties. It is transparent to radiation from 2000 angstroms
to 3 microns. Other more costly materials are required for transmission
beyond this range.

The spectroradiometer is a versatile instrument, capable of both
spatial and spectral scanning for quantitative emission and absorption
measurements from the ultraviolet to the infrared spectral regions.
It consists of a grating monochromator, detectors, entrance optics,
radiation calibration sources, a tuning fork radiation chopper capable
of rapid startup or stop, and a zone ranging device, which enables the
instrument to spatially scan across the exhaust plume. It can be used
in a conventional manner to obtain spectral radiance and spectral
absorption coefficients of a body of gas as a function of wavelength.
Also, it can be used at a fixed wavelength to obtain spectral radiance,
absorption coefficients, temperatures, and partial pressures of species
as a function of spatial position.

The LASS consists of a McPherson Model 216 combination spectrometer
and spectrograph having a relative aperture of f/8.7 and a resolution
of 0.1A. It is trailer mounted with entrance optics, calibration
source, and fiducial camera integrated into the assembly. When utilized
as a spectrometer the LASS provides, by means of photoelectric detection,
an immediate record of spectral wavelength and intensity. If photographic
records are desired, it can be converted, within seconds, to a spectograph.
The determination of temperatures and combustion specie concentration,

e.g., OH, can be accomplished when the LASS is used in conjunction with a water discharge absorption source. The resolution capabilities of the LASS are two orders of magnitude superior to the telespectrograph, originally planned for use on this program. The instrument was designed for observations in the spectral region from 2500 to 8000 angstroms.

The ultraviolet photographic pyrometer produces a photographic record of the spatial distribution of the apparent spectral radiance of the mixing region, or its equivalent brightness temperature, at low spectral resolution. Included in its field of view are both the hot gases to be measured and a radiation standard. The radiation standard consists of a calibrated tungsten filament lamp and a set of neutral density filters. The optical components of the pyrometer all transmit or reflect ultraviolet light.

The application of these Rocketdyne-developed optical instruments to the study of mixing of the practical composite propulsion system propellant combination of LOX/GH_2 and hot air* will provide, for the first time, high precision measurements of the parameters that affect mixing. It is anticipated that the approach taken will establish a concrete experimental basis for the evaluation of the available theories in addition to providing the designer with empirical information.

The 12-month Phase II portion of the program entitled, "Performance Analysis of Composite Propulsion Systems," was initiated by the Rocketdyne Research Division under Contract NAS7-521 on 25 March 1968. The objective of the program is to perform an exploratory experimental investigation of two-dimensional mixing of supersonic hydrogen-oxygen combustion products and a subsonic heated air stream. Utilization of the flow system fabricated during Phase I and the existing optical and

---

* This propellant combination is optically clean, i.e., it does not contain solid particles. Although flows containing solid particles can be handled by appropriate techniques developed by the optics personnel, the complexities introduced do not warrant the study of propellant systems containing solid particles at this time.

selected probe instrumentation systems for measurement of the spatial distributions of the various parameters will allow delineation of the developing free shear layer. The experimentally measured parameters include: concentration of both stable and transient species, temperature, pressure, and velocity.

The Phase II effort discussed in this final report was divided into six tasks consisting of:

1. <u>Facility Checkout</u> – Repair of the combustor components and minor rework of the injector, preparation of the experiment operating manual, and facility activation (cold flow and full-scale hot flow checkout tests).

2. <u>Instrumentation Installation</u> – Installation of the spectro-radiometer, LASS, photographic pyrometer, test-section static pressure taps, and manometer bank.

3. <u>Probe Instrumentation</u> – The evaluation and procurement of special probe-type instrumentation devices for the determination of velocity and total pressure.

4. <u>Testing</u> – The experimental determination of the two-dimensionality of the flow, determination of the effect of test-section film coolant on the mixing process, characterization of a reference configuration, study of the effect of air stream temperature on the mixing process, and evaluation of the effect of relative turbulence level on the two-dimensional developing·free shear layer.

5. <u>Analysis</u> – Support for the previously mentioned tasks and the data analysis required for adequate presentation of the test results.

6. <u>Reports</u> – Writing and processing of all contractually required reports.

A detailed description of the accomplishment of these tasks is presented in subsequent sections of this report.

SUMMARY

This report discusses the Phase II program which is a logical extension
of the Phase I effort described in Ref. 1. The tasks completed under
Phase I consisted of:

1. The design and procurement of an integral, combustor-exhaust
   nozzle and test section.
2. The establishment of test stand subsystems requirements.
3. The installation of test stand propellant and coolant
   subsystems.

Figure 1 shows the apparatus prior to final assembly and installation
of the optical instrumentation. A schematic of the mixing chamber
is given in Fig. 2.

Major accomplishments made in this second phase of the program consisted
of:

1. Optical instrumentation systems including the zone radiometer
   and greybody source, the LASS, and the photographic pyrometer
   were readied for data collection. These instruments are used
   for a non-interference determination of partial pressure,
   temperature, and specie concentration in the flow field.
2. Both cold flow and hot flow check-out tests of the individual
   sub-system were successfully completed.
3. A probe instrumentation survey was accomplished. A commercial
   probe fulfilling the program requirements was procured, and
   the traversing mechanism designed.
4. A hot fire data reduction computer program was written and
   checked out.
5. Full integrated hot-fire testing was initiated, however, as
   a result of previous and subsequent problems, the planned
   test matrix was not completed.

Although the quantity of data did not meet expectations, this phase
demonstrated that successful data collection is imminent.

5
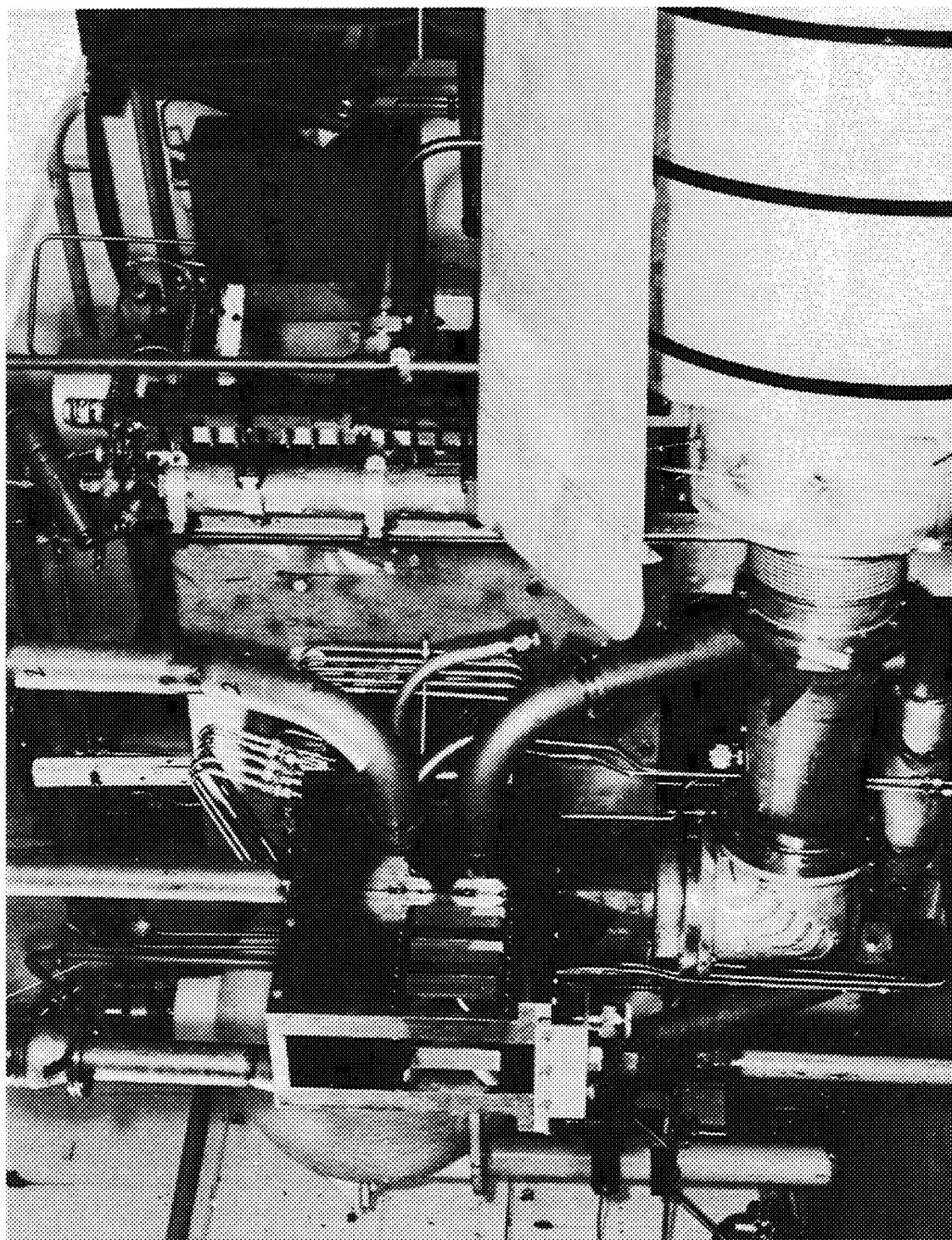
Figure 1. Mixing Apparatus Prior to Final Assembly
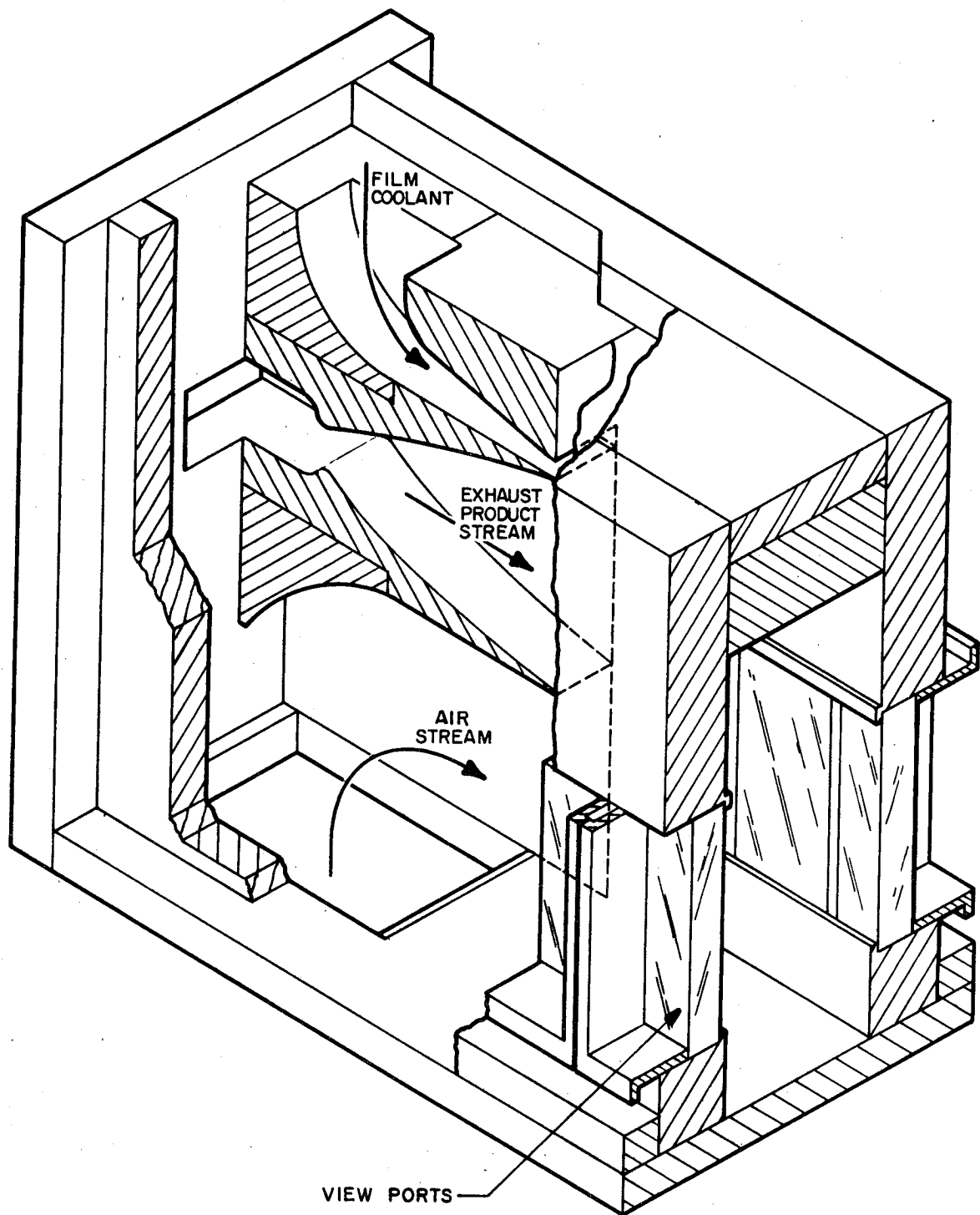
Figure 2. Combustor Exhaust Nozzle and Test Section Schematic

This program was plagued with a wide variety of difficulties. The most incessant problem was coolant water leakage. Its elimination required four modifications to the assembled hardware. This precluded the gathering of a wide range of experimental data.

DISCUSSION

A number of systems analyses have theoretically proven that airbreathing rocket vehicles can outperform any existing rocket engine in the arsenal of weapons and space boosters of the United States. Although these analyses are extremely optimistic about the improvements that can be made within the constraints of existing propulsion systems, e.g., a tripling of range or a doubling of payload, practical problems do exist. These problems, both fundamental and developmental in nature, include:

(1) mixing between the combustor exhaust and the air stream

(2) ignition delay vis-a-vis mixing chamber residence time

(3) cooling of the vehicle and combustion chamber with fuels rather than oxidizers which have higher specific heats

(4) a practical determination of the optimum method of air ingestion.

Discussed below is the second phase of a program to provide precise experimental data for the elucidation and delineation of the mixing problem.

FACILITY CHECKOUT

The small amount of test-stand plumbing remaining from the Phase I effort was completed. This included welding of the film coolant ducting, attachment of the cooling water drain lines to the test section, extension of the LOX bleed line, insertion of an LN_2 line to simplify injector chill-down, and installation of the engine afterburner and facility torches. The apparatus was subsequently removed from the thrust mount to facilitate combustor refurbishment. A handling fixture for ease of removing and replacing the apparatus was fabricated.

Combustor refurbishment included enlargement of the GH_2 orifices in the injector to accomodate the 1 lb/sec hydrogen flow required for

9

the mixing experiments. In addition, a number of water coolant passage leaks on the combustor body were repaired with silver braze and all sealing surfaces between combustor body sections were cleaned. Proof tests of the water coolant passages at full water coolant flow rates were successful.

Prior to final assembly of the apparatus a water coolant leak was noted (Appendix 1). After repairs were completed, the apparatus was mounted in the test stand and all utility, engine, and test section instrumentation was attached. Following this, all sub-system checkouts were successfully completed. These included flows of the water coolant, film coolant, injector chilldown system, engine and pad Firex, hot air system, liquid oxygen, hypergol, facility torches, and gaseous hydrogen. The response and operating characteristics of these sub-systems were deemed satisfactory to proceed with fully integrated checkout firings.

Full-scale system checkout tests, utilizing cold air, were conducted. Two ignition sequence tests and a 150-millisecond mainstage test were successful; however, significant errosion of the upper combustion chamber was experienced during a 2-second mainstage test (Appendix 1). No damage to the 2-D contoured exhaust nozzle or injector occurred.

A new combustor was assembled utilizing additional upper combustion chambers from the storage yard, and the propellant feed lines and coolant water lines were attached. An available nozzle was utilized in place of the 2-D contoured exhaust nozzle that is integrally attached to the mixing chamber. Coolant water blow-downs were made, and the combustor was successfully hot fired. Firing durations were 1, 2, and 5 seconds, respectively. Steady-state heat transfer rates to the coolant were extablished in approximately one second. Therefore, the ability of the combustor to meet the planned 22-second test duration was proven.

This completed the Facility Checkout task.

INSTRUMENTATION INSTALLATION

A 50-tube manometer bank for mapping the test-section static pressure
was procured and installed adjacent to the test pit (Fig. 3). A
total of 30 static pressure taps were located on the four test-section
walls and were plumbed to the bank. The manometer bank is also used
to monitor the pressure in the air heater transfer ducting.

Buildup for the optical instrumentation was completed. The required
control wiring for the instruments was installed in instrumentation
boxes at two locations: in the pit adjacent to the location of the
spectroradiometer and on the exterior of the blockhouse wall near
the location of the LASS and photographic pyrometer.

A mounting fixture for the zone radiometer was fabricated and installed,
and an optical tunnel/mirror system that attaches to the spectroradiometer
and provides an optical access to the mixing region that is free of
atmospheric water vapor was fabricated.

Figure 4 shows schematically the arrangement of the major system
components. The folded optical path allows the spectroradiometer to
be protected by a blast wall and also provides the proper path length
for forming an image of the mixing region on the monochromator entrance
slit. Prevention of excessive vibrations in the tunnel was provided
by structural supports that mount to the blast plate and test stand
floor.

The zone radiometer was inactive for more than a year and required a
modest effort to return it to operational status. Several electronic
components were relocated to provide increased protection from the
elements. The instrument was then placed in the test pit, and wired
to its instrumentation box. Dust was observed in the zone radiometer
after some particularly windy weather and it was necessary to clean the
instrument prior to connection to the optical tunnel and attachment of
the GN_2 environmental purge.
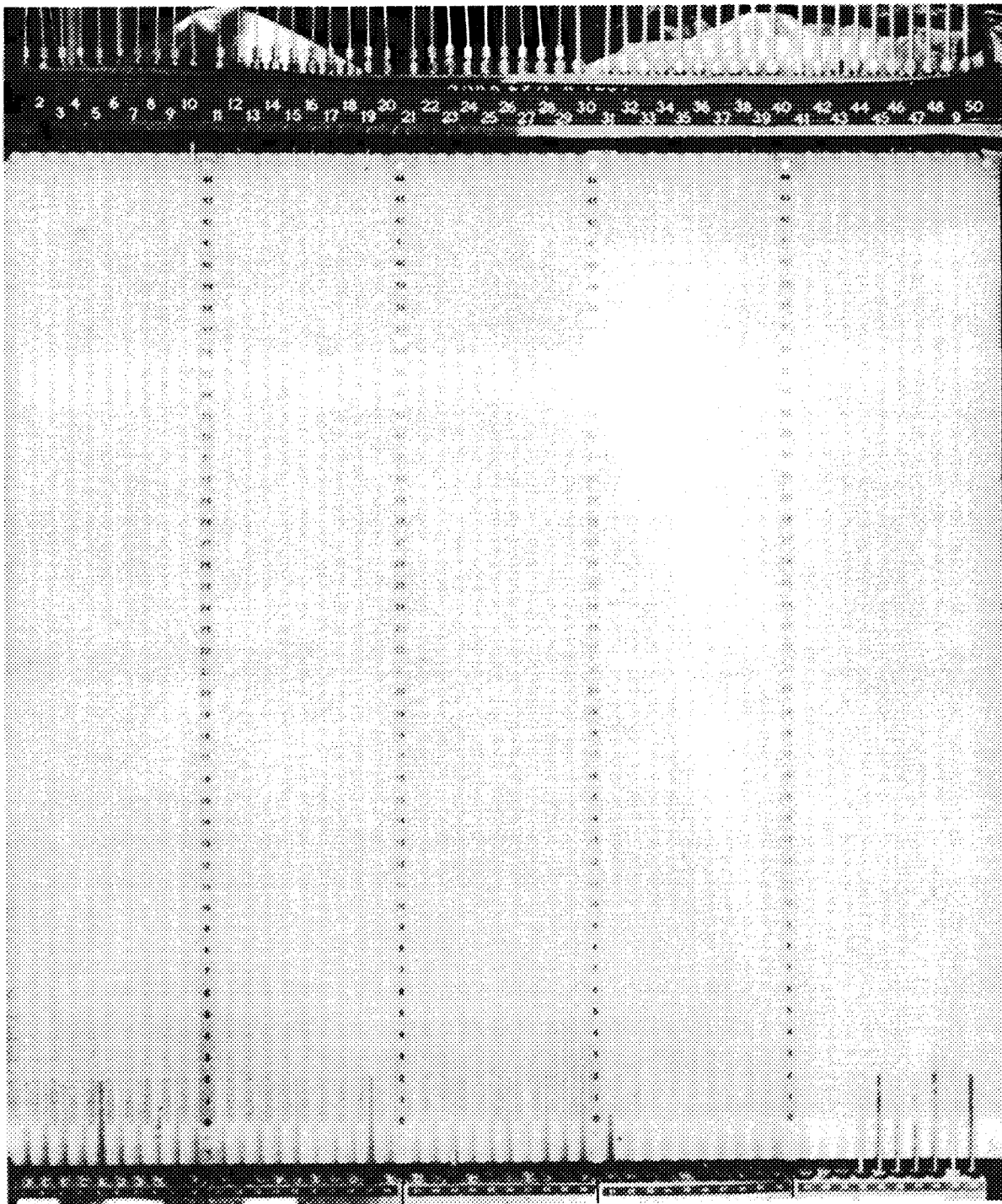
Figure 3.   50-Tube Manometer Bank
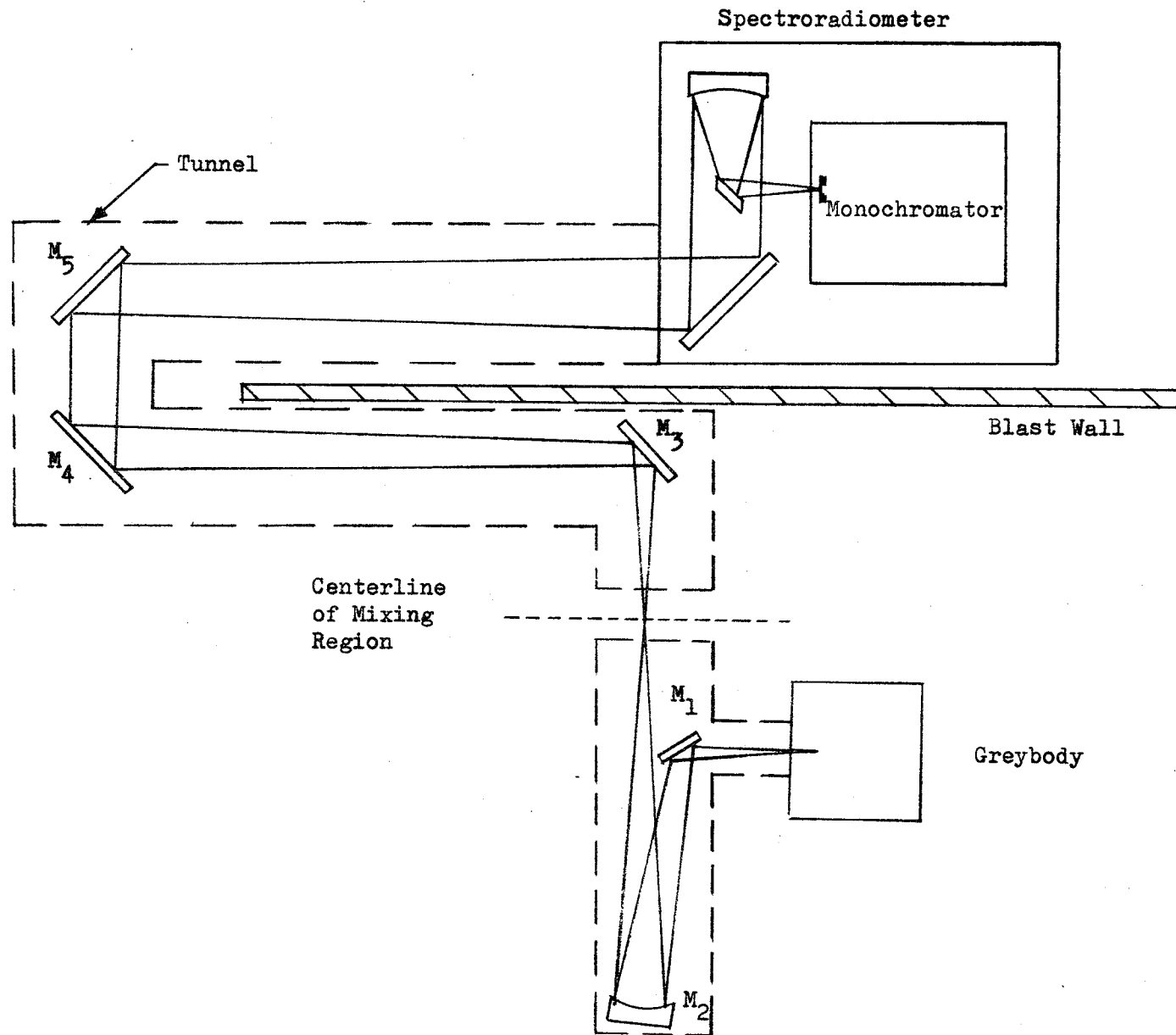
Figure 4. Zone Radiometry Schematic

13

The extra dry GN_2 purge prevents contamination of the instrument by dust and water vapor. The purge exhausts at the junction of the optical tunnel and the mixing chamber and serves the additional purpose of keeping the optical line of sight free of atmospheric water vapor during a test firing.

The greybody source is mounted above the mixing chamber on the opposite side of the zone radiometer line-of-sight. The structural supports for the source and its optical tunnel were located so that they would not block the view into the mixing region for the LASS, photopyrometer, and motion picture cameras.

The two-dimensional flow experiments require the zone radiometer to view the mixing region in the vertical direction. Special mirror mounts with their attendant optical tunnel were fabricated and modifications to the existing tunnel were made to accommodate this fixture. A comprehensive description of zone radiometry is given in Appendix 2.

The assembly of the LASS was completed under a Rocketdyne capital job order (Fig. 5). All subsystem components were mounted in the LASS trailer and the instrument successfully passed checkout. Mounting the instrument in a trailer makes it easily portable and enables installation at any facility in a matter of a few hours. The LASS is used for the spectroscopic determination of OH rotational temperature in the excited and ground state, identification of reaction zones and distinguishment of these zones from zones of thermal emission, and measurement of OH concentration. A detailed description of the instrument, the measurement technique, and the methods of data reduction are given in Appendix 3.

The location and types of photographic coverage for the mixing experiments was formulated and the requirements for the experiments were delivered to photographic personnel. This information included the film, filters, lenses, camera placement, and cameras to be utilized for high-speed photography, photopyrometry, schlieren photography,
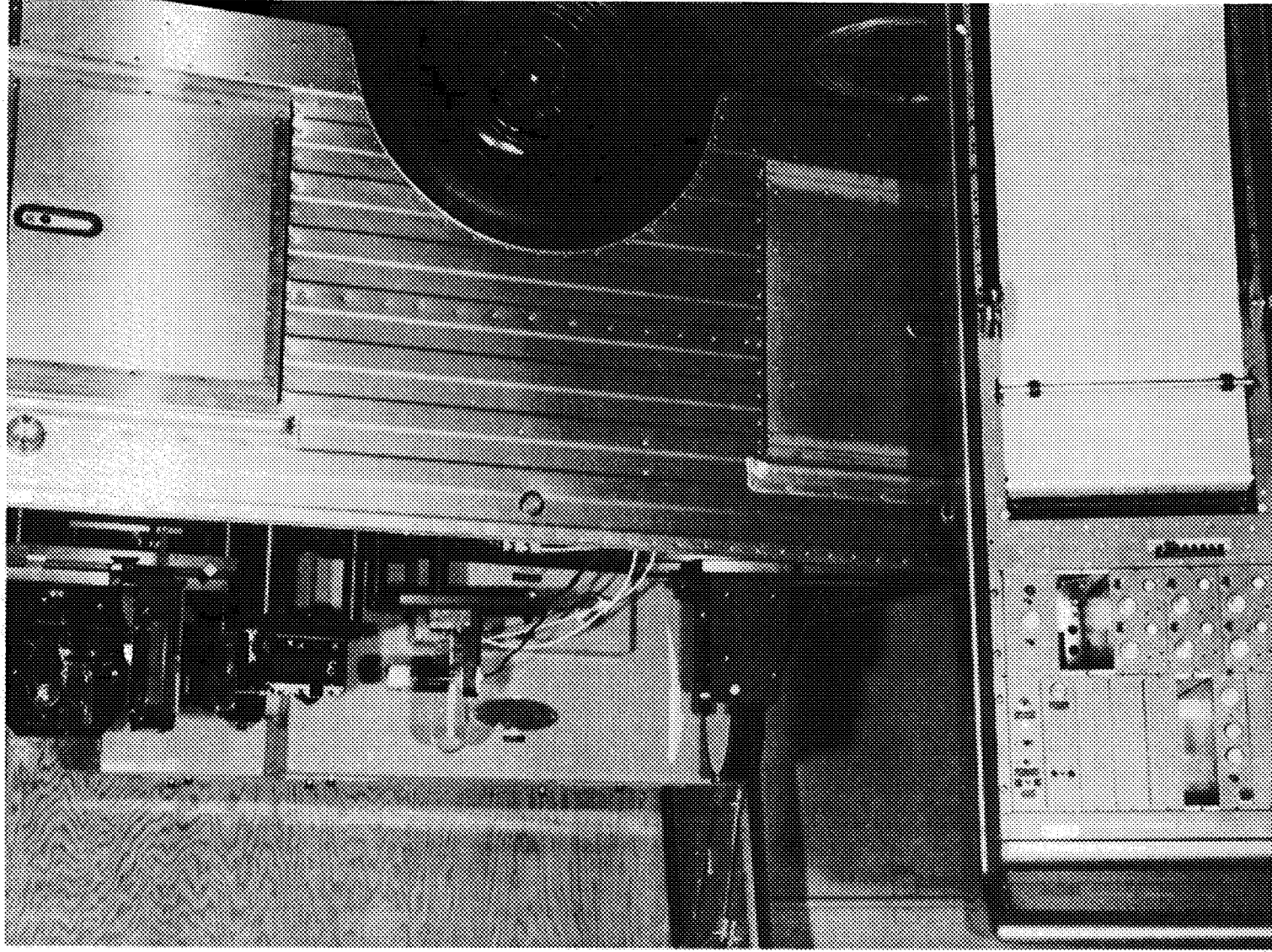
Figure 5. Large Aperture Spectrometer/Spectrograph

15

and overall photography. Low framing rate cameras are utilized to monitor the manometer bank, the back side of the injector, and the entire facility. Various camera speed ranges are required for coverage of the mixing region in the visible, ultraviolet, and infrared spectral regions. All cameras have been located in the test pit.

For the initial runs, a full gamut of photographic coverage was employed. After a critical evaluation of the initial photographic information, infrared photography was eliminated and only those camera settings that yielded specifically useful information were used.

A more compressive discussion of the photographic techniques employed is given in Appendix 4.

PROBE INSTRUMENTATION

For the probe instrumentation survey, available literature was gathered and reviewed. Emphasis was placed on methods that did not interfere with optical data acquisition while allowing the determination of velocity and total pressure; however, consideration was given for future use of these systems for collection of data identical to that gathered by the optical devices. Articles evaluated are included in Ref. 2 through 21. This evaluation concluded that probes satisfying the program requirements were commercially available.

Upon concurrence of the technical monitor, a Greyrad (Model G-13D-3) 3/8-inch, high sensitivity probe with static pressure taps was purchased, Figure 6. The probe can withstand the extreme thermal environment of a rocket exhaust while being capable of the determination of velocity, static pressure, total pressure, static temperature, stagnation temperature, enthalply, and specie concentration.

Design of the probe traversing mechanism was completed. Fabrication of the mechanism will be accomplished during the anticipated follow-on program.
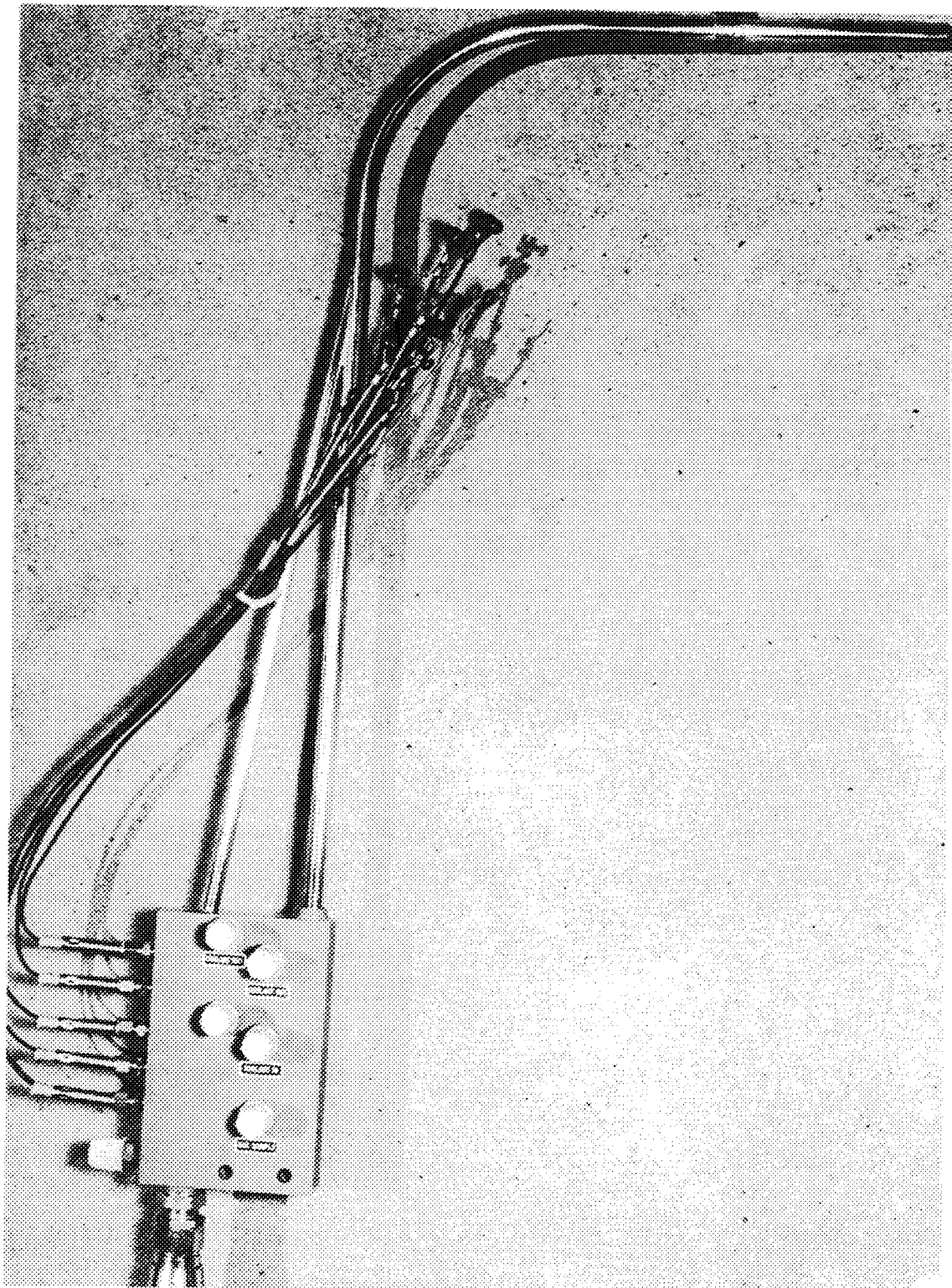
Figure 6. Greyrad Probe

17

TESTING

Following successful demonstration of the integrity of the new combustor,
it was mated with the two-dimensional nozzle which is integrally attached
to the mixing chamber. Leak tests of the assembled apparatus indicated
water leaks at some of the brazed joints on the 2-D contoured exhaust
nozzle. The apparatus was disassembled and the faulty braze joints were
repaired, i.e., TIG welded. The mixing chamber was then reassembled and
mounted in the test stand.

Preliminary to full-scale hot firing tests a determination of the two-
dimensional properties of the film coolant and air stream was made.
Measurements of the film coolant and air stream velocity profiles were
taken at the entrance to the mixing chamber with pitot probe rakes
(0.060 diameter). The total pressure was measured by a mercury-filled
manometer bank.

The velocity profile data for the air and film coolant streams are
presented in Fig. 7 and 8. It should be noted that the air stream
is reasonably two-dimensional except near the bottom wall where a
separate flow region exists. The separated flow region at the bottom
of the air stream is a consequence of the sharp turning angle of the
flow upstream of its entrance to the mixing chamber. Since this region
is relatively far from the theoretically calculated mixing region, it
should have a negligible influence on the mixing. Further, it should
be noted that the film coolants are reasonably two-dimensional at the
interfaces of the primary streams, i.e., air and combustor exhaust
products. Again, a separated flow region is evident near the side wall.
This, also, should have a minimal influence on the mixing region.
The tabs depicted on the figures are used to retain the quartz windows.

The present configuration of the mixing apparatus in total is approxi-
mately 3-inches shorter than the original engine-mixing chamber
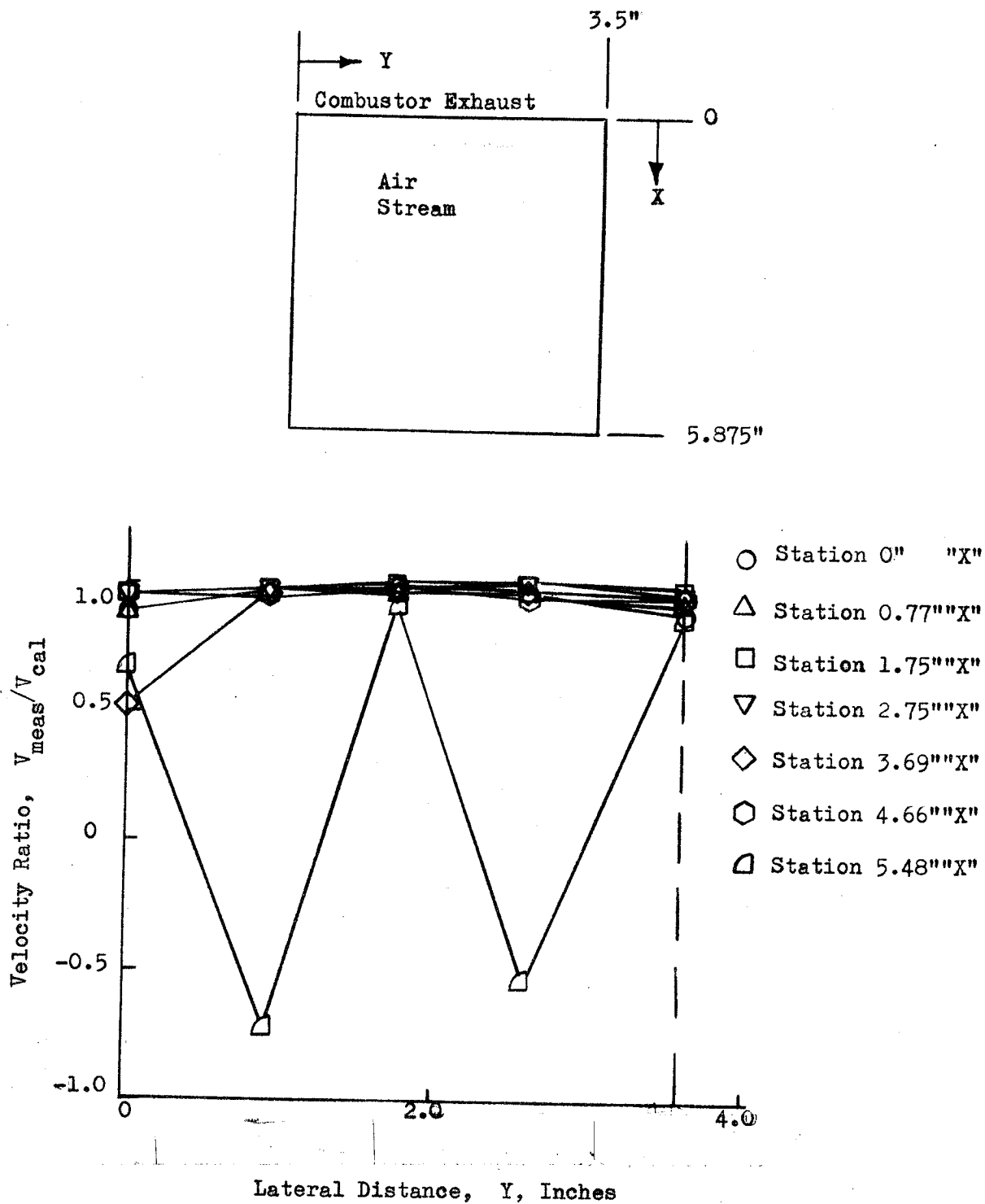
Figure 7.   Air Stream Velocity Profiles
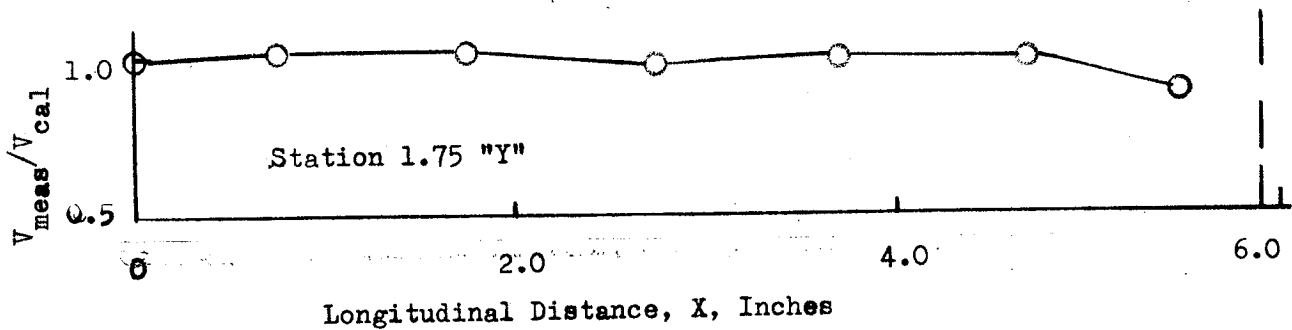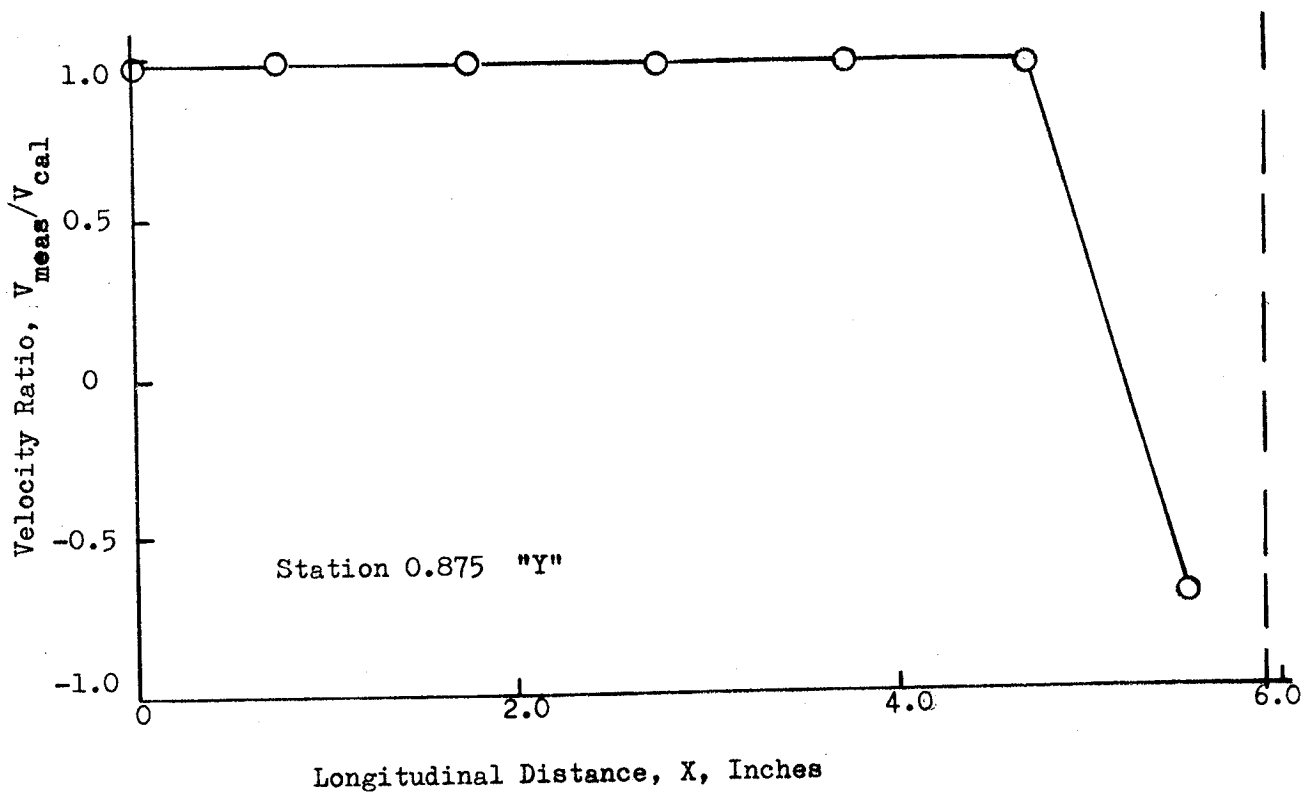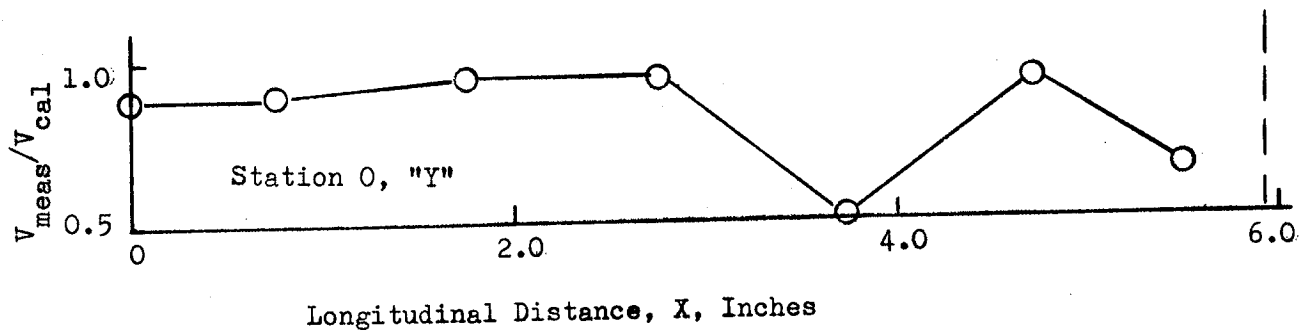
Figure 7 (Cont). Air Stream Velocity Profiles

20
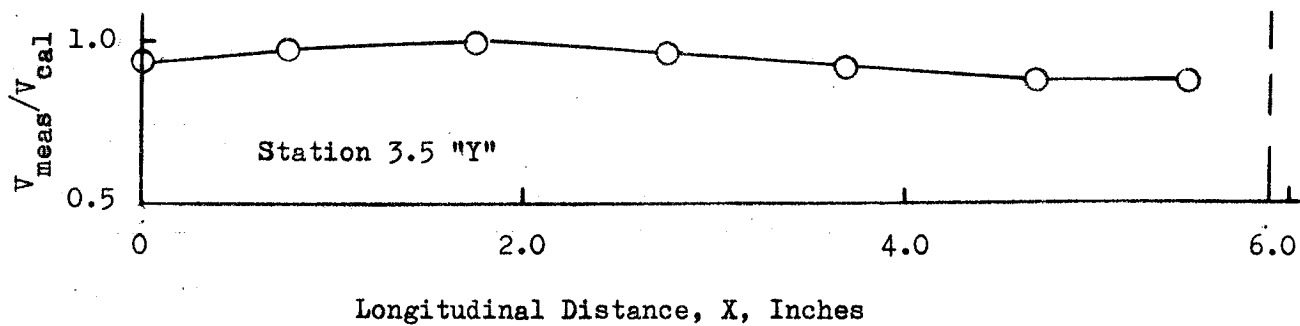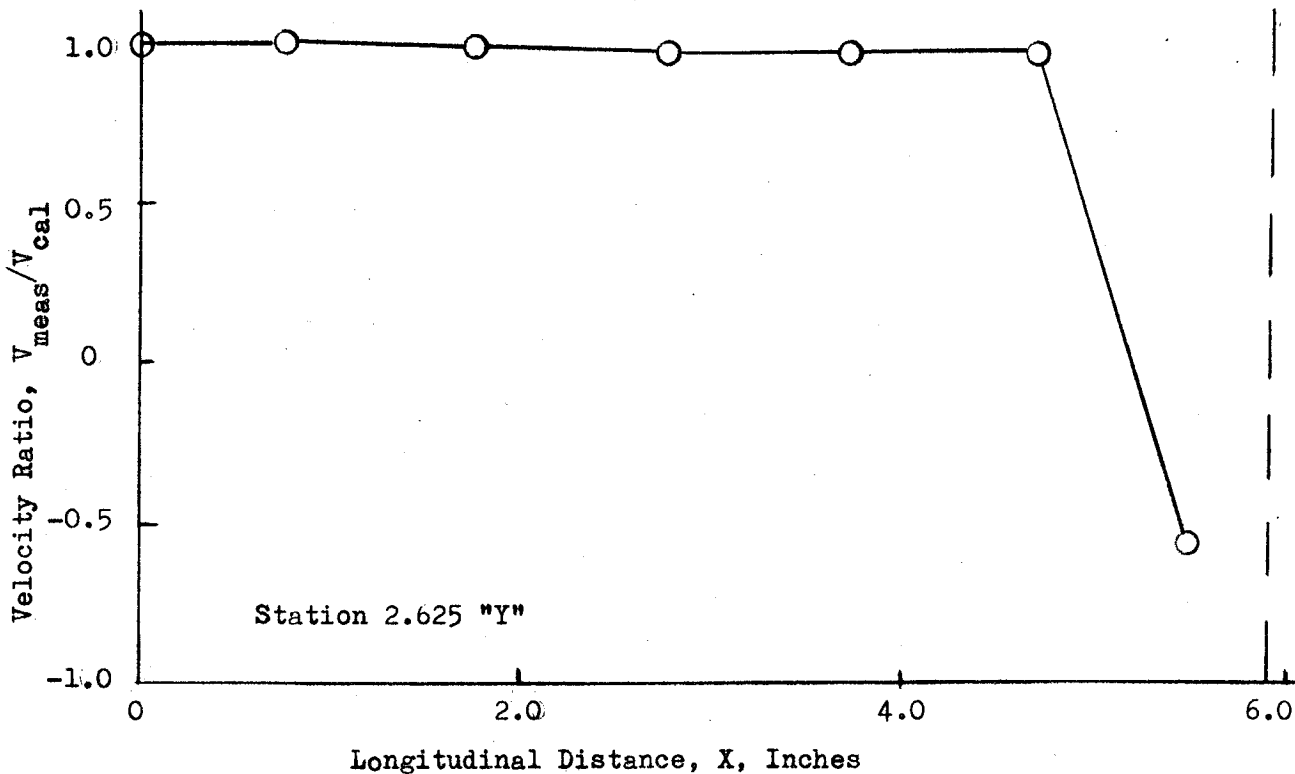
Figure 7 (Cont). Air Stream Velocity Profiles

TOP WALL FILM COOLANT
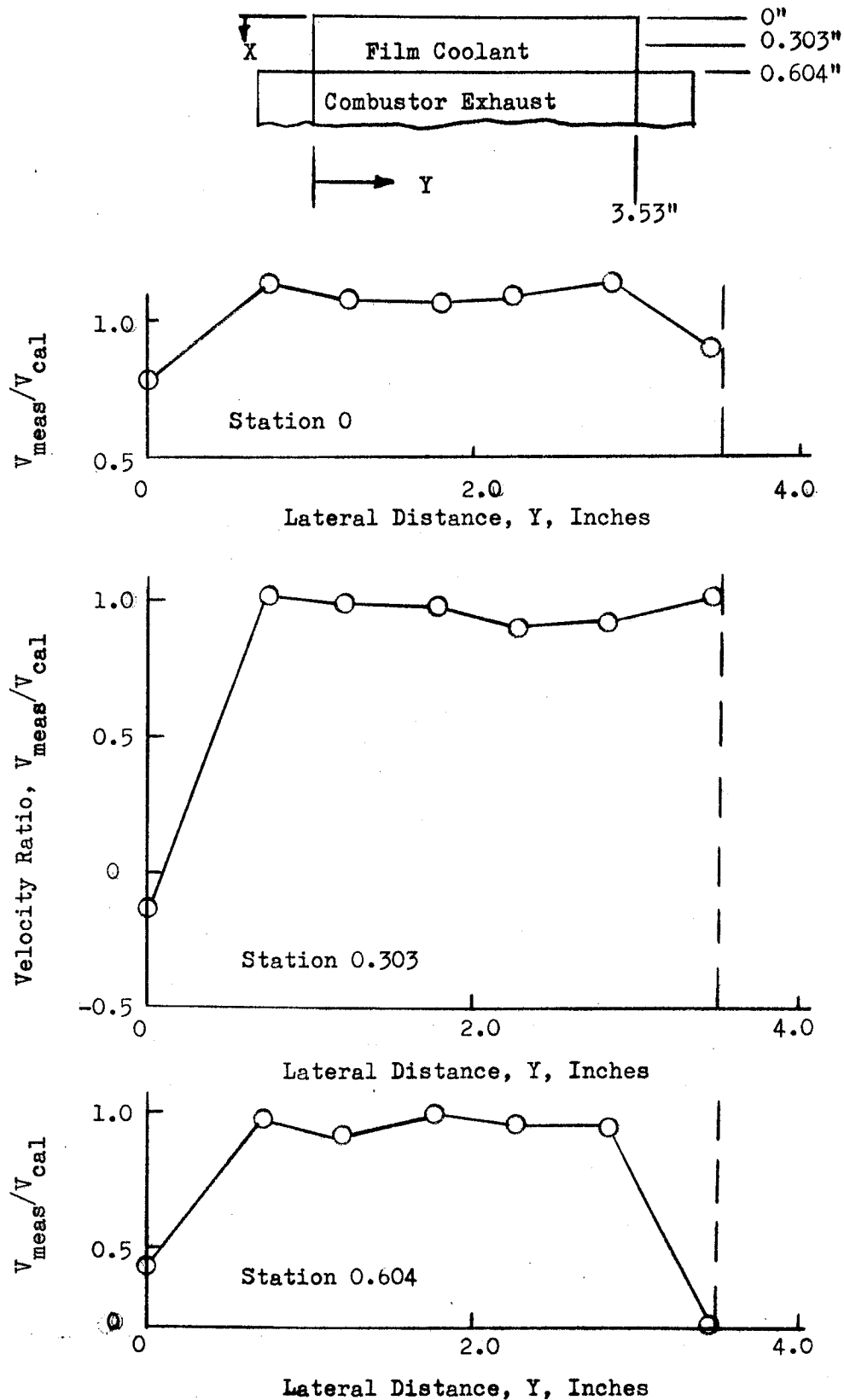
Figure 8. Film Coolant Velocity Profiles

HIGH PRESSURE FILM COOLANT
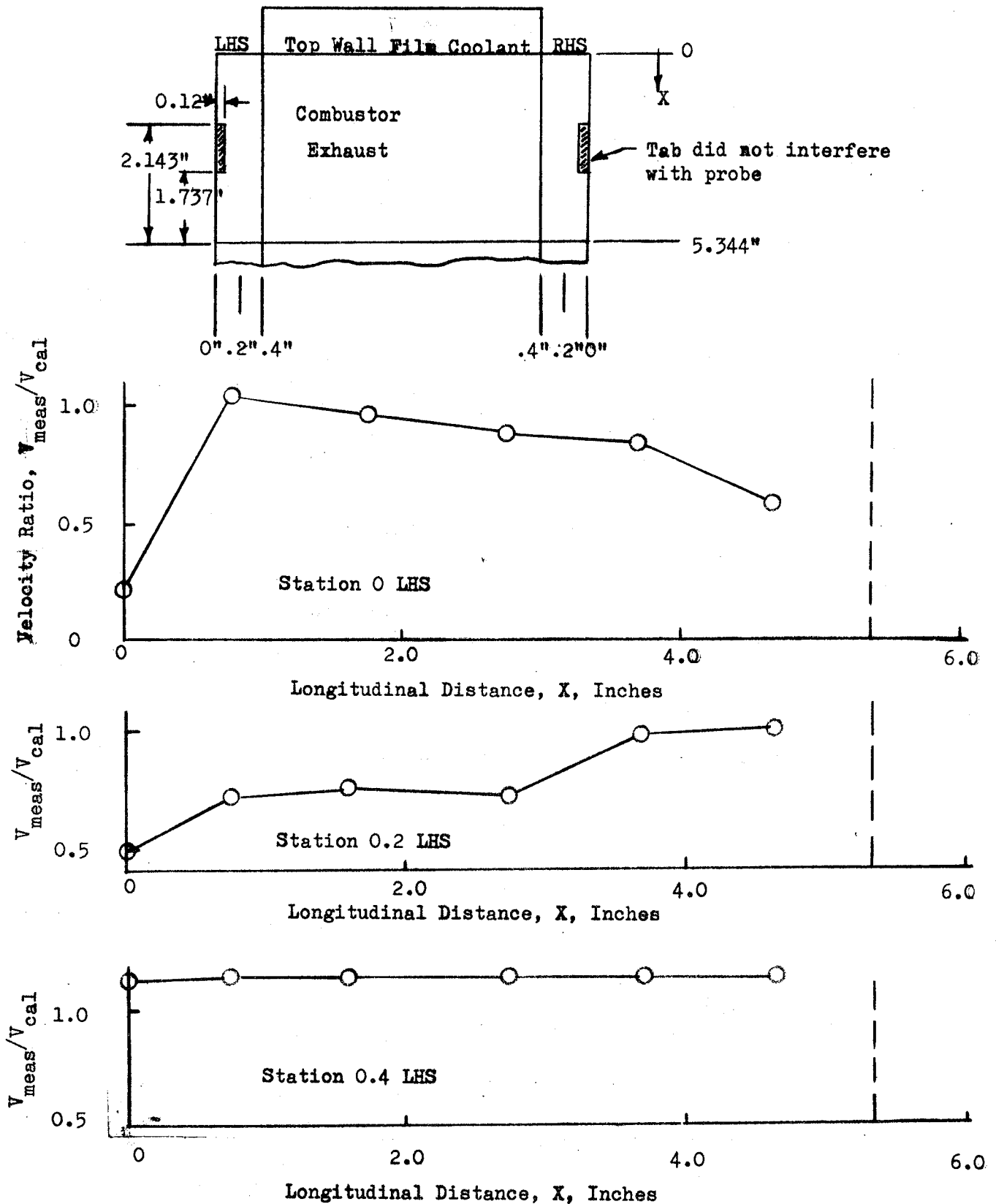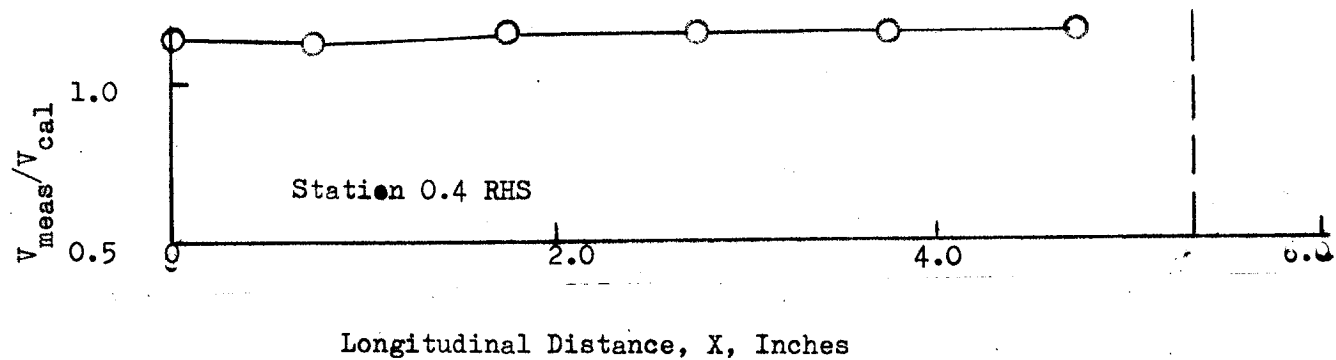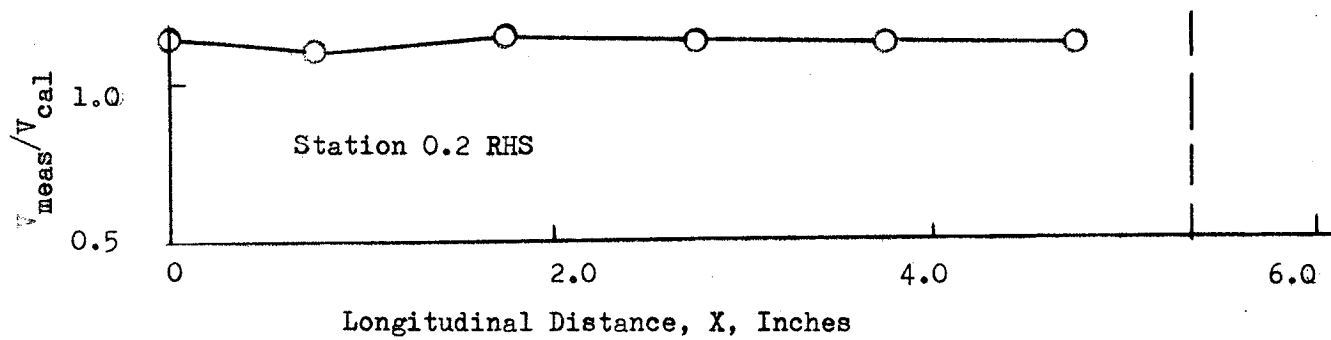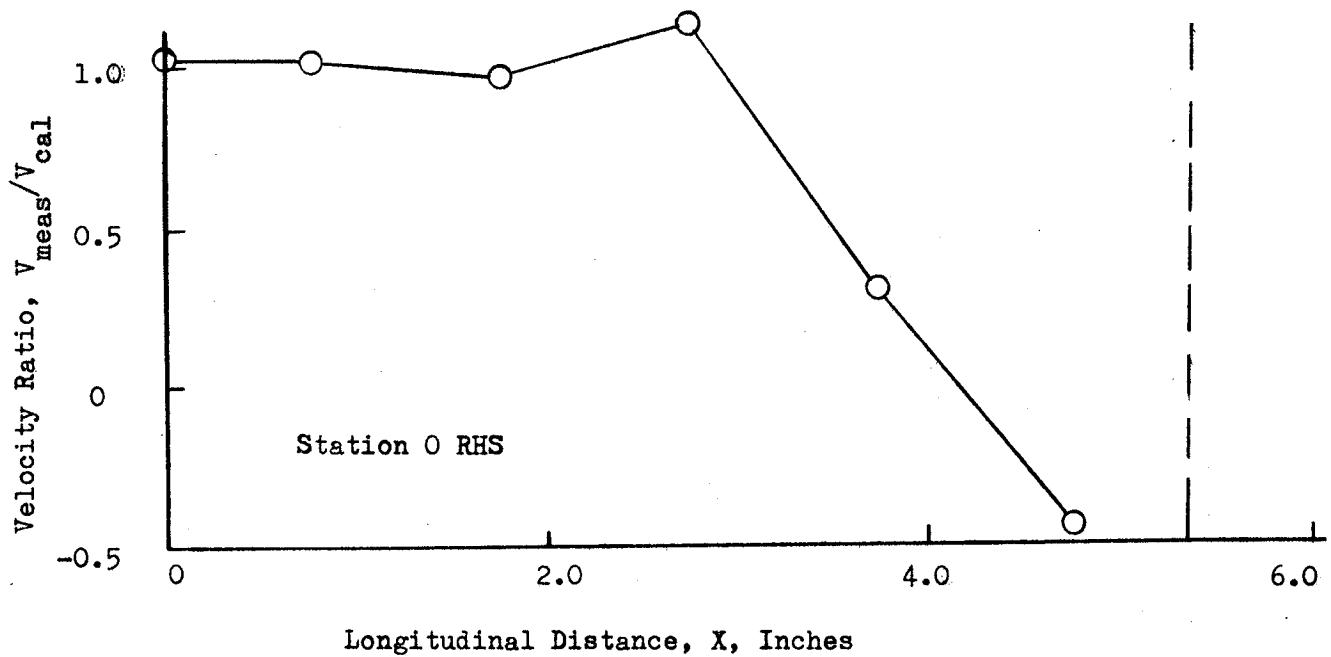
Figure 8 (Cont). Film Coolant Velocity Profiles

Figure 8 (Cont). Film Coolant Velocity Profiles

24

LOW PRESSURE FILM COOLANT

Figure 8 (Cont). Film Coolant Velocity Profiles

25
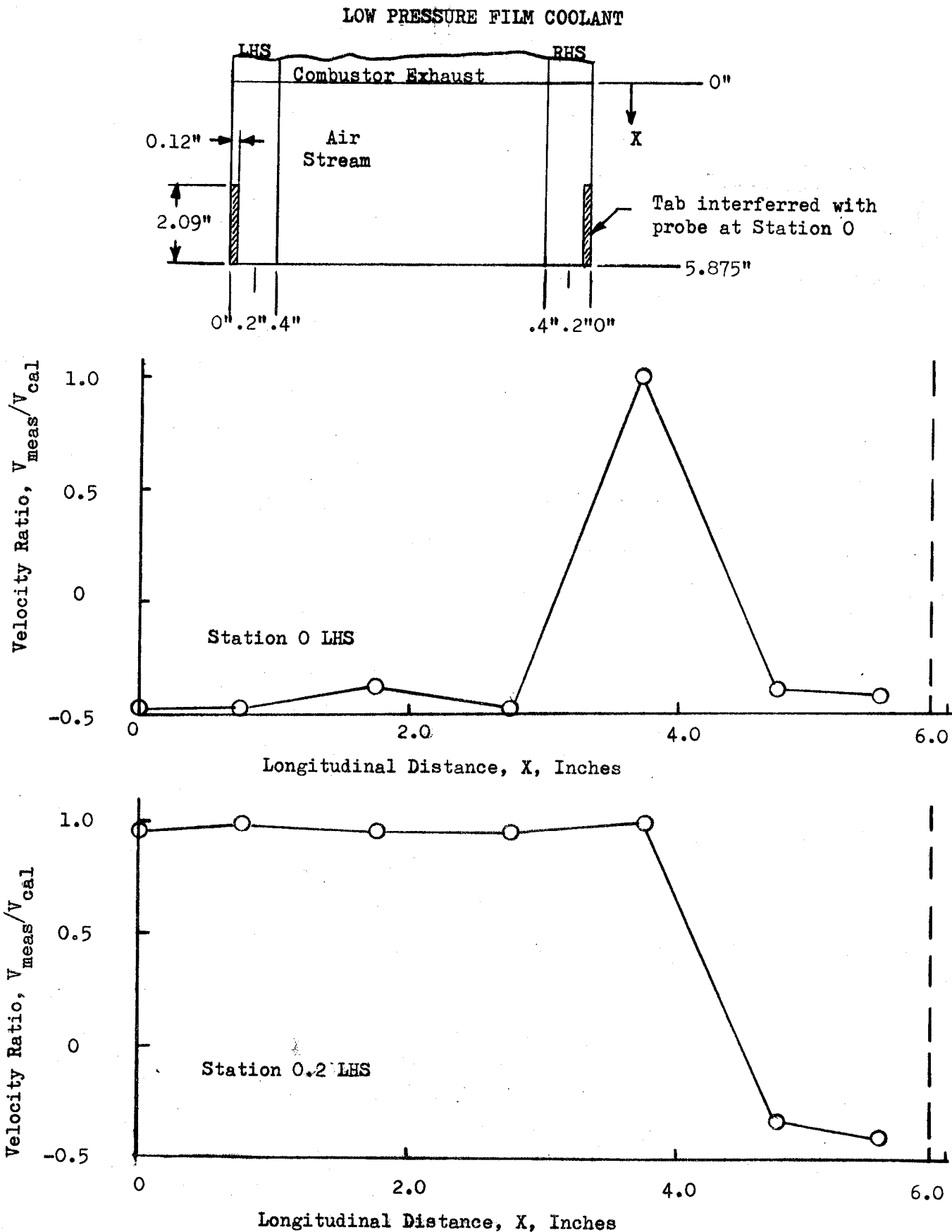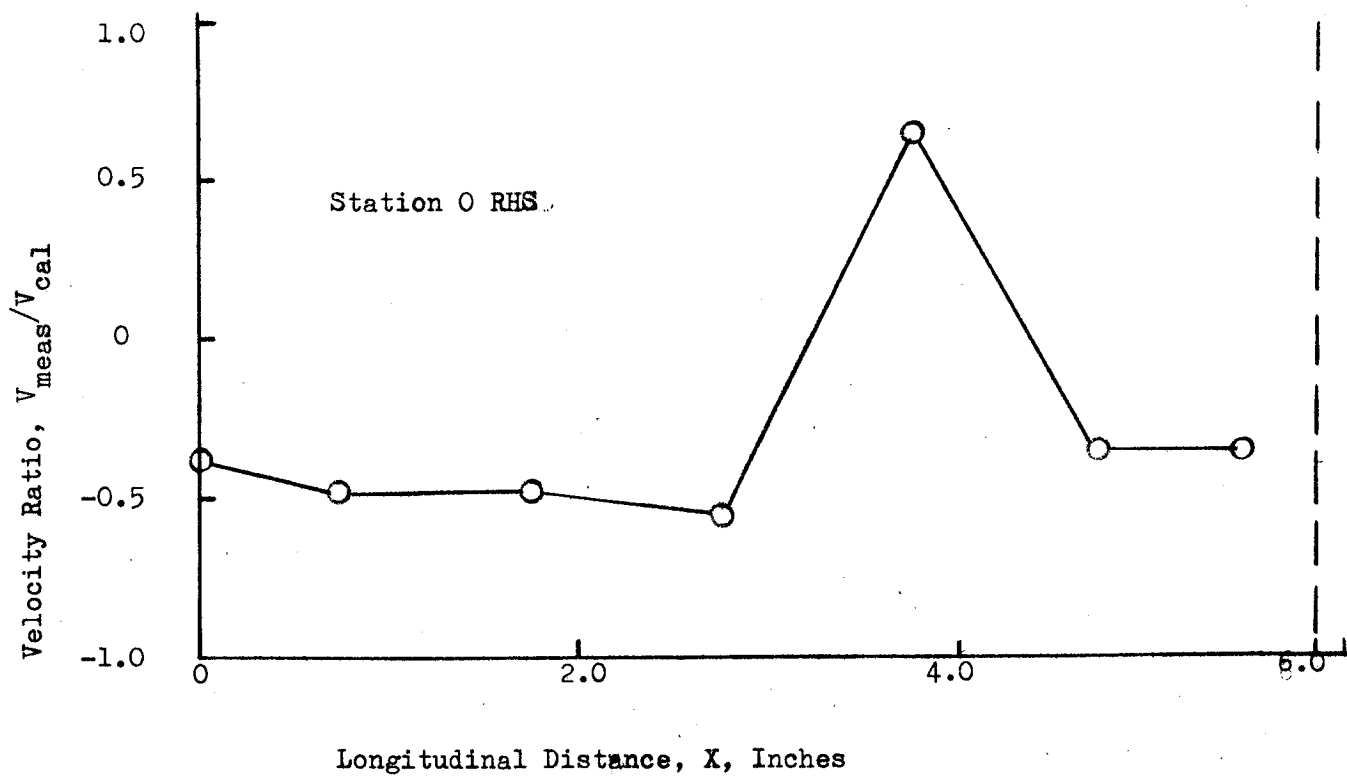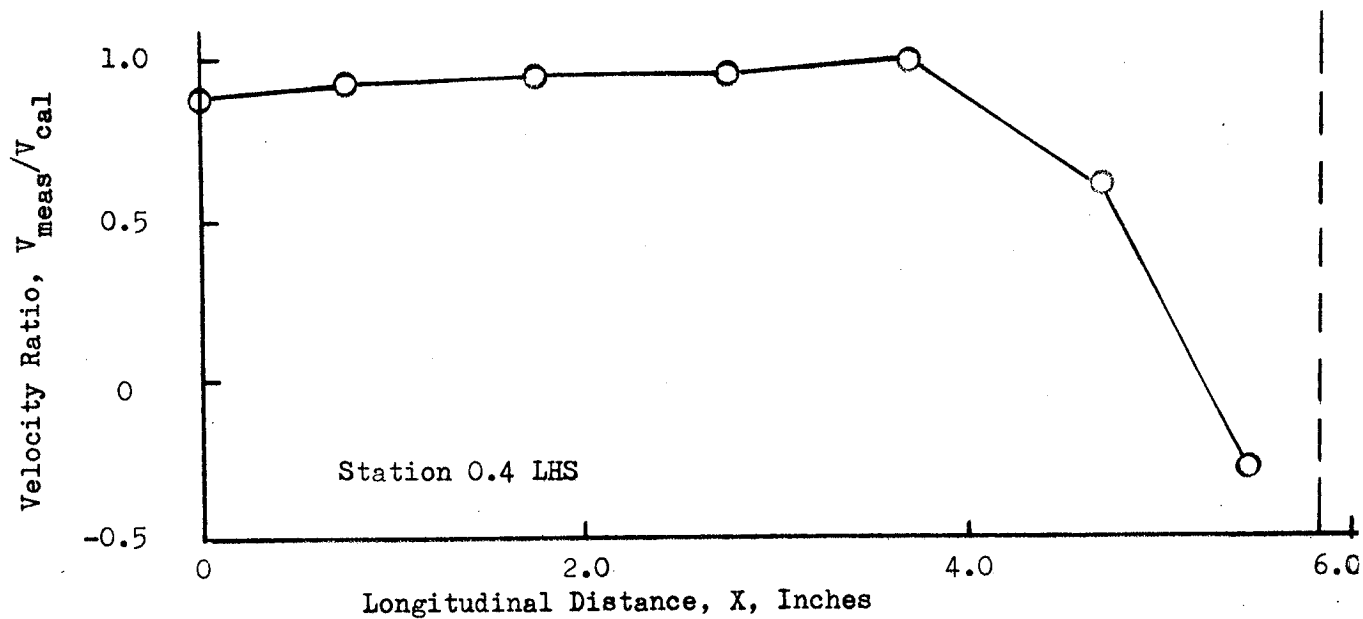
Figure 8 (Cont). Film Coolant Velocity Profiles
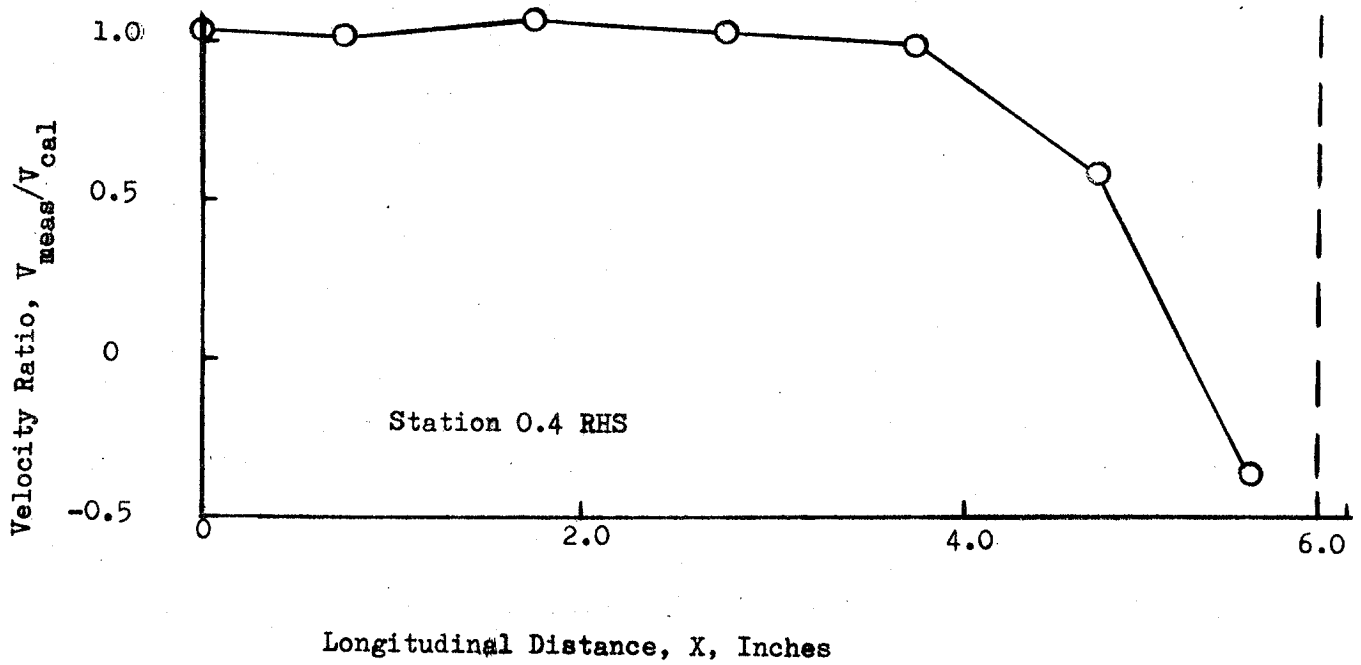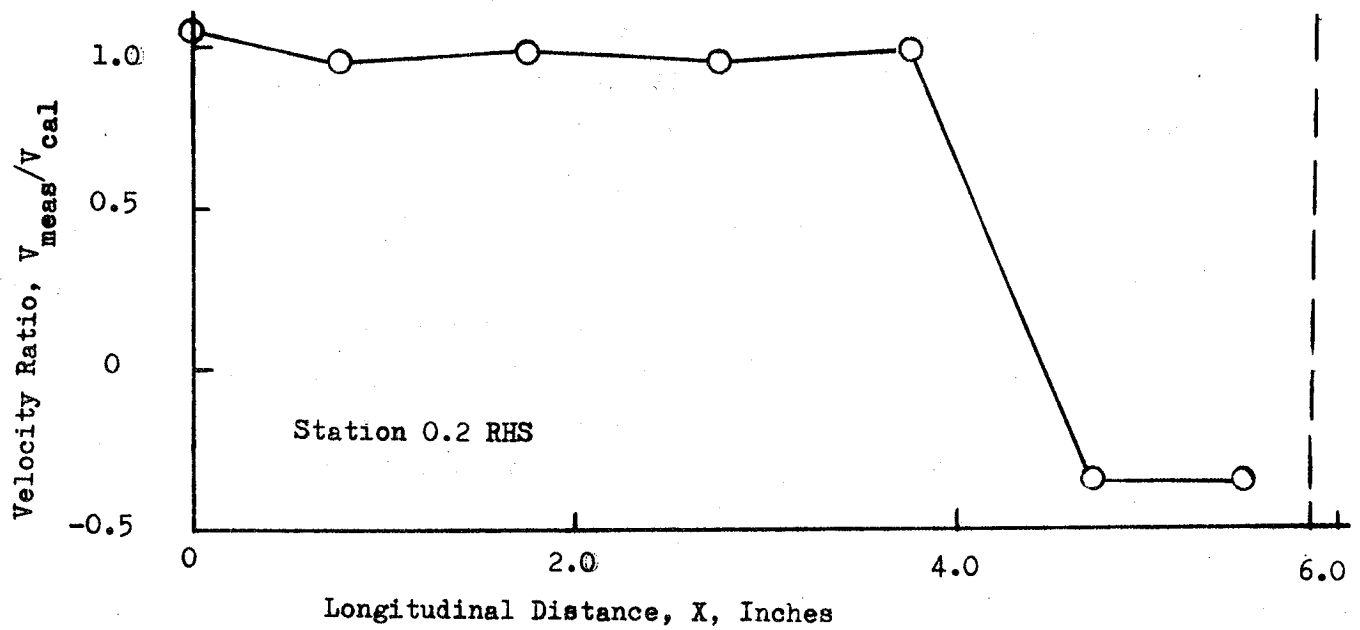
Figure 8 (Cont). Film Coolant Velocity Profiles

configuration. This decrease in length occurs in the combustor length. The new combustor was assembled entirely from existing additional upper combustion chambers found in the storage yard. However, there were not sufficient existing chambers to return the new combustor to its original size. While this caused no problem with c^* efficiency (tests revealed it to be greater than 95 percent), it did require all film coolant and certain water flow connections to be shortened three inches.

In addition, analysis of past data obtained during firings of the original combustor and the 2-D nozzle revealed a potential thermal distortion problem at the edge of the thin lip separating the combustor gases from the air stream. This problem was alleviated by changing the water distribution to allow more coolant flow from the high pressure water tank to pass through the nozzle section and by making additional allowances for thermal expansion at the intersection of the nozzle lip with the side wall.

The modifications to the water coolant system required that the water distribution tests be rerun. These tests were conducted and no maldistribution of coolant water was noted. The changes in the plumbing of the water supply permit operation at a safety factor of 3 which is an increase of 0.8 over that obtainable with the previous setup. The water coolant safety factor is defined as the actual water flowrate divided by the theoretical water flowrate required for marginal cooling.

Because of the changes in the water coolant plumbing, long duration firings (greater than 15 seconds) required total coolant water in excess of that available. Installation of a higher capacity water tank was subsequently completed under a Rocketdyne capital job order. The new tank increased the high pressure water supply from 150 to 600 gallons.

Full scale testing commenced on 16 January after a delay of approximately one week because of alignment problems with the zone radiometer and the demonstration of a need for an effective system to eliminate frost on the test section windows. Frost was eliminated by ducting the cold GN_2 exhaust well aft of the test section during the chilldown. The duct was removed just prior to an engine firing. Three successful firings were conducted with durations of 1, 2, and 5 seconds, respectively. Close examination of the hardware revealed a slight amount (.020 x .050 x 3.0) of erosion of the nozzle tip during the 5-second firing. The cause of the erosion was traced to a gross underestimate (by a factor of four) of the heat flux at the tip which was originally calculated based upon the Bartz equation. A revised calculation of the temperature encountered at the tip, utilizing the actual test data, indicated that the minimum distance from the tip to the first coolant passage must be on the order of 0.85 inches. Therefore, the nozzle tip was cut back 0.150 inches. This increased the tip thickness by 0.006 inches. Subsequent firings confirmed this analysis.

An additional difficulty was encountered during the aforementioned tests. The gaseous nitrogen bottle bank which feeds the laboratory bottle bank was reduced in pressure while the laboratory was on the red light. This resulted in a shift in the water tank and hydrogen regulators during the run causing a slightly decreasing water flow rate and a much reduced hydrogen flow rate, i.e., operation at mixture ratio of 10 rather than 5. This condition contributed to the erosion of the nozzle tip. Corrective action, consisting of closing the main gaseous nitrogen bottle bank fill valve prior to testing, was taken to eliminate the possibility of a similar occurrence in the future.

No zone radiometer data were obtained during these instrumentation checkout firings because the mirrors shifted at the beginning of the run. The apparent cause was transmission of engine vibrations through the tunnel which is connected to the engine. Corrective action consisted of placing additional attachment screws on the mirror mounts, placing

cushions under all mirrors, and attaching the tunnel to the engine via
a black cloth rather than a direct connection.

The photographic coverage revealed that the UV and IR emission was lower
than anticipated. Consequently, these films were all underexposed and
only yielded information during ignition. The operating speeds of the
cameras were reduced to increase the exposure for subsequent firings.
The color photography yielded a good representation of the visible
emission occurring in the mixing chamber. The growth of the mixing
region into the subsonic stream was clearly depicted, Fig. 9. The
specie causing the emission at present is unidentified. Observations
with the LASS will enable the determination of its identity.

No testing during the weeks of 1/24 and 1/31 was possible due to adverse
weather conditions. Following nine straight days of rain, the tempera-
ture dropped to below 32 F at the test site which caused the water supply
lines to ice up and also conditioned the various utilities to render a
number of control valves inoperable. During this period, a small com-
bustor body water leak was noted dribbling into the air stream. The
flowrate at operating conditions was determined to be 3 ml/sec which
was considered insignificant.

Full-scale testing resumed 4 February 1969. Again, off-design mixture
ratio operation occurred and it was analytically determined to be caused
by too large a GN_2 demand during testing. The only change in testing
procedure between this test and those where this problem did not occur
was a doubling of the H_2O tank pressures. As previously prescribed for
other tests, decay in supply pressure was not the cause since normal
pressures of 2200 psi and 2800 psi were recorded for the laboratory
GN_2 bottle bank and the main supply bottle bank, respectively. In
addition, a more serious problem was evident after post-test inspection
of the hardware. The 2-D nozzle side wall was warped. This problem
is discussed in Appendix 1.
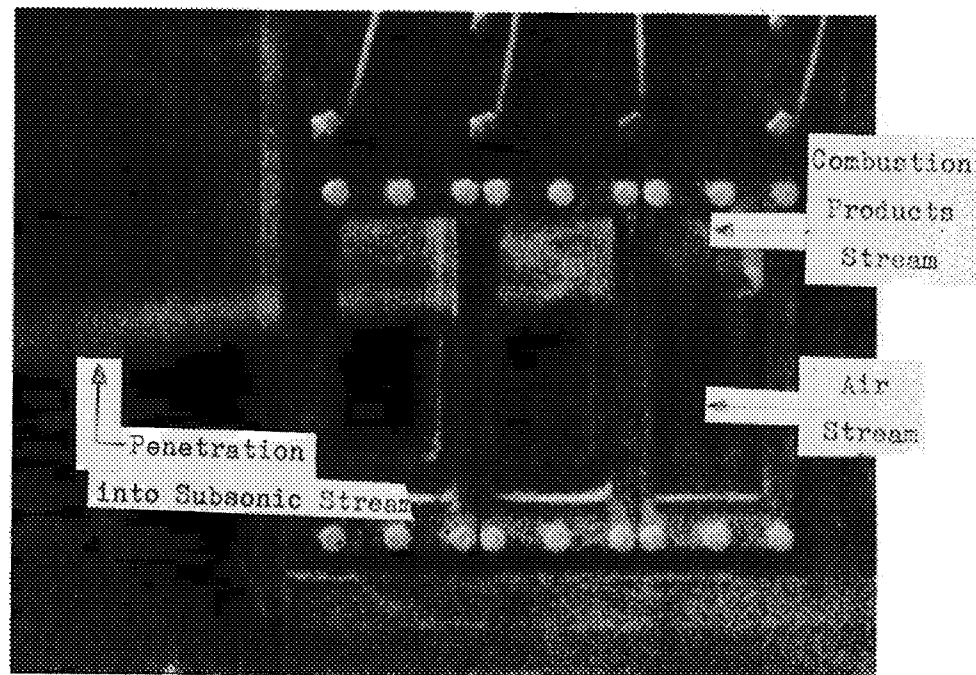
Figure 9.   Mixing Region with Cold Air

A summary of hot fire tests and a summary of principal test parameters
are given in Tables 1 and 2, respectively. A guide to instrumentation
location is shown in Fig. 10.

ANALYSIS

This task was primarily a supporting item for the analytical effort
required under Facility Checkout, Instrumentation Installation, Probe
Instrumentation, and Testing. Whenever the analytical effort was
inextricably linked to the previous items discussed, the results were
presented at that time; however, only those items unique to the
analysis task will be presented in the following paragraphs.

A hot fire data reduction computer program was written to minimize
the time required to reduce the 36 test parameters. Calculations
required to reduce the raw data into a workable form were assembled
and a computational sequence was formulated. The program performs
all the necessary calculations to establish the operating conditions
of the various utilities and the initial conditions of the combustion
gas, air stream, and film coolant as they enter the mixing chamber.
It was utilized in supplying the data for Table 2. A detailed
description of the program is given in Appendix 5.

A cursory review of the photographic data from Run 0101 revealed the follow-
ing information. The UV photograph indicated two distinct boundaries
of ultraviolet emission. It was then postulated that these boundaries
were an indication of a diffuse reaction region with the outer boundary
corresponding to the momentum boundary layer and the inner boundary
representing the termination of the diffusion layer and the start of
a region of intense chemical reaction. (Normally, a photographic
record would be inserted here to illustrate the observation, however,
due to the grainy nature of photographs and the low level of contrast,
adequate reproduction of these photographs is virtually impossible.)
Verification of the preceding interpretation hinges on the correlation

TABLE 1

TESTING SUMMARY

Test No.	Type	Test Duration (Seconds)	Instrumentation & Location	Remarks
0010	Integrated Check-Out	———	Overall, Injector, and Manometer Bank Cameras	Hypergol Function Check
0020	Integrated Check-Out	0.230	Overall, Injector, and Manometer Bank Cameras	Ignition Sequence Check
0030	Integrated Check-Out	0.400	Overall, Injector, and Manometer Bank Cameras	Normal Operation
0040	Integrated Check-Out	2.400	Overall, Injector, and Manometer Bank Cameras	Upper Combustion Chamber Erosion
0050	Combustor Check-Out	1.290	Overall & Injector Cameras	Normal Operation No Film Coolants or Air
0060	Combustor Check-Out	2.355	Overall & Injector Cameras	Normal Operation No Film Coolants or Air
0070	Combustor Check-Out	4.970	Overall & Injector Cameras	Normal Operation No Film Coolants or Air
0080	Instrumentation Check-Out	1.295	Overall, Injector, and Manometer Bank Cameras. Color, False Color, IR & UV Close Up All Three Windows. Zone Radiometer-Window #3 Position 8.	Off Design Mixture Ratio

TABLE 1 (CONT)

TESTING SUMMARY

Test No.	Type	Test Duration (Seconds)	Instrumentation & Location	Remarks
0090	Instrumentation Check-Out	2.095	Overall, Injector, and Manometer Bank Cameras. Color, False Color, IR & UV Close Up All Three Windows. Zone Radiometer-Window #3 Position 8.	Off Design Mixture Ratio
0100	Instrumentation Check-Out	5.265	Overall, Injector, and Manometer Bank Cameras. Color, False Color, IR & UV Close Up All Three Windows. Zone Radiometer-Window #3 Position 8.	Off Design Mixture Ratio – Nozzle Tip Erosion
0101	Instrumentation Check-Out	4.245	Overall, Injector, and Manometer Bank Cameras. Color, False Color, IR & UV Close Up All Three Windows. Zone Radiometer-Window #3 Position 8. Schlieren – Window #1.	Off Design Mixture Ratio – Repeat of Test 0100

34

TABLE 2

TEST PARAMETERS*

Test No.	Date	P_{atm} psia	T_{atm} F	Relative Humidity %	Air System					
					Flowrate lb/sec	T_{mc} F	P_{mc} psig	ρ_{mc} lb/ft^3	V_{mc} ft/sec	Mach No.
0010	7-18-68	13.8	88	25	2.86	82	0.28	0.0703	284.2	0.249
0020	7-18-68	13.8	88	25	3.15	81	0.31	0.0707	311.7	0.273
0030	7-18-68	13.8	88	25	3.30	81	0.34	0.0709	324.7	0.285
0040	7-18-68	13.8	88	25	4.33	77	0.63	0.0728	415.7	0.366
0050	8-28-68	13.75	94	18	—	—	—	—	—	—
0060	8-28-68	13.75	94	18	—	—	—	—	—	—
0070	8-28-68	13.75	94	18	—	—	—	—	—	—
0080	1-16-69	13.9	70	88	3.45	64	0.50	0.0739	326.6	0.291
0090	1-16-69	13.9	72	88	3.44	66	0.45	0.0736	327.7	0.291
0100	1-16-69	13.9	72	88	3.50	65	0.25	0.0737	331.9	0.296
0101	2-4-69	13.82	74	38	3.42	68	0.36	0.0729	327.7	0.291

*All parameters evaluated at mid duration.

TABLE 2 (CONT)

| Test No. | Low Pressure Film Coolant | | | | | | $\overset{\bullet}{w}_{LOX}$ lb/sec | $\overset{\bullet}{w}_{GH_2}$ ft/sec | P_c psig |
	Flowrate lb/sec	T_{mc} F	P_{mc} psig	ρ mc, lb/ft	V_{mc} ft/sec	Mach No.			
0010	0.86	41	−0.26	0.0718	411.1	0.368	3.63	——	——
0020	0.79	46	−0.25	0.0712	379.8	0.338	3.28	1.07	353.8
0030	0.73	54	−0.25	0.7010	359.2	0.318	5.79	1.06	394.0
0040	0.83	52	−0.26	0.0704	404.8	0.359	5.88	1.06	456.0
0050	——	—	——	——	——	——	5.11	1.10	372.0
0060	——	—	——	——	——	——	5.24	1.12	372.0
0070	——	—	——	——	——	——	5.51	1.09	369.0
0080	1.17	−8	−0.18	0.0802	501.8	0.473	6.54	0.65	316.0
0090	1.17	−9	−0.18	0.0804	501.2	0.473	6.63	0.62	324.0
0100	1.22	−3	−0.18	0.0794	528.5	0.496	6.58	0.62	321.0
0101	1.25	−2	−0.31	0.0780	551.0	0.513	6.63	0.66	334.2

TABLE 2 (CONT)

	Low Pressure Film Coolant								
Test No.	Flowrate lb/sec.	T_{mc} F	P_{mc} psig	P_{mc} lb/ft^3	V_{mc} ft/sec	Mach No.	Mixture Ratio	$\dot{w}_{TOT}$	η_{c*}
0010	4.21	−52	0.80	0.0882	1008.3	1.0	——	3.63	——
0020	4.18	−50	0.70	0.0879	1010.4	1.0	3.06	4.35	131.1[+]
0030	4.08	−43	0.49	0.0864	1018.6	1.0	5.48	6.84	99.7
0040	4.04	−42	0.38	0.0861	1020.6	1.0	5.55	6.94	113.3[△]
0050	——	——	——	——	——	——	4.64	6.21	100.9
0060	——	——	——	——	——	——	4.70	6.36	98.8
0070	——	——	——	——	——	——	5.06	6.60	95.6
0080	4.26	−80	0.40	0.0955	972.7	1.0	10.12	7.19	89.5
0090	4.31	−81	0.50	0.0957	971.6	1.0	10.71	7.25	93.0
0100	4.21	−74	0.20	0.0940	980.1	1.0	10.56	7.21	91.9
0101	4.33	−69	0.85	0.0923	986.5	1.0	10.06	7.29	94.2

[+] Duration too short for acurate flowrate measurement

[△] Includes effects of copper and water vaporization
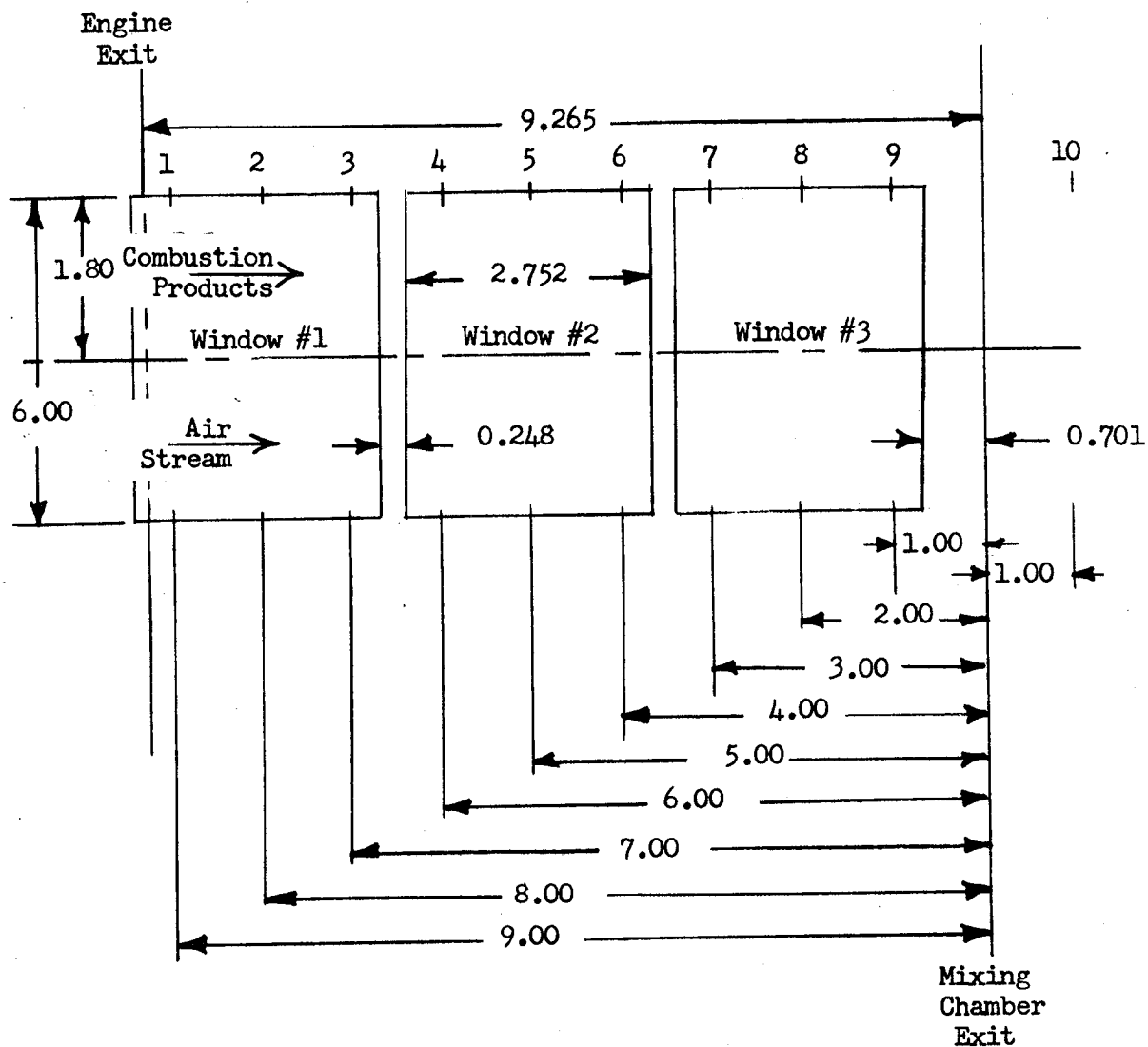
Position	Distance from Start of Mixing Region
1	0.265
2	1.265
3	2.265
4	3.265
5	4.265
6	5.265
7	6.265
8	7.265
9	8.265
10	10.265

All dimensions in inches

Figure 10.   Instrumentation Location Positions

of the observations with the color photographs of the mixing region, Fig. 9, and the schlieren data for window No. 1, Fig. 11.

The edge of the mixing region indicated on the schlieren is at an angle of 12.5 degrees which roughly corresponds with the 14 degree angle of the outer boundary on the UV photograph. However, of more significance is the correspondence in both space and angle of the inner boundary and the radiation displayed on the color photograph. The location was identical and the angles were 5.5 and 6.0 degrees, respectively. The above clearly indicates that an appreciable air-exhaust products reaction layer exists even when cold air is utilized. Final proof of these observations must await more accurate spectroscopic data. Figure 12 is a schematic depicting the location of the boundaries, the edge of the mixing region, and the visible emission with respect to a computer prediction (furnished by the contract monitor) of the temperature profiles for mixing between ambient air and a GH_2-LOX combustor exhaust.
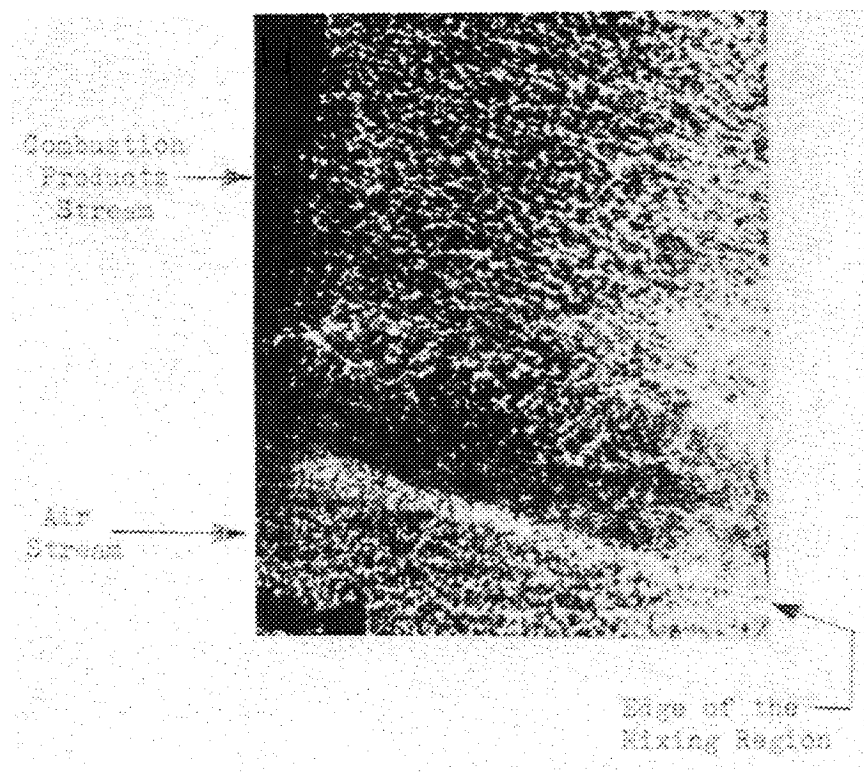
Figure 11. Schlieren through Window No. 1

40
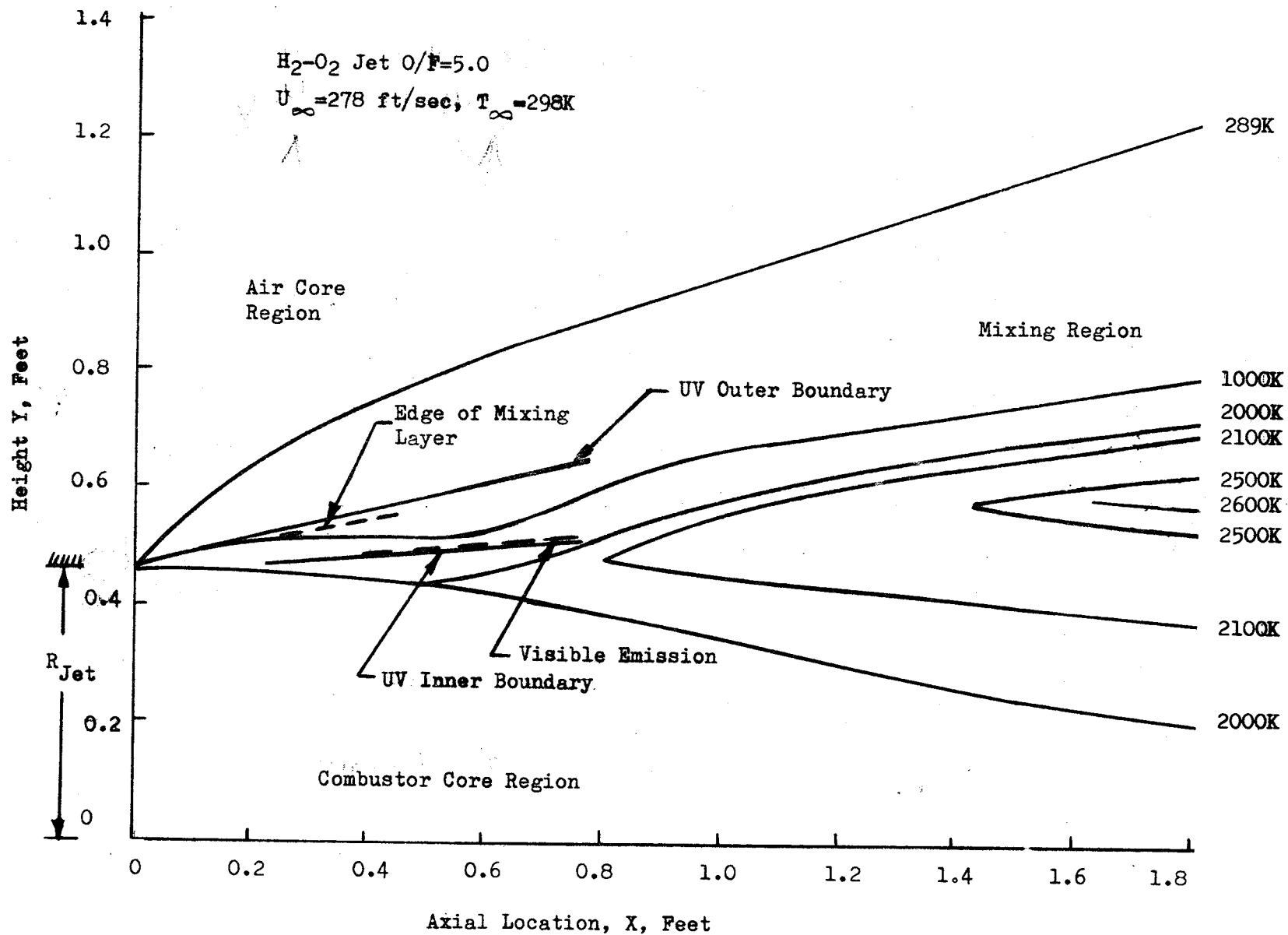
Figure 12. Schematic of Mixing Region

41/42

RECOMMENDATIONS

A carefully designed flow facility, appropriate test hardware, and optical instrumentation systems have been assembled for the study of two-dimensional mixing of supersonic hydrogen-oxygen combustion products with a subsonic heated air stream.

It is recommended that the apparatus be utilized in a comprehensive experimental program. This program would provide well controlled precise experimental data for the determination of the effects of temperature ratio, turbulence level, velocity ratio, and changes in ambient conditions upon the mixing. The characterization of the mixing region should include a mapping of temperature, velocity, pressure, concentration, and enthalpy. Recommended experiments that will help to gather the required data are as follows:

1. Diagnostic experiments to determine the two dimensionality of the flow field and the effect of film cooling on the mixing region.

2. A mixing study that includes a precise mapping of the mixing region for the basic case, then a determination of the effects upon the mixing layer produced by changes in the air turbulence level, air temperature, inlet geometry, and velocity ratio.

3. Tests with a CO_2 seeded air stream. The use of this tracer enables further elucidation of the penetration of the air stream into the combustion products stream.

4. Testing, which would require additional hardware, over a more complete range of experimental variables. These would include different mixture ratios, a wide range of combustion product-air stream velocity ratios, and elevated test section pressures.

5. Mixing studies utilizing different propellant combinations at similar conditions tested with the LOX-GH_2 combustor.

REFERENCES

1. Wrubel, J. A.: <u>Performance Analysis of Composite Propulsion Systems</u>, Phase I Final Report, Contract NAS7-521, Rocketdyne, a Division of North American Rockwell Corporation, Canoga Park, California, January 1968.

2. Incropera, F. P., and G. Leppert: "Investigation of Arc Jet Temperature Measurement Techniques," Stanford University, <u>ISA Transactions</u>, Vol. 6, No. 1, January 1967.

3. Vassallo, F. A.: "A Fast Acting Minature Enthalphy Probe," Cornell Aeronautical Lab," AIAA 3rd Aerodynamic Testing Conference, Preprint No. 68-391, April 1968.

4. Kilburg, R. F.: "A High Response Probe for Measurement of Total Temperature and Total Pressure Through a Turbulent Boundary Layer with High Heat Transfer in Supersonic Flow," General Dynamics, AIAA 3rd Aerodynamic Testing Conference, Preprint No. 68-374, April 1968.

5. McCroskey, W. J.: "Density and Velocity Measurements in High Speed Flows," NASA Ames Research Center, AIAA 3rd Aerodynamic Testing Conference, Preprint No. 68-392, April 1968.

6. Anderson, L. A., and R. E. Sheldahl: "Flow-Swallowing Enthalphy Probes in Low Density Plasma Flows," NASA Ames Research Center, AIAA 3rd Aerodynamic Testing Conference, Preprint No. 68-390, April 1968.

7. Buckingham, D. J.: <u>An Optical Method of Measuring Flow Velocity in Arc-Heated Wind Tunnels</u>, Aeronautical Research Council, Great Britain, ARCR & N No. 3439, March 1965.

8. Kenworthy, M. J.: "New Techniques for Supersonic Combustion Measurements," General Electric Company, AIAA Paper 67-223, January 1967.

9. Goodier, B. G.: "Cooled High Temperature Thermocouples for Phoebus Reactors," Los Alamos Scientific Laboratory of the University of California, AIAA 2nd Propulsion Joint Specialists Conference, AIAA Paper 66-556, June 1966.

10. Muntz, E. P., Harris, C. J., and E. M. Kaegi: Techniques for Experimental Investigation of the Properties of Electrically Conducting Hypersonic Flow Fields, General Electric Company, R63SD27, March 1963.

11. Rocketdyne: An Instrumentation System to Study Rocket Exhaust Plume Radiative Processes, R-6288, August 1965.

12. Kenworthy, M. J., Stanforth, C. M., and W. C. Colley: Investigation of Instrumentation and Simulation Techniques for the Supersonic Combustion Process, General Electric Company, AFAPL-TR-66-76, October, 1966.

13. Gordon, S. A.: The Use of Ionization Probes to Determine Rocket Motor Parameters, Aerochem Research Labs, TP-120, September 1965.

14. Nye, J. O. and R. S. Brodkey: "Light Probe for Measurements of Turbulent Concentration Fluctuations," Ohio State University, Review of Scientific Instruments, 38, 26-29, January 1967.

15. Frohm, A.: "Measurement of Concentration Profiles in Jets Using Fizeau Fringes," Cornell University, AIAA Journal, Vol. 5, No. 1, January 1967.

16. Judge, J. F.: "Greyrad Building a Market in Heat Transfer Measurement," Aerospace Technology, January 1968.

17. Ahlborny, A. and A. J. Barnard: "Velocity Measurement by Doppler Effect," University of British Columbia, AIAA Journal, Vol. 4, No. 6, June 1966.

18. Grey, J.: "Cooled Probe Diagnostics of Dense Plasma Mixing and Heat Transfer Processes," Greyrad Corporation, AIChE Journal, Preprint No. 9C, November 1967.

19. Grey, J.: "Thermodynamic Methods of High Temperature Measurements," Princeton University, ISA Transactions, Vol. 4, No. 2, April 1965.

20. Grey, J., Jacobs, P. F., and M. P. Sherman: "Calorimetric Probe for the Measurement of Extremely High Temperature," Princeton University, *Review of Scientific Instruments*, Vol. 33, No. 7, July 1962.

21. Grey, J. and P. F. Jacobs: "Cooled Electrostatic Probe," Princeton University, *AIAA Journal*, Vol. 5, No. 1, January 1967.

APPENDIX 1

MAJOR PROGRAM DIFFICULTIES

A wide variety of difficulties were encountered on this program. Presented below is a detailed discussion, in cronological order, of major problems and their solutions.

The initial proof test of the water coolant feed lines for the combustor exhaust nozzle/test section assembly indicated seepage past one of the O-ring seals between the nozzle and the test section side wall. After repeated attempts to effect a positive seal, the problem was traced to a mismatch between one of the O-ring/water manifolds and warpage of the test section side wall.

The mismatch was repaired by placing a spacer in the water manifold to assure a positive O-ring seal, planing the side wall in the area of the water manifolds to reduce the warpage, and custom fitting the hardware during assembly. The side wall warpage occurred when the film coolant ducting was welded in place. After completion of the repairs and assembly of the apparatus, a successful proof test was accomplished at twice the operating pressure of the coolant water. The apparatus was then re-installed on the stand; however, due to the leakage problems a three-week-time delay was incurred.

Prior to the first full-scale integrated checkout of the entire system, anomalous behavior (bed temperature greater than the preset value) of the air heater was noted. The countdown was stopped prior to final propellant loading operations and heater electrical power was turned off. An attempt was made to reduce the bed temperature before continuing with the test preparations by actuating the system and blowing air through the bed. After approximately 5 seconds, sparks were observed in the hot air stream and the blower was immediately shut off. At this time the heater burst into flame and before the fire was brought under control

the heater was destroyed (Fig. Al-1). The cause of the incident was traced to the inadvertent use of zirconium tubing rather than what was believed to be stainless steel tubing in the heater bed. Zirconium is highly reactive with air at approximately 1000F, the operating temperature of the air heater. Replacement of the air heater under a Rocketdyne capital job was completed toward the end of this program.

During full scale system check-outs significant erosion of the upper combustion chamber was experienced (Fig. Al-2 and Al-3) during a 2-second mainstage test. The cause of the erosion was attributed to the formation of ice in the coolant passages during the injector chilldown. Post-test inspection indicated an appreciable quantity of water vapor (from aspiration of the trapped coolant water downstream of the main valves) in the gaseous nitrogen water coolant purge.

Modifications to the coolant water sub-system to prevent freezing in the coolant water passages during injector chill-down were made. An 80 psi water flush was plumbed downstream of the water mains to establish water flow through the coolant passages during the chill-down operation. The signal that opens the water mains also closes the water flush mains, providing a rapid flow transition without permitting stagnation.

The most serious problem was noted after post-test inspection of the hardware for the 4 February test. The 2-D nozzle side wall was warped. This relieved the compression on the O-rings causing an excessive water leak during post-test checkouts. It did not appear that any water leakage occurred during the test. The test apparatus was disassembled to facilitate hardware modifications pending a determination of the cause of the warpage. The thermal and stress analysis indicated that the warpage was caused by pressure loading in the divergent section and thermal stress in the convergent section of the two-dimensional nozzle.

50
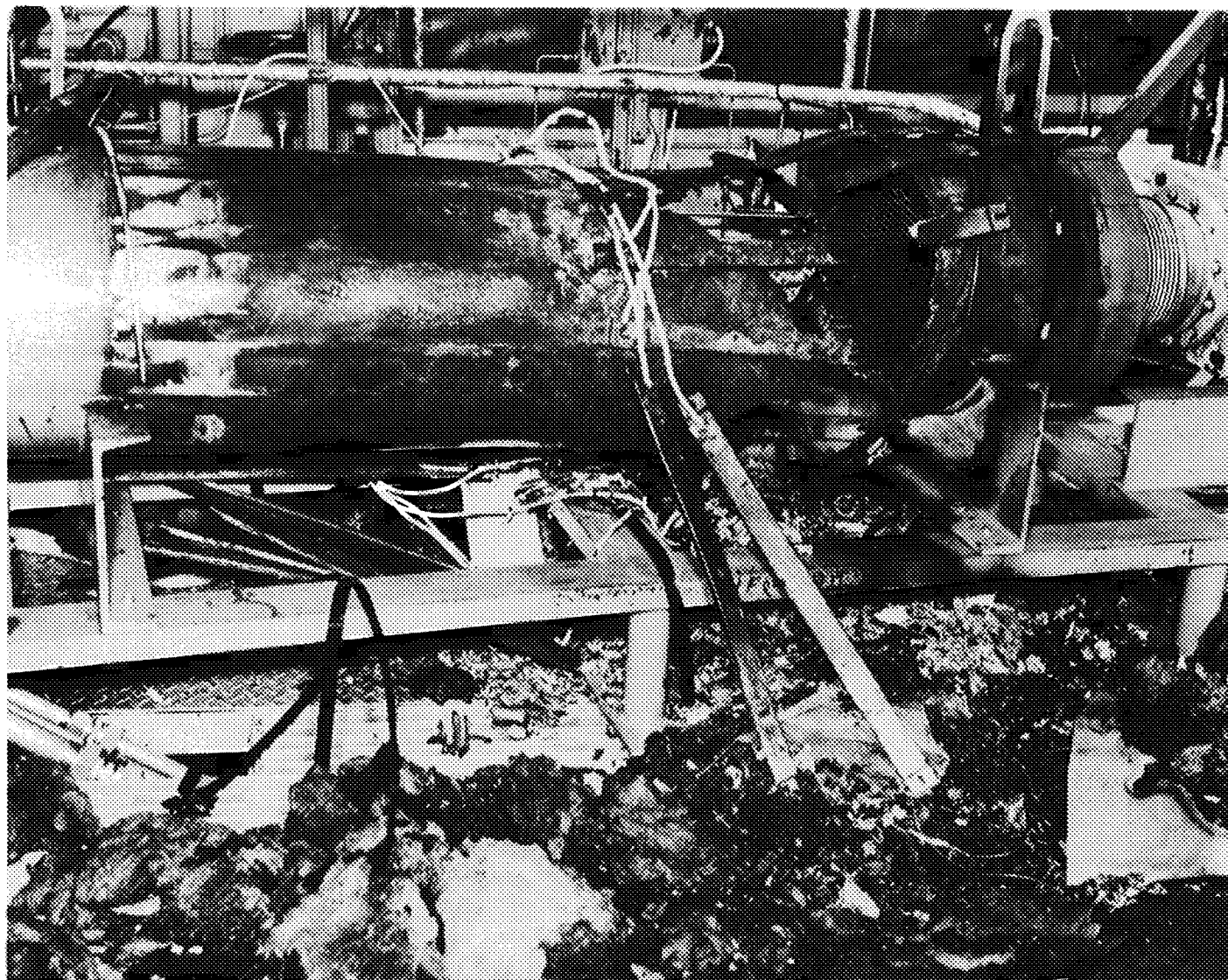
Figure Al-1. Air Heater After Incident

Figure A1-2. Eroded Upper Combustion Chamber — Right Hand Side

52
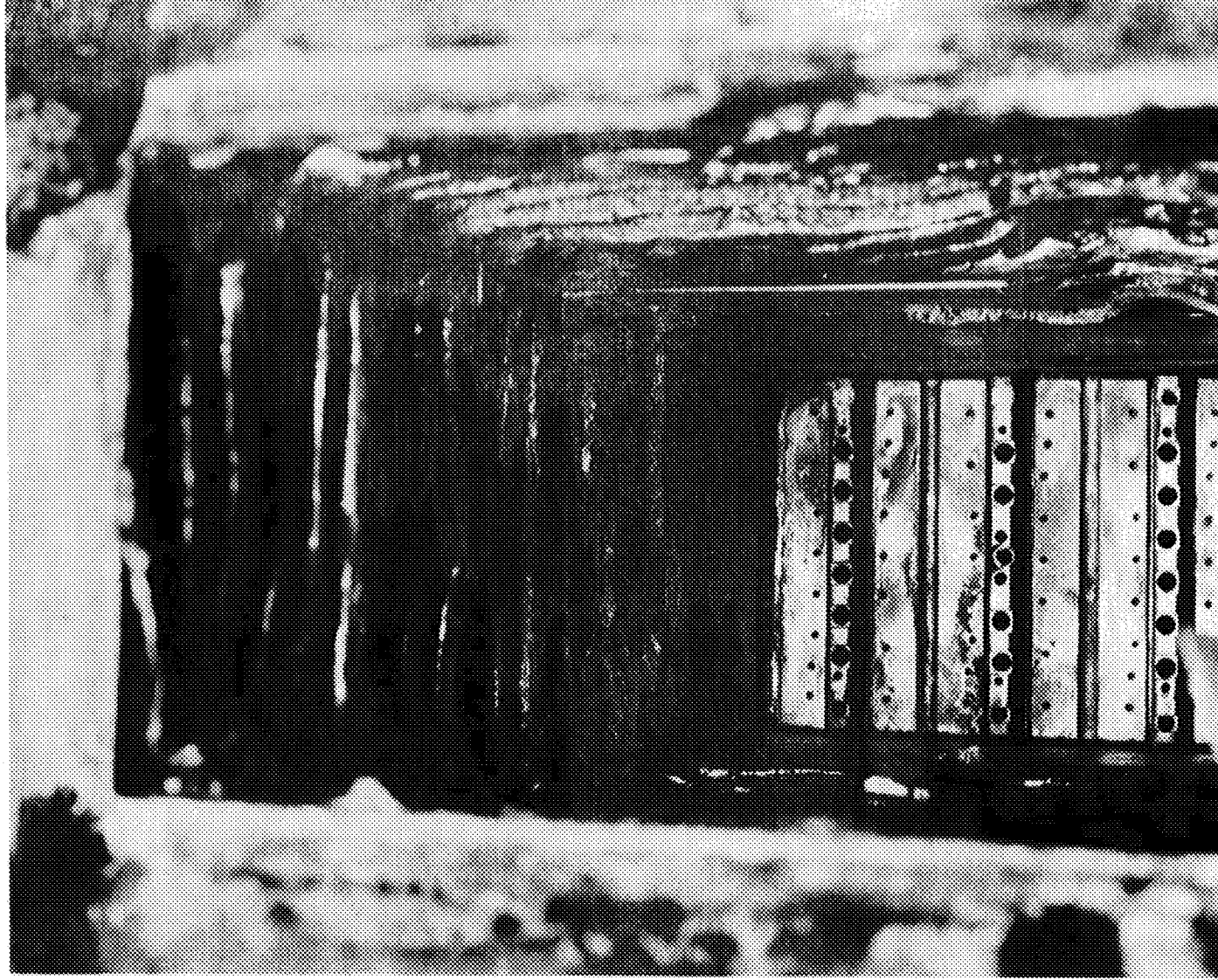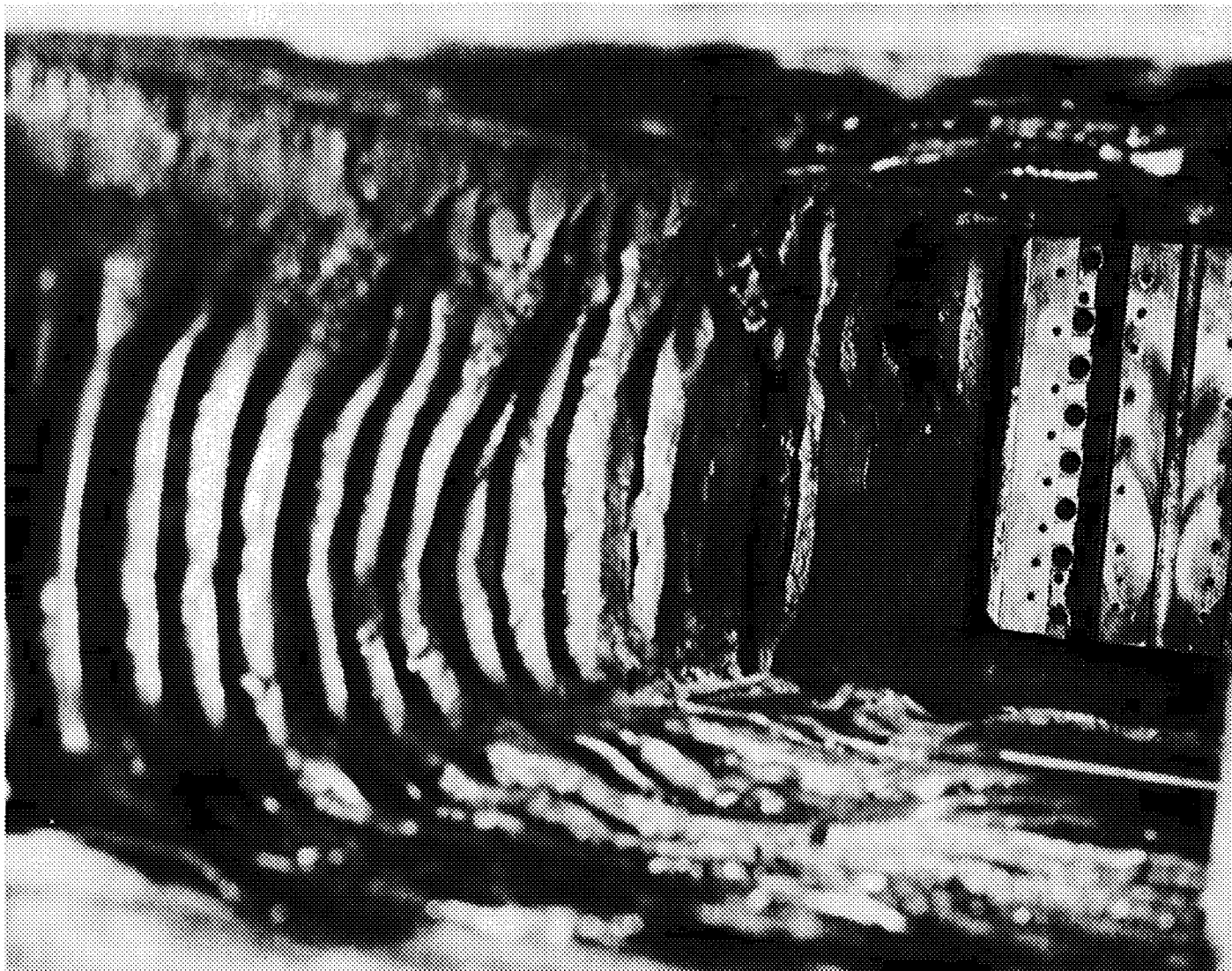
Figure Al-3.   Eroded Upper Combustion Chamber - Left Hand Side

Redesign of the hardware has been completed; however, fabrication
has been deferred to the anticipated follow-on contract. The
modifications consist of reducing the water manifold pressure and
welding the water inlet and outlet directly to the nozzle. This
eliminates the water leak problem and allows testing to continue even
if additional warpage occurs. The present condition of the internal
contour of the nozzles is such that it could be fired without
significantly altering the 2-D flow field if the water leak did not
exist.

APPENDIX 2

ZONE RADIOMETRY

INTRODUCTION

The primary aim of the spectroscopic instrumentation is to experimentally measure temperature and concentration distributions across the mixing region. In particular, the zone radiometer system, developed to study rocket exhaust radiative processes under Contract NAS8-11261 (Ref. A2-1), will be used to determine the temperature and partial pressure profiles for the H_2O molecule from measurements of the spectral emissivity and spectral radiance for various lines of sight. In this Appendix a description is given of the experimental arrangement for zone radiometry measurements, the type of measurements to be carried out, and the data reduction procedures.

EXPERIMENTAL ARRANGEMENT

The zone radiometer spectroscopy system is shown schematically in Fig. 4 of the main text. The greybody source and spectroradiometer were described in complete detail in Ref. A2-1, and will therefore be discussed only briefly here.

The greybody source consists of a 6-inch long, 3/8-inch diamter, electrically heated graphite rod that is mounted in a water-cooled, argon-purged housing. Greybody radiation is optically chopped with a cylindrical "squirrel-cage" chopper to produce an AC signal for absorption measurements. The housing is equipped with a shutter.

Flat mirror M_1 and an 8-inch diameter spherical mirror M_2 form a 1:1 image of the greybody source across a vertical plane perpendicular to the flow axis in the mixing region. The greybody housing is actually mounted above the horizontal optical plane of the system so that it does not obscure a view of the mixing region from other instrumentation. The greybody source optics and flat mirror M_3 may be moved parallel to the flow axis to change the horizontal field of view of the system.

Flat mirrors M_4 and M_5 relay radiation from that part of the mixing region under study to the spectroradiometer.

An optical diagram of the spectroradiometer is shown in Fig. A2-1. Figure A2-2 is a photo of the instrument. The optical path, which is enclosed and purged with dry nitrogen, is of such a length that a 10:1 reduced image of a portion of the mixing region is formed at the mono-chromator entrance slit by the telescope objective mirror. The field of view of the spectroradiometer at the mixing region is rectangular in cross section (on the order of 3 x 3 millimeters) and perpendicular to the flow axis. The width of this field of view is 10 times the width of the entrance slit. The height of the field of view is determined by an adjustable aperture at the entrance slit. During a test this cam driven aperture will scan different zones (zone radiometry) of the mixing region in the vertical direction. The cross sectional size of the field of view is determined from a trade-off between desired spectral and spatial resolution and available energy.

For emission measurements, the greybody shutter is closed and radiation from the mixing region is optically chopped at the monochromator exit slit. (This chopper is not used during absorption measurements).

The Perkin-Elmer Model 98-G monochromator is equipped with a 240-groves-per-millimeter grating blazed at 3.75 microns and used in first order. Overlapping orders are eliminated by a germanium filter. For the subject program, an uncooled PbS detector is used. The AC output from the detector is amplified, synchronously rectified, and displayed on a strip chart recorder.

An additional flat mirror relay system has been assembled so that the spectroradiometer can view the mixing region outside the combustor from above, rather than horizontally. This system will be used to assist in checking the two-dimensionality of the flow field.

POSITION OF CALIBRATION
MIRROR DURING FIRING

LENS

BLACKBODY

FIDUCIAL
AND
BORESIGHTING
CAMERA

TELESCOPE
OBJECTIVE
MIRROR

TRACKING
MIRROR

CALIBRATION MIRROR

57

GRATING

FILTER WHEEL

DETECTOR
CHANGE MIRROR

SLIT WIDTH ADJUST

S_1

S_2

OFF-AXIS ELLIPSE

S_1 = ENTRANCE SLIT
S_2 = EXIT SLIT

Pb Se DETECTOR

NOT SHOWN

1. INTERNAL CHOPPER
   (LOCATED AT S_2)
2. ZONE RANGER
   (SPATIAL SCAN OF
   PLUME OR
   BLACKBODY IMAGE
   OCCURS AT S_1)

WAVELENGTH DRUM

Pb S DETECTOR

WAVELENGTH
DRIVE MECHANISM

MONOCHROMATOR

Figure A2-1. Optical Diagram of the Spectroradiometer

FILTER WHEEL MECHANISM

ZONE RANGER SYSTEM

OPTICAL TUNNEL

Pb Se DETECTOR
HOUSING

BLACKBODY
CALIBRATION
SOURCE
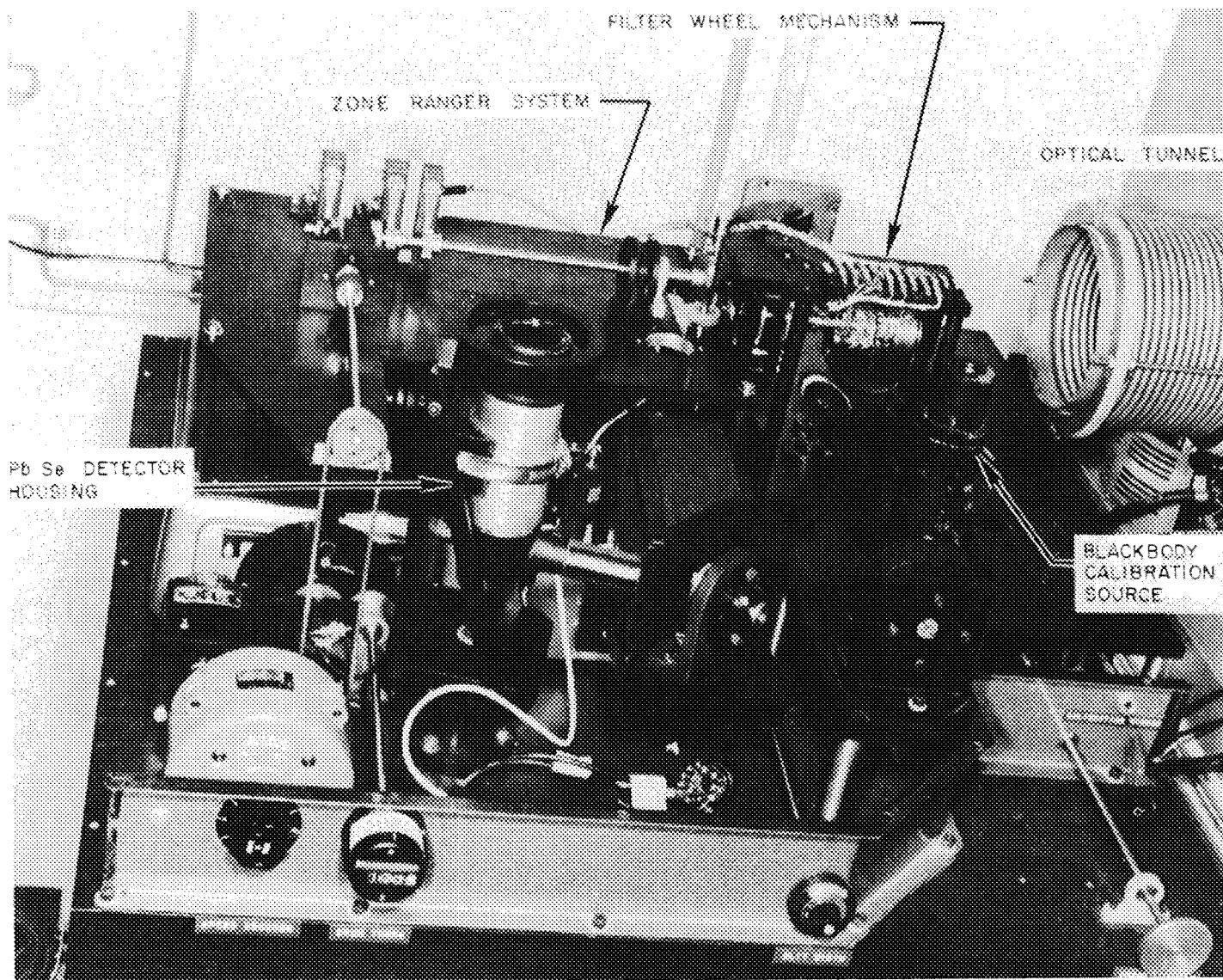
Figure A2-2.   Infrared Spectroradiometer

58

MEASUREMENT TECHNIQUES

Two-Dimensionality Check

The mixing chamber has been designed to produce a two-dimensional flow field, i.e., no gradients in temperature or concentration along horizontal lines-of-sight perpendicular to the flow direction. One method of verifying the two-dimensionality is to view the mixing region along various vertical lines-of-sight lying in a plane perpendicular to the flow direction; there should be no variation in spectral radiance observed from one such line of sight to another. This type of measurement will be carried out early in the test program. These measurements will also indicate the effect of the nitrogen film cooling on the mixing characteristics.

Calibration

Wavelength calibration of the spectroradiometer is carried out by recording atmospheric absorption spectra. Intensity calibration for emission data is made with a blackbody radiation source including the effect of the various mirrors and windows in the optical path. The background spectra for absorption measurements is obtained by scanning the greybody prior to a test. Spatial calibration of the spectrometer field of view is obtained by using the travelling aperature to scan the images of small light sources placed at known positions with respect to the mixing region.

Spectral Scans

The spectroradiometer can be used in a conventional spectral scan mode for either emission or absorption measurements with a fixed line-of-sight through the mixing region. The primary purpose of the spectral scans is to furnish data to allow selection of the optimum wavelength, slit width, and electronic amplification values for the zone radiometry measurements.

Zone Radiometry

On each individual test firing zone radiometry is carried out for emission and absorption measurements at a selected wavelength across a single plane (perpendicular to the flow axis) of the mixing region. Different planes are covered on different tests. On the first half of a test the traveling aperture scans the mixing region image for emission measurements and radiation intensity is recorded as a function of spatial position. For the second half of the test the internal chopper is turned off, and the greybody shutter is opened. Chopped greybody radiation attenuated by combustion products is then recorded as a function of spatial position. Before, or after, a test the blackbody and the greybody are similarly scanned for calibration purposes.

DATA REDUCTION

Because of the two-dimensionality of the flow field, the data reduction procedure is much simpler than described in Ref. A2-1. The data reduction procedure for each line of sight is simply that used for a uniform gas.

Point by point comparison of spatial scans of greybody radiation before a test and greybody radiation attenuated by the flow field during a test allows preparation of graphs of fractional transmission (τ_{LOS}) or emissivity ($\epsilon_{LOS} = 1 - \tau_{LOS}$) as a function of line of sight. In addition, comparison of spatial scans of flow field emission and blackbody emission allows preparation of graphs of spectral radiance. (N_{LOS}) as a function of line of sight.

The line of sight temperature is defined by the relation

$$\frac{N_{LOS}}{\epsilon_{LOS}} = N_{BB} \ (T_{LOS})$$

where $N_{BB} \ (T_{LOS})$ is the spectral radiance of a blackbody at temperature T_{LOS} and at the wavelength at which the measurement was carried out.

The H_2O line of sight partial pressure P_{LOS} is determined from the expression

$$\tau_{LOS} = e^{-KL\,P_{LOS}}$$

where L is the path length of the flow field along the line of sight and K is the value of the spectral absorption coefficient of H_2O at T_{LOS} and the wavelength of measurement.

REFERENCES

A2-1   Rocketdyne, <u>An Instrumentation System to Study Rocket Exhaust Plume Radiative Processes</u>, Final Report NAS8-11261, August 1965.

APPENDIX 3

LASS

SPECTROSCOPY WITH THE LASS

A spectroscopic study of the ultraviolet radiation emitted and absorbed by the OH radical in the $^2\Sigma^+ - ^2\Pi$ electronic transition can yield significant information on the kinetic processes causing the radiation, Ref. A3-1 to A3-4 .

The measurements to be taken include:
1. partial pressure of the OH radical
2. effective rotational temperatures of OH in its ground electronic state
3. effective rotational temperatures of OH in its electronically excited state
4. effective electronic excitation temperature of OH.

Measurement 2 is expected to provide the true gas temperature, while the temperatures measured in 3 and 4 may or may not agree with the gas temperature. The agreement is dependent upon whether the region is reacting or in thermal equilibrium. When the temperature measurements disagree, the magnitude of disagreement yields information about the chemical kinetics and is indicative of chemiluminencence. Chemiluminencence is radiation emitted by species formed in an exci state, i.e., radiation originating from a combustion zone. When all temperatures agree, it is normally concluded that the radiation arises from thermal rather than chemical processes. It should be noted that the measured temperatures will also be compared with those determined by measurements in the infrared. A complete delination of the meaning of the various temperatures is beyond the scope of this report and will be included when the experimental data are presented.

Measurements 1 and 2 are obtained from the absorption of a suitable discrete OH spectral line source placed behind the engine, Measurement 3 is determined from relative emission line intensities, and Measurement 4 results from comparison of emission and absorption of a given spectral line. The emission and absorption for these measurements is recorded simultaneously by the technique of electronically separating the chopped absorption signals from the emission signal and recording each one individually. Since the spectral region of interest covers a narrow range, all measurements for a particular axial location can be recorded during a single engine firing of 15 seconds duration.

In addition, the spectroscopy study provides a survey spectra of the ultraviolet and visible radiation from the combustion gases. This will assist in the motion picture photography studies to be described in a later section of this report. These data also allow identification of species, such as the unidentified emitter recorded in the color motion picture.

MEASUREMENT TECHNIQUE

A brief description of the measurements and the relevant data reduction equations are presented below. A more detailed description is available in the references.

Concentration of OH

The concentration of the OH radical is determined from a measurement of absorption of discrete spectral lines. In this technique, the light source, a radio frequency discharge in a tube containing low pressure water vapor, produces an OH emission spectrum of narrow spectral lines. The emission line from this source is absorbed by the broader line in the combustion chamber so that only absorption at the line center is measured.

The concentration of OH is given by the expression (Ref. A3-5)

$$N_{OH} = \frac{Q_R \, Q_V \, b_d P'}{FA_k \, T_{J'J''}} \exp \left(\frac{E_k}{kT} \right) \times 2.40 \times 10^{12} \qquad (1)$$

where E_k is the rotational energy level, k is Boltzmann's constant, Q_R and Q_V are the rotation and vibration partition functions, and b_d is the doppler line half-width. Also, $FA_k = \frac{f}{2J'' + 1}$, where f is the oscillator strength, J'' is the ground state quantum number, $T_{J'J''}$ is a correction factor for vibration-rotation interaction, and T is the rotational temperature.

In addition, $P' = P_{\nu_0} \left\{ [\exp (a^2)] \, [\text{erfc} \, (a)] \right\}^{-1}$

where P_{ν_0} is the absorption coefficient measured at the line center, and

$$a = \frac{b_n + b_c}{b_d} \, (\ln 2)^{1/2},$$

where b_n and b_c are the natural and collisional half-widths.

In Eq. (1), the values of k, Q_R, Q_V, $T_{J'J''}$, FA_k, b_d, E_k, and a are available in appropriate references. Thus, N_{OH} is determined from a measurement of P_{ν_0} and T.

P_{ν_0} is given by

$$P_{\nu_0} = \frac{I_0}{I}$$

where I and I_0 are the transmitted intensities of a line from the discharge lamp through the engine, with and without combustion, respectively. The rotational temperature, T, is measured from P_{ν_0} by the line slope technique.

Measurement of Rotational Temperature of OH Ground State

A. Line Slope Technique

The rotational temperature is determined from the following

equation relating the measured absorption at a line center to the temperature (Ref. A3-2):

$$\log \frac{P_{\nu_0}}{A_k \, T_{J'J''}} = C - \frac{E_k}{kT} \log e \qquad (2)$$

where C is a constant.

When P_{ν_0} is measured, the temperature is determined from the reciprocal of the slope of a graph of

$$\log \frac{P_{\nu_0}}{A_k \, T_{J'J''}} \quad \text{versus } E_K.$$

B. Iso-Intensity Technique

Another approach for determination of the rotational temperature is given in Ref. A3-1

$$T_R = \frac{\left(E_x - E_b\right) \log e}{k \left(\log FA_x \, T_{J'J''} - \log FA_b \, T_{J'J''}\right)} \qquad (3)$$

This technique depends upon the absorption of two lines being equal. The subscripts b and x refer to two lines of equal absorption.

Measurement of Rotational Temperature of OH Excited State

The excited state rotational temperature is measured using equations identical to Eq. (2) and (3), except that the intensity I' of a spectral line emitted by the combustion gas is used in place of P_{ν_0} and E, respectively.

Measurement of Electronic Temperature of OH

The electronic temperature, T_e, is determined from the equation

$$N_g = \frac{I}{I_0} N_{BB} \left(\lambda, T_e\right)$$

where N_g is the measured radiance of the gas and N_{BB} is the radiance

of a blackbody at the same temperature as the OH electronic temperature, T_e. T_e is determined from tables of the blackbody function.

INSTRUMENT SUB-SYSTEMS

The construction of the spectrum resolving and recording instrument has been completed by the Rocketdyne Research Division. It is a versatile instrument for applications involving the examination and analysis of the ultraviolet and visible radiation emitted by rocket engines and similar sources.

Figure A3-1 is an optical schematic of the LASS. Its principal parts are: (1) a combination spectrograph/spectrometer, (2) the entrance optics, (3) a system for wavelength and intensity calibration, and (4) the electronics (not shown in the figure) for photodetection, data recording, and calibration.

Spectrometer-Spectrograph

A schematic of the combination spectrometer/spectrograph is shown in Figure A3-2. Made by the McPherson Instrument Company, the Model 216 is a 1-meter focal length, stigmatic, Czerny-Turner optical system having an f/no. of 8.7. By using different gratings, the instrument covers a wavelength range from 2000 A to 8 microns. The focusing mirror is twice as large as the collimating mirror and thus intercepts a greater portion of the diffracted light rendering eight inches of the focal plane usable. Utilization of a film cassette in the focal plane permits spectrographic operation. In this mode, the instrument is capable of photographing 1700 A of spectra per exposure with a 1200-line-per-millimeter grating. Since the grating may be rotated between exposures, a series of exposures can cover any desired spectral range. Multiple exposures on each film are made by translating the cassette.
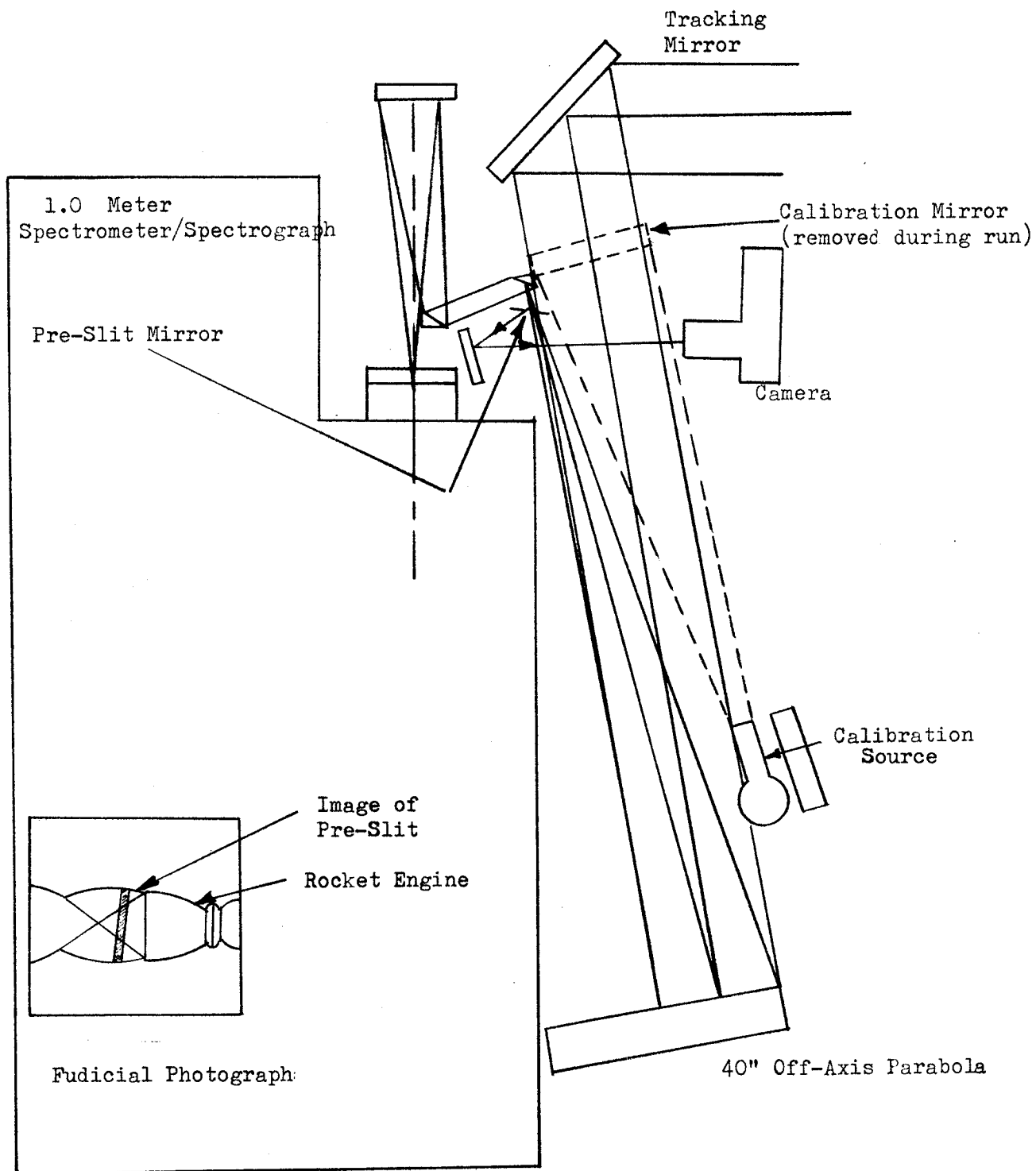
Figure A3-1. Optical Diagram of Large Aperture Spectrometer/Spectrograph

Focusing
mirror

Point of symmetry
location of bilateral
monochromator exit slit

Photomultipliers
(Up to 18 on
three tracks)

Light-tight
housing

Focal curve
location of
multiple exit
slits and photo-
graphic film
cassette

Grating

Bilateral
entrance
slit

Collimator mirror
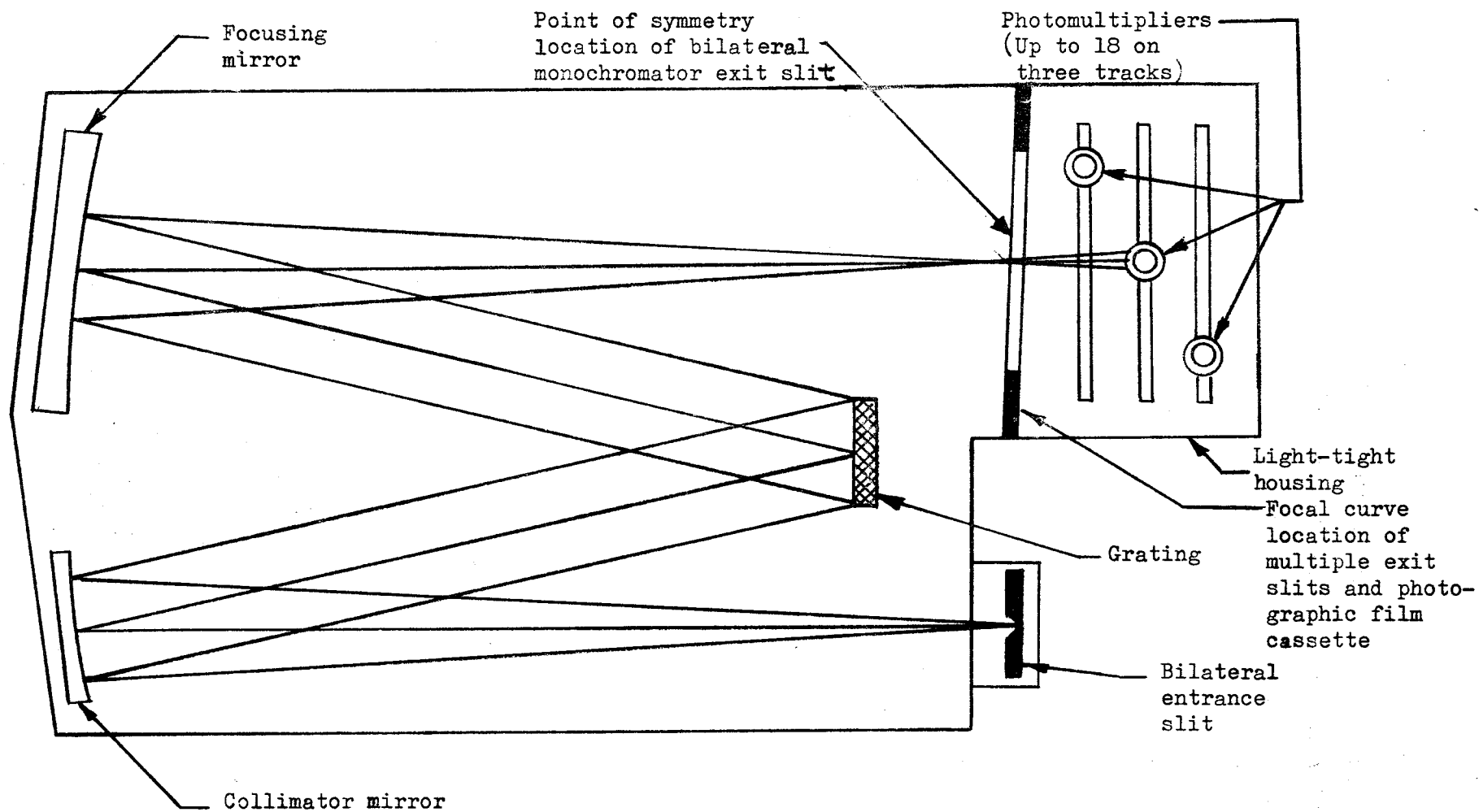
Figure A3-2. Optical Arrangement of the McPherson Model 216 Spectrometer/Spectrograph

For use as a spectrometer, a single adjustable exit slit is mounted at
the center of the focal plane. All of the diffracted light corresponding
to the wavelength at the observation location passes through the exit
slit. The light is detected by a photomultiplier tube mounted on a
rack in a light-tight enclosure behind the focal plane. Wavelength
scanning is accomplished automatically at a range of speeds from 1 A
per minute to 4000 A per minute with a 1200 line per millimeter
grating. Utilization of a 600-line-per-millimeter grating doubles
the scan rate.

Entrance Optics

The entrance optics consist of two optical subsystems, the collecting
optics and the fiducial optics. The collecting optics focus the source
radiation onto the entrance slit of the spectrometer/spectrograph, while
the fiducial optics show the location of the source on the entrance
slit. Since the McPherson Model 216 instrument is stigmatic,
the image of the source on the entrance slit has a point-to-point
correspondence with the image of the slit on the focal plane of the
instrument. In addition, it should be noted that the optical system
was designed for minimum optical aberrations.

As shown in Fig.A3-1, the collecting optics gather radiation from the
source with a tracking flat mirror and a 6-inch diameter 40-inch
focal length off-axis parabolic mirror. These mirrors focus the light
on a plane which intersects the plane of the preslit mirror (a mirror
with a narrow slice cut through it). Light passing through the pre-
slit mirror is reflected off a small plane mirror just behind the
pre-slit mirror to a second flat mirror. The light is then reflected
by a spherical mirror which focuses the pre-slit onto the entrance slit
of the McPherson instrument.

In the fiducial sub-system, the portion of the light striking the
pre-slit mirror is reflected onto a flat diagonal mirror and is
imaged on the film or view finder in the camera. The image in the

view finder is used to boresight the instrument while the image on the film produces a fiducial photograph as shown schematically in the inset on Fig. A3-1. The shadow of the pre-slit in the fiducial photograph locates the region of the source under investigation.

Calibration System

The calibration system utilizes a calibrated tungsten ribbon filament lamp for intensity calibration and a hollow cathode iron discharge lamp for calibrating wavelength and spectral line intensity. The calibration mirror directs the lamp radiation through the same number of reflections as traversed by the source radiation. Each lamp is operated from separately regulated DC power supplies and the calibration source is selected by a small angular rotation of the calibration spherical mirror. When not in use, this mirror is removed.

Electronics

A highly regulated DC high voltage supply is used for the photomultiplier tubes which can supply power up to the maximum spectrometer capacity of eighteen tubes. The photomultiplier output is normally recorded by an Offner 7-channel strip chart pen recorder system. When the LASS is operated at high scanning speeds, a higher response recording system is required; then the photomultiplier outputs are recorded on magnetic tape.

The absorption source is a water vapor discharge lamp which is excited by a 100 watt, 2450 megahertz RF power generator. The light from this source is mechanically chopped at 400 hertz in order that it can be electronically separated from the combustion radiation.

REFERENCES

A3-1 - Dieke, G. H., and H. M. Crosswhile: <u>Bumblebee Series Report,</u>
<u>No. 87</u>, John Hopkins University, 1948.

A3-2 Kostkowski, H. J., and H. P. Broida: <u>National Bureau of</u> <u>Standards Report 4418</u>, Dec. 1954 – Dec. 1955.

A3-3 Lezberg, E. A., Rose, C. M., and R. Friedman: NASA TND-2883, June 1965.

A3-4 Padley, P. J.: <u>Faraday Society</u>, Vol. 56, 1960.

A3-5 Lezberg, E. A., and D. R. Buchels: NASA TND-2441, 1964.

APPENDIX 4

PHOTOGRAPHIC MEASUREMENTS

A number of photographic measurements are utilized to provide supplemental information for comparison with the previously discussed optical methods of data collection. These measurements include schlieren, ultraviolet, infrared, color, false color, and photopyrometry photography. A brief discussion of these techniques follows.

SCHLIEREN PHOTOGRAPHY

Schlieren photography is one approach for the determination of the boundaries of the mixing region in both the horizontal and vertical directions for the check on two-dimensionality of the flow and film coolant effects experiments. This technique provides a cross reference with the data gathered with the zone radiometer and furnishes a visual picture of the phenomena of interest. Utilization was made of Rocketdyne's test site schlieren apparatus. Simple efficient operation is achieved through the use of a specially-designed schlieren lens attachment for a 16-millimeter Fastax camera and a portable parabolic mirror with a rigid mounting base. A high intensity pulsed light source is provided by an EG&G, Inc., Model 501 high-speed stroboscope. The test set-up is shown schematically in Fig. A4-1. For these experiments the knife edge was oriented vertically to accentuate horizontal density gradients. A discussion of the theory of operation of a schlieren system will not be presented here since it is adequately covered in the open literature, e.g., Ref. A4-1 and A4-2.

MOTION PICTURE PHOTOGRAPHY

The initial photographic studies incorporated an array of five cameras to record radiation from the following spectral regions:

1. 3100 A - corresponds to the (0,0) OH band, the region where OH radiates most intensely

WINDOWED
TEST
SECTION

EG & G MODEL 50I

STROBOSCOPE
POWER SUPPLY &
CONTROLS

FLASHER

CONVERGENT
MIRROR

FASTAX
CAMERA

LIGHT PATHS

ROCKETDYNE SCHLIEREN LENS
ATTACHMENT CONTAINS A
LIGHT SPLITTER AND KNIFE
EDGE

Figure A4-1. Schematic of Schlieren Apparatus

APPENDIX 4

PHOTOGRAPHIC MEASUREMENTS

A number of photographic measurements are utilized to provide supplemental information for comparison with the previously discussed optical methods of data collection. These measurements include schlieren, ultraviolet, infrared, color, false color, and photopyrometry photography. A brief discussion of these techniques follows.

SCHLIEREN PHOTOGRAPHY

Schlieren photography is one approach for the determination of the boundaries of the mixing region in both the horizontal and vertical directions for the check on two-dimensionality of the flow and film coolant effects experiments. This technique provides a cross reference with the data gathered with the zone radiometer and furnishes a visual picture of the phenomena of interest. Utilization was made of Rocketdyne's test site schlieren apparatus. Simple efficient operation is achieved through the use of a specially-designed schlieren lens attachment for a 16-millimeter Fastax camera and a portable parabolic mirror with a rigid mounting base. A high intensity pulsed light source is provided by an EG&G, Inc., Model 501 high-speed stroboscope. The test set-up is shown schematically in Fig. A4-1. For these experiments the knife edge was oriented vertically to accentuate horizontal density gradients. A discussion of the theory of operation of a schlieren system will not be presented here since it is adequately covered in the open literature, e.g., Ref. A4-1 and A4-2.

MOTION PICTURE PHOTOGRAPHY

The initial photographic studies incorporated an array of five cameras to record radiation from the following spectral regions:

1. 3100 A - corresponds to the (0,0) OH band, the region where OH radiates most intensely

Figure A4-1. Schematic of Schlieren Apparatus

2. 3500-4500 A - the "blue continuum" which may be caused
    by the recombination reaction

$$H + OH \longrightarrow H_2O + h\nu$$

3. infrared from 7000-8500A - corresponds to weak water
    emission bands which have been recorded in previous
    work at Rocketdyne

4. visible from 4000-6300 A - includes some of the blue
    continuum and impurities which may be present

Table A4-1 presents the spectral regions recorded, the possible emitter
species, and types of lens, filters, and films utilized. The film
records of the initial test runs were evaluated for their information
content and only those spectral regions that yield specifically useful
information were used for monitoring subsequent tests.

The cameras were located in a cluster approximately 10 feet from the
engine with a direct line of sight perpendicular to the windows. Full
photographic coverage was employed on tests 0080 through 0101. Initially,
Fastax cameras capable of framing rates up to 8000 frames per second
were utilized, however, optical emission was too weak to be recorded
at high framing rates. Therefore, on subsequent tests lower framing
rate Bell and Howell and Millikan cameras were employed.

The objectives of the motion picture coverage are to 1) determine the
spatial distribution of emission from each emitting species, 2) assist
in identification of species by intercomparison of the spatial distri-
bution of emission from the different film records, 3) determine the
stability of the flow field with respect to time, and 4) provide a
visual analog to the spectroscopic data.

For the initial engine tests, photographic coverage was intended to
determine the proper film exposures, film and filter combinations,
and the spectral region most favorable for flow diagnostics. The
partially completed accomplishments to date include:

TABLE A4-1

FASTAX EQUIPMENT SPECIFICATIONS

FOR COMPOSITE PROPULSION SYSTEM

Spectral Region ($\overset{\circ}{A}$)	Chief Emitter	Lens Type	Filter	Film
2850-3150	OH	Quartz, Ultra-violet transmitting	OCLI	2498 RAR
3500-4500	O + OH Recombination	Glass	Corning 0-52 plus Wratten 39	2498 RAR
4000-6300	H_2O, O + OH Recombination, Impurities	Glass	Wratten 2B	Ektachrome EF Daylight
7000-8500	H_2O	Glass	Wratten 89B	False Color IR
3500-6300	H_2O, O + OH Recombination, Impurities	Glass	None	Ektachrome EF Daylight

(1) Emission in the visable spectral region was successfully recorded. Proper exposure is f/2.5 at 64 frames per second.

(2) An unidentified species was recorded in the 7000-8500 A spectral region. Spectroscopic measurements are required for its identification.

(3) Ultraviolet radiation was recorded in the 3100 A spectral region. Proper exposure is f/3.5 at 8 frames per second.

(4) No IR emission was detected, even at the maximum exposure setting of the Bell & Howell camera (f/2.5 and 8 frames per second). However, since the radiation from normal sunlight did not appear on the film for this camera setting, it is possible that a time exposure will reveal IR radiation in the mixing region. This approach will be attempted on future tests.

(5) The 3500-4500 spectral region was not successfully recorded. Further attempts are planned.

PHOTOPYROMETRY

The photopyrometer consists of a Nikon F 35 mm camera equipped with an automatic rewind motor and an ultraviolet transmitting lens, optical interference filters to isolate a narrow band of radiation in the desired spectral region, a tungsten ribbon filament lamp, and an optical calibration system consisting of mirrors and an attenuating step filter, Fig. A4-2.

With the ultraviolet photopyrometer, the radiation from the OH radial can be photographed and a contour map of the OH brightness temperature can be obtained. The map is an aid in defining the spatial extent of combustion. A tungsten lamp ribbon filament of known spectral radiance is also imaged on the film record. The ribbon filament is attenuated by a step filter of known attenuation and thus provides a calibration source for data reduction. The initial step in flow field maping utilizes an automatic-scanning microdensitometer which produces an

To
Engine

Camera

Mirror

Step
Filter

Collimating
Mirror

Mirror

Tungsten
Lamp

Collimating
Mirror
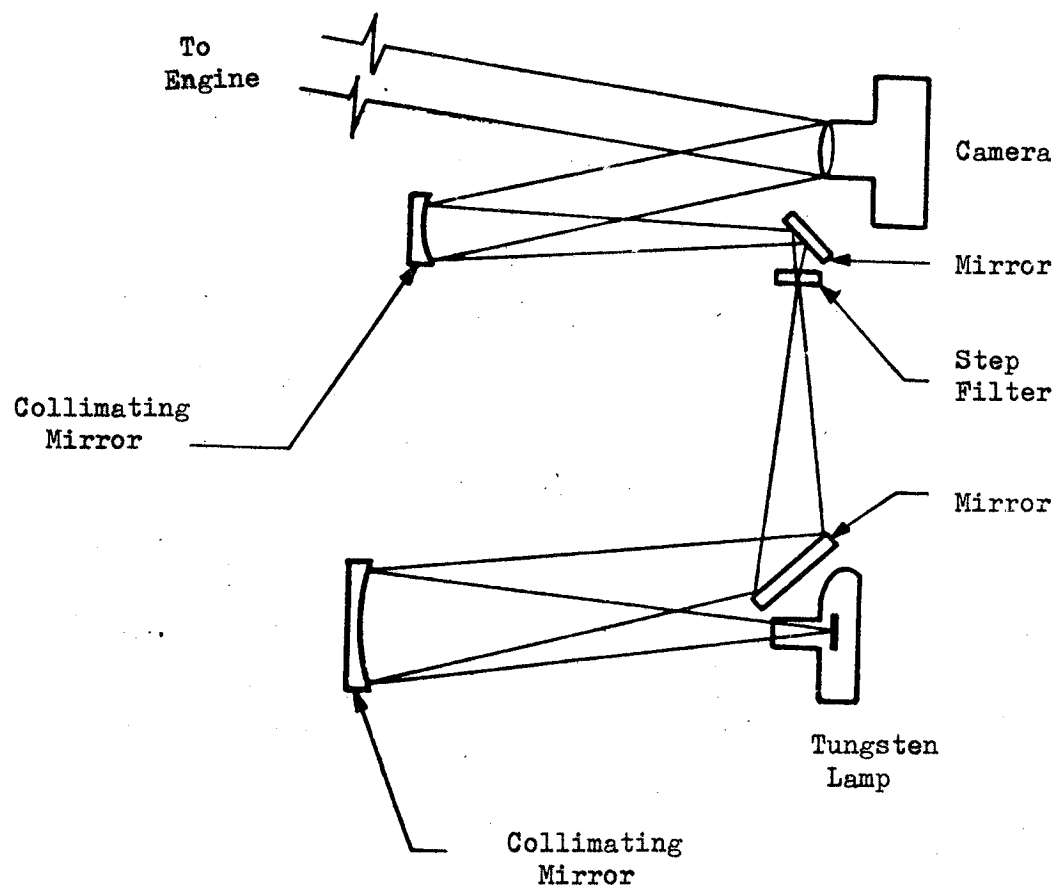
Figure A4-2. Optical Diagram of Photographic Pyrometer

isodensity contour map of the gas flow image. In addition, the microdensitometer produces a density measurement of each zone of the step filtered lamp image. The film response is then determined by graphing the film density of each zone versus the logarithm of radiance. A value of radiance or its equivalent brightness temperature can them be assigned to each isodensity contour in the exhaust plume.

The OH brightness temperature at a given point in the flow field is a function of both OH concentration and the electronic excitation temperature, which may be equal to or greater than the gas translational temperature. Complete interpretation of the photopyrograms is difficult and the various postulations can only be resolved through correlation with the LASS spectroscopic data.

REFERENCES

A4-1. Shapiro, A. H.: The Dynamics and Therodynamics of Compressible Fluid Flow, The Ronald Press Company, New York, 65-67, 1963.

A4-2. Keagy, W. R., Jr., and H. H. Ellis: "The Application of the Schlierin Method to the Quantitative Measurement of Mixing Gases and Jets," Third Symposium on Combustion, Flame, and Explosion Phenomena, Williams & Wilkins Co., Baltimore, Md., 1949.

HOT FIRE DATA REDUCTION COMPUTER PROGRAM

A computer program has been written in FORTRAN language to reduce hot firing data with the General Electric 420 Timesharing Computer.

The program, entitled SSMIX, consists of a main program which handles the majority of the data reduction, two "function" sub-routines which convert millivolt values to temperatures in degrees fahrenheit for chromel-alumel and iron-constantan thermocouples, and a "function" which provides compressible isentropic flow parameters as a function of Mach number.

Attached hereto are the following: program summaries, a definition of program variables (Table A5-1), program listings (Table A5-2), a data input list, and a printout for a typical run (Table A5-6).

PROGRAM SSMIX

This program reduces desired parameters from test firing raw data. Three major sub-systems are involved: (1) LOX-GH$_2$ rocket motor, (2) GN$_2$ Film Coolant, and (3) Heated Air. For data reduction purposes these three sub-systems are further divided as follows:

1. LOX-GH$_2$ Rocket Motor
    a. High Pressure Coolant Water
    b. Low Pressure Coolant Water
    c. LOX Oxidizer
    d. GH$_2$ Fuel
    e. Engine Performance

2. GN$_2$ Film Coolant
    a. High Pressure GN$_2$ Film Coolant
    b. Low Pressure GN$_2$ Film Coolant

3. Heated Air
    a. Air Stream
    b. Air Heater

Data reduction for each of the above is handled separately in a labeled section of the program.

TABLE A5-1
SSMIX PROGRAM VARIABLES

GENERAL

IRUN	—	Run Number	(Integer)
IDATE	—	Run Date	(Integer)
PA	—	Atmospheric Pressure	(psia)
TATM	—	Atmospheric Temperature	(F)
RH	—	Relative Humidity	(Percent)

HIGH PRESSURE COOLANT WATER

CWH	—	Flowmeter Cycles	(Cycles)
PWHT	—	Tank Pressure	(psig)
PWHI	—	Inlet Pressure	(psig)
VWHT	—	Tank Temperature	(MV)
VWH1	—	1/4-Inch Outlet Temperature	(MV)
VWH2	—	3/4-Inch Outlet Temperature	(MV)
VWH3	—	$1\frac{1}{2}$-Inch Outlet Temperature	(MV)
WWH	—	Flowrate	(lbs/sec)
TWHT	—	Tank Temperature	(F)
TWH1	—	1/4-Inch Outlet Temperature	(F)
TWH2	—	3/4-Inch Outlet Temperature	(F)
TWH3	—	$1\frac{1}{2}$-Inch Outlet Temperature	(F)
DWH1	—	1/4-Inch Outlet Delta Temp	(F)
DWH2	—	3/4-Inch Outlet Delta Temp	(F)
DWH3	—	1-1/2-Inch Outlet Delta Temp	(F)

LOW PRESSURE COOLANT WATER

CWL	—	Flowmeter Cycles	(Cycles)
PWLT	—	Tank Pressure	(psig)
PWLI	—	Inlet Pressure	(psig)
VWLT	—	Tank Temperature	(MV)
VWL1	—	1-Inch Outlet Temperature	(MV)

WWL	—	Flowrate	(lbs/sec)
TWLT	—	Tank Temperature	(F)
TWL1	—	1-Inch Outlet Temperature	(F)
DWL1	—	1-Inch Outlet Delta Temperature	(F)

AIR STREAM

PSD	—	Stream Pressure in Duct	(psig)
VSD	—	Stream Temperature in Duct	(MV)
TSD	—	Stream Temperature in Duct	(F)
RSD	—	Stream Density in Duct	(lbs/ft^3)
PRA	—	Pressure Ratio PA/PSD	
YA	—	Expansion Factor	
WA	—	Flowrate	(lbs/sec)
TA	—	Mixing Chamber Inlet Air Temperature	(R)
TAC	—	Mixing Chamber Inlet Air Temperature	(F)
RA	—	Mixing Chamber Inlet Air Density	(lbs/ft^3)
VA	—	Mixing Chamber Inlet Air Velocity	(ft/sec)
AA	—	Mixing Chamber Inlet Air Acoustic Velocity	(ft/sec)
XMA	—	Mixing Chamber Inlet Air Mach Number	
PPA	—	Isentropic Flow Pressure Ratio P/Po	
AAA	—	Isentropic Flow Area Ratio A/A*	
PAMC	—	Mixing Chamber Inlet Air Pressure	(psig)

LOW PRESSURE GN_2 FILM COOLANT

PNL	—	Manifold Pressure	(psig)
VNL	—	Manifold Temperature	(MV)
TNL	—	Manifold Temperature	(F)
PRNL	—	Pressure Ratio PA/PNL	
YNL	—	Expansion Factor	
WNL	—	Flowrate	(lbs/sec)
TNLMC	—	Mixing Chamber Inlet Temperature	(R)
TNLMCC	—	Mixing Chamber Inlet Temperature	(F)
RNL	—	Mixing Chamber Inlet N_2 Density	(lbs/ft^3)

VENL	—	Mixing Chamber Inlet N_2 Velocity	(ft/sec)
ANL	—	Mixing Chamber Inlet N_2 Acoustic Velocity	(ft/sec)
XMNL	—	Mixing Chamber Inlet N_2 Mach Number	
PPNL	—	Isentropic Flow Pressure Ratio P/Po	
AANL	—	Isentropic Flow Area Ratio A/A*	
PNLMC	—	Mixing Chamber Inlet N_2 Pressure	(psig)

HIGH PRESSURE GN$_2$ FILM COOLANT

PNH	—	Manifold Pressure	(psig)
VNH	—	Manifold Temperature	(MV)
TNH	—	Manifold Temperature	(F)
PRNH	—	Pressure Ratio PA/PNH	
YNH	—	Expansion Factor	
WNH	—	Flowrate	(lbs/sec)
TNHMC	—	Mixing Chamber Inlet N_2 Temperature	(R)
TNHMCC	—	Mixing Chamber Inlet N_2 Temperature	(F)
RNHMC	—	Mixing Chamber Inlet N_2 Density	(lbs/ft^3)
VENH	—	Mixing Chamber Inlet N_2 Velocity	(ft/sec)
ANH	—	Mixing Chamber Inlet N_2 Acoustic Velocity	(ft/sec)
PNHMC	—	Mixing Chamber Inlet N_2 Pressure	(psig)

LOX OXIDIZER

PC	—	Chamber Pressure	(psig)
COX	—	Flowmeter Cycles	(Cycles)
POXT	—	Tank Pressure	(psig)
POXI	—	Inlet Pressure	(psig)
VOXI	—	Inlet Temperature	(MV)
VOXC	—	Injector Cooldown Temperature	(MV)
TOXI	—	Inlet Temperature	(F)
TOXC	—	Injector Cooldown Temperature	(F)
TK	—	Inlet Temperature	(K)
RS	—	Saturation Density	(lbs/ft^3)
PV	—	Vapor Pressure	(psia)
B	—	Adiabatic Compressibility	

ROX	–	LOX Density	(lbs/ft^3)
WOX	–	LOX Flowrate	(lbs/sec)
DPOXI	–	Injector Delta Pressure	(psi)

HYDROGEN FUEL

PHVI	–	Venturi Inlet Pressure	(psig)
PHI	–	Inlet Pressure	(psig)
VHI	–	Inlet Temperature	(MV)
THI	–	Inlet Temperature	(F)
XKH	–	Isentropic Flow Coefficient	
PHIC	–	Inlet Pressure	(psia)
ZH	–	Compressibility Factor	
WH	–	Flowrate	(lbs/sec)
DPHI	–	Injection Delta Pressure	(psi)

PERFORMANCE PARAMETERS

PRPC	–	Pressure Ratio PC/PA	
XMR	–	Mixture Ratio	
WT	–	Total Flow	(lbs/sec)
CSTAR	–	C*	(ft/sec)
TC4	–	Theoretical C* @ MR = 4.0	(ft/sec)
TC5	–	Theoretical C* @ MR = 5.0	(ft/sec)
TC6	–	Theoretical C* @ MR = 6.0	(ft/sec)
TCSTAR	–	Theoretical C* @ MR of Test	(ft/sec)
CN	–	C* Efficiency	(Percent)

AIR HEATER

VAH1	–	Heater Bed Temperature 1	(MV)
VAH2	–	Heater Bed Temperature 2	(MV)
VAH3	–	Heater Bed Temperature 3	(MV)
VAH4	–	Heater Bed Temperature 4	(MV)
TAH1	–	Heater Bed Temperature 1	(F)
TAH2	–	Heater Bed Temperature 2	(F)
TAH3	–	Heater Bed Temperature 3	(F)
TAH4	–	Heater Bed Temperature 4	(F)

SSMIX - LOGIC

```
5C  *  *  *  *  PRØGRAM SSMIX      1/9/69      J T. SABØL  *  *  *  *
10C
15 CALL ØPENF (1,"XDATA",2)
20 READ(1,)IRUN,IDATE,PA,TATM,RH
25C       *****HIGH PRESSURE WATER SYSTEM*****
30 READ(1,)CWH,PWHT,PWHI,VWHT,VWH1,VWH2,VWH3
35 WWH=.1129*CWH
40 TWHT=ICØN(VWHT)
45 TWH1=ICØN(VWH1)
50 TWH2=ICØN(VWH2)
55 TWH3=ICØN(VWH3)
60 DWH1=TWH1-TWHT
65 DWH2=TWH2-TWHT
70 DWH3=TWH3-TWHT
75C      *****LØW PRESSURE WATER SYSTEM*****
80 READ(1,)CWL,PWLT,PWLI,VWLT,VWL1
85 WWL=.1102*CWL
90 TWLT=ICØN(VWLT)
95 TWL1=ICØN(VWL1)
100 DWL1=TWL1-TWLT
105C              *****AIR SYSTEM*****
110 READ(1,)PSD,VSD
115 TSD=CRAL(VSD)
120 RSD=2.7*(PSD+PA)/(TSD+460.)
125 PRA=PA/(PSD+PA)
130 YA=SQRT(((1.-.732**4.)/((1.-.732**4.)*PRA**1.42857))*(((3.5*
135&PRA**1.42857)*(1.-PRA**.285714))/(1.-PRA)))
140 WA=16.27*YA*SQRT(PSD*RSD)
145 TA=(PRA**.286)*(TSD+460.)
150 TAC=TA-460.
155 RA=2.7*(PSD+PA)/(TSD+460.)
160 VA=6.99*WA/RA
165 AA=49.*TA**.5
170 XMA=VA/AA
175 CALL CFLØW(XMA,PPA,AAA)
180 PAMC=((WA*SQRT((TSD+460.)/.997)*AAA*PPA)/10.959)-PA
185C      *****LØW PRESSURE NITRØGEN SYSTEM*****
190 READ(1,)PNL,VNL
195 TNL=ICØN(VNL)
200 PRNL=PA/(PNL+PA)
205 YNL=SQRT(((1.-.577**4.)/((1.-.577**4.)*PRNL**1.42857))*(((3.5*
210&PRNL**1.42857)*(1.-PRNL**.285714))/(1.-PRNL)))
215 WNL=4.79*YNL*SQRT(((PNL+PA)/(TNL+460.))*PNL)
```

```
220  TNLMC=((.989*PA/(PNL+PA))**.286)*(TNL+460.)
225  TNLMCC=TNLMC-460.
230  RNL=2.61*PA/TNLMC
235  VENL=34.4*WNL/RNL
240  ANL=49.9*(TNLMC**.5)
245  XMNL=VENL/ANL
250  CALL CFLOW(XMNL,PPNL,AANL)
255  PNLMC=((WNL*SQRT((TNL+460.)/.997)*AANL*PPNL)/2.2333)-PA
260C       *****HIGH PRESSURE GN2 FILM COOLANT*****
265  READ(1,)PNH,VNH
270  TNH=ICON(VNH)
275  IF((PNH+PA).GE.(1.7*PA)) GO TO 10
280  PRNH=PA/(PNH+PA)
285  YNH=SQRT(((1.-.475**4.)/((1.-.475**4.)*PRNH**1.42857))*(((3.5*
290 &PRNH**1.42857)*(1.-PRNH**.285714))/(1.-PRNH)))
295  WNH=6.88*YNH*SQRT(((PNH+PA)/(TNH+460.))*PNH)
300  TNHMC=((PA*.988/(PNH+PA))**.286)*(TNH+460.)
305  TNHMCC=TNHMC-460.
310  RNHMC=2.61*PA/TNHMC
315  VENH=22.7*WNH/RNHMC
320  ANH=49.9*(TNHMC**.5)
325  GO TO 20
330  10 WNH=3.38*(PNH+PA)/SQRT(TNH+460.)
335  TNHMC=.8333*(TNH+460)
340  TNHMCC=TNHMC-460.
345  RNHMC=2.61*PA/TNHMC
350  VENH=49.9*TNHMC**.5
355  20 PNHMC=(.1563*WNH*SQRT((TNH+460.)/.997))-PA
360C       *****LOX OXIDIZER CALCULATIONS*****
365  READ(1,)PC,COX,POXT,POXI,VOXI,VOXC
370  TOXI=ICON(VOXI)
375  TOXC=ICON(VOXC)
380  TK=(TOXI+459.668)/1.8
385  RS=62.428227*(1.414202-.001033016*TK-2.23E-5*TK**2.)
390  PV=PA*EXP(5.238279-7.2953481/TK-41958.931/TK**2.)
395  B=8.05790431E-5-1.8993851E-6*TK+1.2860036E-8*TK**2.
400  ROX=RS*(10.**B*(POXI+PA-PV)+1.)**.1
405  WOX=.297E-3*COX*ROX
410  DPOXI=POXI-PC
415C       *****HYDROGEN FUEL CALCULATIONS*****
420  READ(1,)PHVI,PHI,VHI
425  THI=ICON(VHI)
430  XKH=(((THI+60.)/200.)*.00013)+.01362
435  PHIC=PHI+PA
440  ZH=4.62585E-5*PHIC+.99
445  WH=((PHVI+PA)/SQRT(THI+460.))*SQRT(1./ZH)*XKH
```

```
450 DPHI=PHI-PC
455C      *****PERFØRMANCE PARAMETERS*****
460 PRPC=(PC+PA)/PA
465 XMR=WØX/WH
470 WT=WØX+WH
475 CSTAR=130.*(PC+PA)/WT
480 TC4=((((PC+PA)-300.)/200.)*15.)+8146.
485 TC5=((((PC+PA)-300.)/200.)*30.)+7893.
490 TC6=((((PC+PA)-300.)/200.)*40.)+7600.
495 IF(XMR-5.)30,40,50
500 30 TCSTAR=((5.-XMR)*(TC4-TC5))+TC5
505 GØ TØ 55
510 40 TCSTAR=TC5
515 GØ TØ 55
520 50 TCSTAR=TC5-((XMR-5.)*(TC5-TC6))
525 55 CN=(CSTAR/TCSTAR)*100.
530C      *****AIR HEATER TEMPERATURES*****
535 READ(1,)VAH1,VAH2,VAH3,VAH4
540 TAH1=CRAL(VAH1)
545 TAH2=CRAL(VAH2)
550 TAH3=CRAL(VAH3)
555 TAH4=CRAL(VAH4)
560C            *****PRINTØUTS*****
565 PRINT,"          * * * * * *M I X I N G   P R Ø G R A M * *
570&* * * "
575 PRINT,↑2,"    NØTE:  DIMENSIØNS FØR PARAMETERS ARE AS FØLLØWS:"
580 PRINT,↑," TEMPERATURES - F          DENSITIES - #/FT3"
585 PRINT,"           PRESSURES - PSIG        FLØWS - #/SEC"
590 PRINT,"           VELØCITIES - FT/SEC"
595 PRINT,↑2,"       * * * * * * * * * * * * * * * * * * *
600&* * *"
605 PRINT,↑2,"RUN - ",IRUN,"              ","DATE - ",IDATE
610 PRINT 70,PA,TATM,RH
615 PRINT,↑2,↑,"         ***** HIGH PRESSURE WATER SYSTEM *****"
620 PRINT 75,WWH,PWHT,PWHI,TWHT,DWH1,DWH2,DWH3
625 PRINT,↑2,↑,"         ***** LØW PRESSURE WATER SYSTEM *****"
630 PRINT 80,WWL,PWLT,PWLI,TWLT,DWL1
635 PRINT,↑2,↑,"              ***** AIR SYSTEM *****"
640 PRINT 85,WA,PSD,PAMC,TSD,TAC,RA,VA,AA,XMA
645 PRINT,↑2,↑,"         ***** LØW PRESSURE NITRØGEN SYSTEM *****"
650 PRINT 90,WNL,PNL,PNLMC,TNL,TNLMCC,RNL,VENL,ANL,XMNL
655 PRINT,↑2,↑,"         ***** HIGH PRESSURE NITRØGEN SYSTEM *****"
660 IF((PNH+PA).GE.(1.7*PA)) GØ TØ 60
665 PRINT 95,WNH,PNH,PNHMC,TNH,TNHMCC,RNHMC,VENH,ANH
670 GØ TØ 65
675 60 PRINT 100,WNH,PNH,PNHMC,TNH,TNHMCC,RNHMC,VENH
```

```
680 65 PRINT,†2,†,"          ***** LØX ØXIDIZER CALCULATIØNS *****"
685 PRINT 105,WØX,PØXT,PØXI,TØXI,TØXC,DPØXI
690 PRINT,†2,†,"          ***** HYDRØGEN FUEL CALCULATIØNS *****"
695 PRINT 110,WH,PHVI,PHI,THI,DPHI
700 PRINT,†2,†,"          ***** PERFØRMANCE PARAMETERS *****"
705 PRINT 115,PC,PRPC,XMR,WT,CSTAR,TCSTAR,CN
710 PRINT,†2,†,"          ***** AIR HEATER BED TEMPERATURES *****"
715 PRINT 120,TAH1,TAH2,TAH3,TAH4
720 70 FØRMAT(/,"P ATM - "F5.2,5X,"T ATM - "F4.0,5X,"RH - "F4.1,
725&5X,"PC/PA IDEAL - 29.35")
730 75 FØRMAT(/,"FLØW - "F5.2,5X,"P TANK - "F6.1,5X,"P IN - "F6.1,
735&5X,"T TANK - "F4.0,//,"DT1 - "F4.0,5X,"DT2 - "F4.0,5X,
740&"DT3 - "F4.0)
745 80 FØRMAT(/,"FLØW - "F5.2,5X,"P TANK - "F6.1,5X,"P INLET - "
750&F6.1,//,"T TANK - "F4.0,7X,"DELTA T - "F4.0)
755 85 FØRMAT(/,"FLØW - "F4.2,5X,"P SD - "F4.3,5X,"P MC - "F4.2,
760&//,"T SD - "F5.0,5X,"T MC - "F5.0,5X,"RHØ MC - "F5.4,//,
765&"V MC - "F6.1,5X,"A - "F6.1,5X,"M - "F4.3)
770 90 FØRMAT(/,"FLØW - "F4.2,5X,"P N2 - "F4.2,5X,"P MC - "F6.2,//,
775&"T N2 - "F3.0,5X,"T MC - "F3.0,5X,"RHØ MC - "F5.4,//,
780&"V MC - "F6.1,5X,"A - "F6.1,5X,"M - "F4.3)
785 95 FØRMAT(/,"FLØW - "F4.2,5X,"P N2 - "F4.1,5X,"P MC - "F6.2,
790&5X,"T N2 - "F3.0,//,"T MC - "F4.0,5X,"RHØ MC - "F5.4,5X,
795&"VEL N2 - "F6.1,5X,"A - "F6.1)
800 100 FØRMAT(/,"FLØW - "F4.2,5X,"P N2 - "F4.1,5X,"P MC - "F6.2,
805&5X,"T N2 - "F3.0,//,"T MC - "F4.0,5X,"RHØ MC - "F5.4,5X,
810&"VEL N2 - "F6.1)
815 105 FØRMAT(/,"FLØW - "F4.2,5X,"P TANK - "F5.1,5X,"P IN - "F5.1,
820&//,"T IN - "F5.0,5X,"T CØØL - "F5.0,5X,"DP INJ - "F5.1)
825 110 FØRMAT(/,"FLØW - "F4.2,5X,"P VEN IN - "F6.1,5X,"P IN - "F6.1,
830&//,"T H2 - "F4.0,5X,"DP INJ - "F5.1)
835 115 FØRMAT(/,"PC - "F5.1,5X,"PC/PA - "F5.2,5X,"MR - "F5.2,5X,
840&"TØTAL FLØW - "F4.2,//,"C* - "F5.0,5X,"THEØR C* - "F5.0,5X,
845&"ETA C* - "F5.1)
850 120 FØRMAT(/,"T BED 1 - "F5.0,3X,"T BED 2 - "F5.0,3X,
855&"T BED 3 - "F5.0,3X,"T BED 4 - "F5.0)
860 PRINT,†2,†,"          * * * * * * * * * * * * * * * * * * *
865&* * * *"
870 PRINT,†2,†2
999 END
```

SSMIX DATA INPUT

Data are entered in permanent file XDATA. Nine lines of data are
inputted as shown below.

1	IRUN, IDATE, PA, TATM, RH
2	CWH, PWHT, PWHI, VWHT, VWH.1, VWH2, VWH3
3	CWL, PWLT, PWLI, VWLT, VWL1
4	PSD, VSD
5	PNL, VNL
6	PNH, VNH
7	PC, COX, POXT, POXI, VOXI, VOXC
8	PHVI, PHI, VHI
9	VAH1, VAH2, VAH3, VAH4

It should be noted that a line number is required and a comma is
needed to separate each data variable.

SUBROUTINES

Function Icon

This function performs temperature scaling of millivolt values from
iron-constantan thermocouples with a 150F reference junction in the
range of -11.2 to +53.2 millivolts (-320 to 1800F). Scaling is
accomplished by separating the 64.4 millivolt range into smaller
ranges, each having been fitted with a third-order polynomial
equation. The breakdown is as follows:

.2 MV Range	-11.2 to -11.0 MV
1.0 MV Range	-11.0 to -10.0 MV
2.0 MV Ranges	-10.0 to 0 MV
4.0 MV Ranges	0 to +52.0 MV
1.0 MV Range	+52.0 to +53.0 MV
.2 MV Range	+53.0 to +53.2 MV

The program (Table A5-3) selects the correct equation from the millivolt value and solves for the temperature. Accuracy is $\pm$ 1.0 F of NBS standards.

Function Cral

This function performs temperature scaling of millivolt values of chromel-alumel thermocouples with a 32 F reference junction in the range 0 to 55 millivolts (32 to 2504 F). Scaling is accomplished by treating the 55-millivolt range as eleven 5-millivolt ranges, each having been fitted with a third order polynomial equation. The program (Table A5-4) selects the correct equation from the millivolt value and solves for the temperature. Accuracy is $\pm$ 1.0 F of NBS standards.

Function CFlow

This function provides the compressible isentropic flow parameters P/P_o (pressure ratio) and A/A* (area ratio) in the Mach number range from .20 to .60 for a perfect gas, k = 1.4.

The program (Table A5-5) contains arrays of P/Po and A/A* for .01 Mach number increments. The tables were abstracted from <u>The Dynamics and Thermodynamics of Compressible Fluid Flow</u>, Vol. I, by Ascher H. Shapiro, Ronald Press Co., New York, 1953.

Operation of this function is based upon the Mach number calculated in the main program. It first checks the Mach number to insure it is within the range of .20 to .60. If not, values of zero are returned to the main program. If the Mach number is in the proper range, the program enters a loop comparing the input Mach number to those stored in the array. When the array Mach number equals or exceeds the input Mach number the two bracketing values of P/Po and A/A* are chosen and a linear interpolation performed. The interpolated values are then returned to the main program.

FUNCTION ICON - LOGIC

```
7000 FUNCTION ICON(XMV)
7005C
7010C IRON CONSTANTAN THERMOCOUPLE MILLIVOLT TO DEGREES F CONVERSION
7015C 150 DEGREE REFERENCE JUNCTION TEMPERATURE
7020C      J T. SABOL   12/18/68
7025C
7030      IF(XMV.GE.-11.2.AND.XMV.LE.53.2) GO TO 5
7035      T=9999.
7040      GO TO 140
7045   5 IF(XMV) 10,50,50
7050  10 IF(XMV.LT.-10..AND.XMV.GT.-11.) GO TO 40
7055      IF(XMV.LE.-11.) GO TO 45
7060      N=IABS(INT(XMV/2))
7065      I=N+1
7070      V=XMV+2.*N
7075      GO TO (15,20,25,30,35,35),I
7080  15 T=-.15*V*V+33.85*V+150.
7085      GO TO 130
7090  20 T=-.5*V*V+34.5*V+81.7
7095      GO TO 130
7100  25 T=-.8*V*V+35.9*V+10.7
7105      GO TO 130
7110  30 T=-1.3*V*V+38.4*V-64.3
7115      GO TO 130
7120  35 T=-2.65*V*V+43.05*V-146.3
7125      GO TO 130
7130  40 V=XMV+10.
7135      T=-8.*V*V+54.*V-243.
7140      GO TO 130
7145  45 V=XMV+11.
7150      T=-50.*V*V+65.*V-305.
7155      GO TO 130
7160  50 IF(XMV.GT.52..AND.XMV.LT.53.) GO TO 120
7165      IF(XMV.GE.53.) GO TO 125
7170      N=INT(XMV/4.)
7175      I=N+1
7180      V=XMV-4.*N
7185      GO TO (55,60,65,70,75,80,85,90,95,100,105,110,115,115),I
7190  55 T=-.0875*V*V+33.525*V+150.
7195      GO TO 130
7200  60 T=-.05*V*V+32.6*V+282.7
7205      GO TO 130
```

```
7210  65  T=.075*V*V+32.2*V+412.3
7215      GO TO 130
7220  70  T=0.*V*V+32.5*V+542.3
7225      GO TO 130
7230  75  T=-.0125*V*V+32.725*V+672.3
7235      GO TO 130
7240  80  T=-.0375*V*V+32.575*V+803.
7245      GO TO 130
7250  85  T=-.0875*V*V+31.975*V+932.7
7255      GO TO 130
7260  90  T=-.1*V*V+31.1*V+1059.2
7265      GO TO 130

7270  95  T=-.1625*V*V+29.975*V+1182.
7275      GO TO 130
7280  100 T=-.1*V*V+28.7*V+1299.3
7285      GO TO 130
7290  105 T=-.025*V*V+28.15*V+1412.5
7295      GO TO 130
7300  110 T=.375*V*V+27.65*V+1524.7
7305      GO TO 130
7310  115 T=-.0375*V*V+30.575*V+1641.3
7315      GO TO 130
7320  120 V=XMV-52.
7325      T=.4*V*V+29.8*V+1763.
7330      GO TO 130
7335  125 V=XMV-53.
7340      T=20.*V*V+26.*V+1793.2
7345  130 IF(T) 135,140,140
7350  135 ICON=INT(T-.5)
7355      GO TO 999
7360  140 ICON=INT(T+.5)
7365  999 RETURN
7370      END
800
```

FUNCTION CRAL - LOGIC

```
8000 FUNCTION CRAL(XMV)
8005C
8010C CHROMEL-ALUMEL THERMOCOUPLE MILLIVOLT TO DEGREES CONVERSION
8015C 32 DEGREE REFERENCE JUNCTION TEMPERATURE
8020C      J. I. SABOL       12/27/68
8025C
8030     IF(XMV.GE.0.0.AND.XMV.LE.55.) GO TO 5
8035     T=9999.
8040     GO TO 65
8045  5  N=INT(XMV/5.)
8050     I=N+1
8055     V=XMV-5.*N
8060     GO TO (10,15,20,25,30,35,40,45,50,55,60,60),I
8065 10  T=-.216*V*V+44.94*V+32.
8070     GO TO 65
8075 15  T=-.048*V*V+45.*V+251.3
8080     GO TO 65
8085 20  T=-.125*V*V+44.08*V+475.1
8090     GO TO 65
8095 25  T=-.048*V*V+42.72*V+692.3
8100     GO TO 65
8105 30  T=-.016*V*V+42.28*V+904.7
8110     GO TO 65
8115 35  T=.064*V*V+42.36*V+1115.7
8120     GO TO 65
8125 40  T=.168*V*V+42.74*V+1329.1
8130     GO TO 65
8135 45  T=.208*V*V+43.88*V+1547.
8140     GO TO 65
8145 50  T=.176*V*V+45.68*V+1771.6
8150     GO TO 65
8155 55  T=.240*V*V+47.32*V+2004.4
8160     GO TO 65
8165 60  T=.240*V*V+50.2*V+2247.
8170 65  CRAL=INT(T+.5)
8175 99  RETURN
8180     END
```

FUNCTION CFLOW - LOGIC

```
9000 SUBROUTINE CFLOW(XMK,PP0,AAS)
9005C
9010C PROGRAM CALCULATES THE COMPRESSIBLE ISENTROPIC FLOW FUNCTIONS
9015C P/P0 AND A/A* IN THE MACH NUMBER RANGE OF .20 TO .60
9020C          J. T. SABOL          1/29/69
9025C
9030     DIMENSION XM(41),PP(41),AA(41)
9035     DATA XM,PP,AA/.20,.21,.22,.23,.24,.25,.26,.27,.28,.29,
9040&    .30,.31,.32,.33,.34,.35,.36,.37,.38,.39,.40,.41,.42,.43,
9045&    .44,.45,.46,.47,.48,.49,.50,.51,.52,.53,.54,.55,.56,.57,
9050&    .58,.59,.60,.9725,.9697,.9668,.9638,.9607,.9574,.9540,
9055&    .9506,.9470,.9432,.9394,.9355,.9315,.9273,.9231,.9187,
9060&    .9143,.9097,.9051,.9004,.8956,.8907,.8857,.8806,.8755,.8702,
9065&    .8649,.8595,.8541,.8486,.8430,.8373,.8316,.8258,.8200,.8141,
9070&    .8082,.8022,.7962,.7901,.7840,2.96,2.82,2.70,2.59,2.49,
9075&    2.40,2.31,2.23,2.16,2.09,2.035,1.976,1.921,1.870,1.822,1.778,
9080&    1.735,1.696,1.658,1.623,1.590,1.558,1.528,1.500,1.474,1.448,
9085&    1.424,1.401,1.380,1.359,1.339,1.321,1.303,1.286,1.270,1.255,
9090&    1.240,1.226,1.213,1.200,1.188/
9095     IF(XMK.LT..20.OR.XMK.GT..60) GO TO 40
9100     DO 10 I=1,41
9105     IF(XM(I)-XMK) 10,20,30
9110 10 CONTINUE
9115 20 PP0=PP(I)
9120     AAS=AA(I)
9125     GO TO 50
9130 30 J=I-1
9135     A1=(XMK-XM(J))*100.
9140     PP0=PP(J)-((PP(J)-PP(I))*A1)
9145     AAS=AA(J)-((AA(J)-AA(I))*A1)
9150     GO TO 50
9155 40 PP0=0.
9160     AAS=0.
9165 50 CONTINUE
9170     RETURN
9175     END
```

PROGRAM SSMIX TYPICAL OUTPUT

* * * * * * M I X I N G   P R Ø G R A M * * * * *

NØTE: DIMENSIØNS FØR PARAMETERS ARE AS FØLLØWS:

        TEMPERATURES - F   DENSITIES - #/FT3
        PRESSURES - PSIG   FLØWS - #/SEC
        VELØCITIES - FT/SEC

* *

RUN -   101   DATE -   20469

P ATM - 13.82   T ATM - 50.   RH - 38.0   PC/PA IDEAL - 29.35

***** HIGH PRESSURE WATER SYSTEM *****

FLØW - 28.90   P TANK - 1060.0   P IN - 910.0   T TANK - 50.

DT1 - 99.   DT2 - 27.   DT3 - 20.

***** LØW PRESSURE WATER SYSTEM *****

FLØW - 29.20   P TANK - 1050.0   P INLET - 856.0

T TANK - 52.   DELTA T - 26.

***** AIR SYSTEM *****

FLØW - 3.42   P SD - .596   P MC - 0.36

T SD - 74.   T MC - 68.   RHØ MC - .0729

V MC - 327.7   A - 1125.5   M - .291

***** LØW PRESSURE NITRØGEN SYSTEM *****

FLØW - 1.25   P N2 - 1.98   P MC - -.31

T N2 - 22.   T MC - 2.   RHØ MC - .0780

V MC - 551.0   A - 1073.1   M - .513

***** HIGH PRESSURE NITRØGEN SYSTEM *****

FLØW - 4.33   P N2 - 13.9   P MC - 0.85   T N2 - 9.

T MC - -69.   RHØ MC - .0923   VEL N2 - 986.5

***** LØX ØXIDIZER CALCULATIØNS *****

FLØW - 6.63   P TANK - 736.0   P IN - 698.0

T IN - -296.   T CØØL - -146.   DP INJ - 363.8

***** HYDRØGEN FUEL CALCULATIØNS *****

FLØW - 0.66   P VEN IN - 1102.0   P IN - 540.0

T H2 - 69.   DP INJ - 205.8

***** PERFØRMANCE PARAMETERS *****

PC - 334.2   PC/PA - 25.18   MR - 10.06   TØTAL FLØW - 7.29

C* - 6204.   THEØR C* - 6650.   ETA C* - 94.2

***** AIR HEATER BED TEMPERATURES *****

T BED 1 - 50.   T BED 2 - 50.   T BED 3 - 50.   T BED 4 - 50.

* *

REPORT DISTRIBUTION LIST FOR CONTRACT NAS7-521

<u>Copies</u>

NASA Marshall Space Flight Center

Marshall Space Flight Center, Alabama 35812

Attn: Technical Manager, David Seymour, S&E-AERO-AT	5
Office of Technical Information, MS-IP	2
Keith Chandler, S&E-ASTN-PA	1
Technical Library	1
Hans G. Paul, R-P&VED	2
Purchasing Office, PR-EC	1
Don Thompson, S&E-ASTN-PAA	1
Patent Office, M-PAT	1
Technology Utilization Office, MS-T	1

NASA Headquarters, Washington, D.C. 20546

Attn: Chief, Liquid Propulsion Technology, OART, RPL	3
Jack Suddreth, OART, RPL	2
Alfred Gessow, OART, RR-2	1
Director, Launch Vehicles and Propulsion, OSSA, SV	1
Director, Advanced Manned Missions, OMSF, MT	1
Chief, Air Breathing Propulsion, RAP	1
Chief, Fluid Dynamics, RRF	1
Director, Technology Utilization Division, OTU	1

NASA Ames Research Center

Moffett Field, California 94035

Attn: Mission Analysis Division	1
Hans M. Mark	2

NASA Scientific and Technical Information Facility   10

P.O. Box 33

College Park, Maryland 20740

NASA Goddard Space Flight Center

Greenbelt, Maryland 20771

Attn: Merland L. Moseson, Code 620   2

NASA Pasadena Office

4800 Oak Grove Drive

Pasadena, California 91103

Attn: Henry Burlage, Jr., Propulsion Div., 38   2

      JPL Support Contracts Branch, Fred Abbott, Bldg. 150,   1

      Rm. 502

      Patents and Contracts Management   1

      Dr. Duane DipperyMS354-357   1

NASA Langley Research Center

Langley Station

Hampton, Virginia 23365

Attn: Edward Cortwright, Director   2

      Kenneth Pierpont, MS353   2

NASA Lewis Research Center

21000 Brookpark Road

Cleveland, Ohio 44135

Attn: Dr. Abe Silverstein, Director   2

      Irving Johnson, MS500-205   2

Paul Herr, MS500-209   1

Office of Technical Information   1
James Dugan, MS501-2   1

NASA Manned Spacecraft Center

Houston, Texas 77001

Attn: Joseph G. Thibodaux, Jr., Chief, Propulsion and

Power Division   2

Office of Technical Information   1

NASA John F. Kennedy Space Center

Cocoa Beach, Florida 32931

Attn: Dr. Kurt H. Debus   2

Aeronautical Systems Division

Air Force Systems Command

Wright-Patterson Air Force Base

Dayton, Ohio 45433

Attn: D. L. Schmidt, Code ASRCNC-2   1

Air Force Missile Development Center

Holloman Air Force Base, New Mexico

Attn: Maj. R. E. Bracken, Code MDGRT   1

Air Force Missile Test Center

Patrick Air Force Base, Florida

Attn: L. J. Ullian   1

Space and Missile Systems Organization

Los Angeles, California

Attn: Col. Clark, Technical Data Center   1

Arnold Engineering Development Center

Arnold Air Force Station

Tullahoma, Tennessee

Attn: Dr. H. K. Doetsch   1

Bureau of Naval Weapons

Department of the Navy

Washington, D.C.

Attn: J. Kay, RTMS-41   1

Defense Documentation Center Headquarters

Cameron Station, Building 5

5010 Duke Street

Alexandria, Virginia 22314

Attn: TISIA   1

Headquarters, U.S. Air Force

Washington 25, D.C.

Attn: Col. C. K. Stambaugh, AFRST   1

Picatinny Arsenal

Dover, New Jersey 07801

Attn: I. Forsten, Chief   1

        Liquid Propulsion Laboratory, SMUPA-DL

Air Force Rocket Propulsion Laboratory

Research and Technology Division

Air Force Systems Command

Edwards, California 93523

Attn: Mr. H. Main, RPRR   1

U.S. Army Missile Command

Redstone Arsenal

Alabama 35809

Attn: Dr. Walter Wharton   1

U.S. Naval Weapons Station

China Lake, California 93557

Attn: Chief, Missile Propulsion Division, Code 4562   1

Chemical Propulsion Information Agency

Applied Physics Laboratory

8621 Georgia Avenue

Silver Spring, Maryland 20910

Attn: Tom Reedy   1

Aerojet-General Corporation

P.O. Box 296

Azusa, California 91703

Attn: W. L. Rodgers   1

Aerojet-General Corporation

P.O. Box 1947

Technical Library, Bldg. 2015, Dept. 2410

Sacramento, California 95809

Attn: R. Stiff   1

Aeronutronic Division

Philco Corporation

Ford Road

Newport Beach, California 92663

Attn: D. A. Garrison   1

Aerospace Corporation

2400 East El Segundo Boulevard

P.O. Box 95085

Los Angeles, California 90045

Attn: John G. Wilder, MS-2293   1

Arthur D. Little, Inc.

20 Acorn Park

Cambridge, Massachusetts 02140

Attn: Library   1

Astrosystems International, Inc.

1275 Bloomfield Avenue

Fairfield, New Jersey 07007

Attn: A. Mendenhall   1

Atlantic Research Corporation

Edsall Road and Shirley Highway

Alexandria, Virginia 22314

Attn: Dr. Ray Friedman   1

Avco Systems Division

Wilmington, Massachusetts

Attn: Howard B. Winkler   1

Beech Aircraft Corporation

Boulder Division

Box 631

Boulder, Colorado

Attn: J. H. Rodgers   1

Bell Aerosystems Company

P.O. Box 1

Buffalo, New York 14240

Attn: W. M. Smith   1

Bellcomm

955 L'Enfant Plaza, S.W.

Washington, D.C.

Attn: H. S. London   1

Bendix Systems Division

Bendix Corporation

3300 Plymouth Road

Ann Arbor, Michigan

Attn: John M. Brueger   1

Boeing Company

P.O. Box 3707

Seattle, Washington 98124

Attn: J. D. Alexander   1

Boeing Company

1625 K Street, N.W.

Washington, D.C. 20006

Attn: Library   1

Boeing Company

P.O. Box 1680

Huntsville, Alabama 35801

Attn: Ted Snow   1

Missile Division

Chrysler Corporation

P.O. Box 2628

Detroit, Michigan 48231

Attn: John Gates   1

Wright Aeronautical Division

Curtiss-Wright Corporation

Wood-Ridge, New Jersey 07075

Attn: G. Kelley   1

Astropower Laboratory

McDonnell-Douglas Aircraft Company

2121 Paularino

Newport Beach, California 92663

Attn: Dr. George Moe

      Director, Research   1

Missile and Space Systems Division

McDonnell-Douglas Aircraft Company

3000 Ocean Park Boulevard

Santa Monica, California 90406

Attn: R. W. Hallet, Chief Engineer

      Advanced Space Technology   1

Research Center

Fairchild Hiller Corporation

Germantown, Maryland

Attn: Ralph Hall   1

Republic Aviation Corporation

Fairchild Hiller Corporation

Farmingdale, Long Island, New York

Attn: Library   1

General Dynamics/Convair Division

Library & Information Services (128-00)

P.O. Box 1128

San Diego, California 92112

Attn: Frank Dore   1

Missile and Space Systems Center

General Electric Company

Valley Forge Space Technology Center

P.O. Box 8555

Philadelphia, Penna.

Attn: F. Mezger   1

      F. E. Schultz   1

Grumman Aircraft Engineering Corporation

Bethpage, Long Island

New York

Attn: Joseph Gavin   1

Honeywell, Inc.

Aerospace Division

2600 Ridgway Road

Minneapolis, Minnesota

Attn: Gordon Harms   1

Hughes Aircraft Co.

Aerospace Group

Centinela and Teale Streets

Culver City, California

Attn: E. H. Meier, V. P. and Div. Mgr.

      Research and Dev. Div.   1

Walter Kidde and Company, Inc.

Aerospace Operations

567 Main Street

Belleville, New Jersey

Attn: R. J. Manville

      Dir. of Research Engr.   1

Ling-Temco-Vought Corporation

P.O. Box 5907

Dallas, Texas 75222

Attn: Warren C. Trent   1

Lockheed Missiles and Space Company

P.O. Box 504

Sunnyvale, California 94088

Attn: J. Guill, Technical Information Center   1

Lockheed Missiles and Space Company

Huntsville Research and Engineering Center

4800 Bradford Blvd., N.W.

Huntsville, Alabama 35805

Attn: Mrs. Beverly Audah   1

Lockheed Propulsion Company

P.O. Box 111

Redlands, California 92374

Attn: H. L. Thackwell   1

The Marquardt Corporation

16555 Saticoy Street

Van Nuys, California 91409

Attn: Howard McFarland   1

Baltimore Division

Martin Marietta Corporation

Baltimore, Maryland 21203

Attn: John Calathes (3214)   1

Denver Division

Martin Marietta Corporation

P.O. Box 179

Denver, Colorado 80201

Attn: Dr. Morganthaler   1

Orlando Division

Martin Marietta Corporation

P.O. Box 5837

Orlando, Florida

Attn: J. Ferm   1

McDonnell-Douglas Aircraft Corporation

P.O. Box 516

Municipal Airport

St.Louis, Missouri 63166

Attn: R. A. Herzmark   1

Space & Information Systems Division

North American Rockwell Corporation

12214 Lakewood Boulevard

Downey, California 90241

Attn: Library   1

Rocketdyne (Library 586-306)

North American Rockwell Corporation

6633 Canoga Avenue

Canoga Park, California 91304

Attn: Dr. R. J. Thompson, Jr.   1

       S. F. Iacobellis   1

Northrop Space Laboratories

3401 West Broadway

Hawthorne, California

Attn: Dr. William Howard   1

Astro-Electronics Division

Radio Corporation of America

Princeton, New Jersey 08540

Attn: Y. Brill   1

Reaction Motors Division

Thiokol Chemical Corporation

Denville, New Jersey 07832

Attn: Dwight S. Smith   1

Thiokol Chemical Corporation

Huntsville Division

Huntsville, Alabama

Attn: John Goodloe   1

Space Division

Aerojet-General Corporation

9200 East Flair Avenue

El Monte, California 91734

Attn: S. Machlawski   1

Stanford Research Institute

333 Ravenswood Avenue

Menlo Park, California 94025

Attn: Dr. Gerald Marksman   1

TRW Systems Group

TRW Incorporated

One Space Park

Redondo Beach, California 90278

Attn: G. W. Elverum   1

TAPCO Division

TRW, Incorporated

23555 Euclid Avenue

Cleveland, Ohio 44117

Attn: P. T. Angell   1

Research Laboratories

United Aircraft Corporation

400 Main Street

East Hartford, Connecticut 06108

Attn: Erle Martin   1

Hamilton Standard Division

United Aircraft Corporation

Windsor Locks, Connecticut 06096

Attn: R. Hatch   1

United Technology Center

587 Methilda Avenue

P.O. Box 358

Sunnyvale, California 94088

Attn: Dr. D. Altman   1

Florida Research and Development

Pratt and Whitney Aircraft

United Aircraft Corporation

P.O. Box 2691

West Palm Beach, Florida 33402

Attn: R. J. Coar   1

Rocket Research Corporation

520 South Portland Street

Seattle, Washington 98108

Attn: Foy McCullough, Jr.   1

Vickers, Inc.

P.O. Box 302

Troy, Michigan

Attn: Library   1

Louisiana State University

Department of Chemical Engineering

Baton Rouge, Louisiana

Attn: Dr. Richard J. Farmer   1

Sunstrand Aviation

2421 Eleventh Street

Rockford, Illinois 61101

Attn: R. W. Reynolds   1

General Applied Science Laboratory, Inc.

Merrick and Stewart Avenues

Westbury, Long Island

New York 11590

Attn: Dr. Ray Edleman   1

DOCUMENT CONTROL DATA - R & D

(Security classification of title, body of abstract and indexing annotation must be entered when the overall report is classified)

1. ORIGINATING ACTIVITY *(Corporate author)*	2a. REPORT SECURITY CLASSIFICATION
Rocketdyne, a Division of North American Rockwell Corporation, 6633 Canoga Avenue, Canoga Park, California 91304	2b. GROUP

3. REPORT TITLE

PERFORMANCE ANALYSIS OF COMPOSITE PROPULSION SYSTEMS

4. DESCRIPTIVE NOTES *(Type of report and inclusive dates)*
Phase II Final Report (25 March 1968 through 24 March 1969)

5. AUTHOR(S) *(First name, middle initial, last name)*

Wrubel, J. A.

6. REPORT DATE	7a. TOTAL NO. OF PAGES	7b. NO. OF REFS
29 April 1969	116	21

8a. CONTRACT OR GRANT NO.	9a. ORIGINATOR'S REPORT NUMBER(S)
b. PROJECT NO.	R-7825
c.	9b. OTHER REPORT NO(S) *(Any other numbers that may be assigned this report)*
d.	

10. DISTRIBUTION STATEMENT

11. SUPPLEMENTARY NOTES	12. SPONSORING MILITARY ACTIVITY
	National Aeronautics and Space Administration Marshall Space Flight Center

13. ABSTRACT

The improved understanding of gas-stream turbulent mixing is contingent upon obtaining a more comprehensive description of the resultant flow field and a more precise evaluation of the turbulent transport properties. The second phase of a continuing program to accomplish these goals is described herein. The flow field being experimentally studied is the two-demensional mixing of fuel-rich supersonic hydrogen-oxygen combustion products and a subsonic heated airstream. The mixing is accomplished in a chamber accessible to both optical- and probe-type instrumentation systems. The second phase of the program included flow facility check-out, instrumentation installation, probe instrumentation survey, and preliminary testing.

14. KEY WORDS	LINK A		LINK B		LINK C	
	ROLE	WT	ROLE	WT	ROLE	WT
Gas Stream Turbulent Mixing						
Turbulent Transport Properties						
Supersonic Hydrogen-Oxygen Combustion Products						
Subsonic Heated Airstream						